POLITECNICO DI MILANO
DEPARTMENT of Hydraulic Engineering
DOCTORAL PROGRAMME IN Environmental Engineering and Infrastructures

Characterization of groundwater dynamics in response to forcing terms under uncertainty

Doctoral Dissertation of:
Raul Perulero Serrano

Supervisor:
Prof. Alberto Guadagnini

Tutor:
Prof. Monica Riva

The Chair of the Doctoral Program:
Prof. Alberto Guadagnini

2014 – 26th Cycle

Para Elisa, que está en camino.

ACKNOWLEDGEMENTS

I would like to kindly acknowledge Prof. Alberto Guadagnini for his wise words, advice and trust, for his patience and comprehension. Without his support this dissertation would not have seen the light. I would also like to acknowledge the support of Prof. Monica Riva and her thorough scientific discussions carried out during the entire project.

I would like to thank the collaboration of Laura Guadagnini for giving a wider geological perspective to our research work and Prof. Mauro Giudici for his constructive discussions held during the early stages of this project.

A special thanks to everyone I met at the former DIIAR (and currently DICA) Department: professors, fellows, administration staff and IT people. Also thank you to everyone who helped me through the ocean of bureaucracy during these last years: especially people at the H.H.R.R. and financial departments.

I would like to express my appreciation to Giovanna Venuti and Priscila Escobar Rojo for their constructive and very interesting conversations related to work and beyond.

Financial support by Marie Curie Initial Training Network "*Towards Improved Groundwater Vulnerability Assessment (IMVUL)"* is gratefully acknowledged.

I would like to raise a special and big thank you to Dr. Noelle Odling, from the University of Leeds, for her collaboration in a parallel project carried out during the last year of my Ph.D. project, and for helping me in joining the LUWC. Moreover, for welcoming me into the University of Leeds which in turn gave me the chance to apply for the position I am currently performing there. Thank you also to Dr. William Murphy and Dr. Jared West, both from University of Leeds, for offering me the position and their support throughout the training that it involves.

I would like to say thank you to all my family and friends who supported me since I left my hometown pursuing new scientific and life challenges, especially my parents for their unconditional support in all these years and my wife for her patience, comprehension and love. *Vielen dank Dr. Lena Driehaus*! I would not like to end this section without mentioning who has been a good fellow, project companion, flat mate, comrade, adventure sharer and above all a great friend. Огромное спасибо Dr. СергеюЧайниковУ (Sergey V. Chaynikov).

ABSTRACT

We present a numerical study keyed to the analysis of the impact on hydraulic head statistics of two selected methodologies for the stochastic simulation of hydrofacies spatial arrangement. We analyze the distribution of hydraulic heads in a confined aquifer under steady state convergent three-dimensional flow to a fully penetrating well, superimposed to a mean uniform regional gradient. The heterogeneous structure of the system is modelled on the basis of available field information comprising detailed lithological data collected within an aquifer system located in northern Italy. These data are grouped into five lithotype categories and the aquifer system is modelled as a random composite medium. Monte Carlo realizations of the three-dimensional geomaterial distributions are generated through the Sequential Indicator Simulation (SISIM) and the Truncated Plurigaussian Simulation (TPS) methods. The latter enables one to integrate geological conceptual information in the simulation procedure, while the former relies mainly on a variogram-based analysis. Point and vertically averaged hydraulic heads, corresponding to typical observations collected within screened boreholes, are analyzed by evaluating the dependence of their sample probability distributions on (*i*) the hydrofacies generation scheme (*ii*) the extent of the vertical averaging interval and (*iii*) the relative distance between the location of observation boreholes, hydrological boundaries and the source term. Theoretical probability density function models are fitted against numerically simulated distributions within a Maximum Likelihood (ML) context. Our results indicate that hydraulic heads associated with the Truncated Plurigaussian Simulation method exhibit increased variability when compared to their counterparts evaluated upon relying on a Sequential Indicator based modeling strategy of the system heterogeneity. Covariance matrices and probability distributions of point and vertically averaged hydraulic heads display similar key representative features and patterns. This suggests that typical measurements collected in screened boreholes can be used to infer qualitative information about the correlation structure and the statistical properties of heads.

Keywords: Geostatistics; Sequential Indicator Simulation; Truncated Plurigaussian Simulation; Monte Carlo method; head probability distribution.

RIASSUNTO

Vi presentiamo uno studio numerico basato su l'analisi dell'impatto di due metodologie di simulazione stocastica di disposizione spaziale d'idrofacies sulle statistiche della testa idraulica. Analizziamo la distribuzione delle teste idrauliche in un acquifero confinato sotto flusso stazionario convergente tridimensionale a un pozzo pienamente penetrante, sovrapposte a un gradiente medio regionale uniforme. La struttura eterogenea del sistema è modellata sulla base delle informazioni di campo disponibili che comprende dati litologici dettagliati raccolti all'interno di un sistema acquifero situato nel nord d'Italia. Questi dati sono raggruppati in cinque categorie di litotipi e il sistema acquifero è modellato come un mezzo composito casuale. Realizzazioni tridimensionali di Monte Carlo sulle distribuzioni di geomateriali sono generate mediante "*Sequential indicator Simulations and the Truncated Plurigaussian method*". Quest'ultimo metodo permette d'integrare l'informazione concettuale geologica nella procedura di simulazione, mentre il primo si basa principalmente sull'analisi dei variogrammi. Teste idrauliche puntuali e calcolate sulla media nella verticale, corrispondenti a tipici rilevamenti riscossi entro pozzi schermati, vengono analizzati per valutare la dipendenza rispetto le sue distribuzioni di probabilità campionate rispetto (*i*) il sistema di generazione d'idrofacies (*ii*) l'estensione dell'intervallo di media verticale e (*iii*) la distanza relativa tra la posizione dei pozzi di osservazione, i confini idrologici e il termino sorgente. Modelli di funzioni di densità di probabilità teoriche sono adatte contro distribuzioni simulate numericamente in un contesto di Massima Verosimiglianza. I nostri risultati indicano che le teste idrauliche associate al metodo "*Truncated Plurigaussian Simulation*" mostrano una maggiore variabilità rispetto alle loro controparti valutate sulla strategia di modellazione della eterogeneità del sistema basata nell' "*Sequential Indicator Simulation*". Le matrici di covarianza e le distribuzioni di probabilità delle teste idrauliche, di misure puntuali e sulla media nella verticale, mostrano caratteristiche rappresentative chiave e simili. Questo fatto suggerisce che misure tipiche raccolte in pozzi schermati, possono essere usate per dedurre informazione qualitativa sulla struttura di correlazione e proprietà statistiche delle teste idrauliche.

Parole chiave: Geostatistica; Sequential Indicator Simulation; Truncated Plurigaussian Simulation; metodo di Monte Carlo; distribuzioni teste idrauliche.

Index

1. INTRODUCTION 4

1.1. Aims 4

1.2. Objectives 5

1.3. Structure 6

1.4. Originality and principal outcome 7

2. LITERATURE REVIEW 8

2.1. Geostatistical simulations 11

2.2. Hydraulic head pdfs 13

3. CREMONA FIELD CASE STUDY 16

3.1. Area under study 16

3.1.1. Location 16

3.1.2. Previous studies 18

3.1.3. Hydrogeological structure 19

3.1.4. Wells / piezometers 22

3.1.5. Springs 24

3.2. Reference information database 26

3.3. Regional vulnerabilities 30

3.4. Final remark 30

4. METHODOLOGY 31

4.1. Modifying the geological database 31

4.2. Recalling geostatistical concepts 33

4.3. Indicator variogram calculation 34

4.4. SISIM vs TPS (and the geostatistical simulations) 35

4.5. Flow field simulations using VMOD 39

4.6. Workflow for treating the output from the multi-realization scheme 42

5. AQUIFER SYSTEM SIMULATIONS 43

5.1. Modifying the geological database 43

5.2. Variogram analysis and indicator variogram model fitting results 46

5.3. Description of representative results 50
5.3.1. Qualitative analysis of heterogeneity' reproduction for SISIM and TPS 52
5.3.2. Statistical analysis of SISIM and TPS output volumetric proportions 53
5.3.3. Variogram calculations from output simulations (SISIM and TPS) 58
5.3.4. Sample Log*K* fields for mean (μ) and variance (σ^2), from SISIM and TPS 60

6. FLOW FIELD SIMULATIONS 63

6.1. Stating the problem: modeling details and procedure 63
6.1.1. Numerical grid 64
6.1.2. Boundary conditions 66

6.2. N-S and W-E ensemble average drawdown maps 67

6.3. Hydraulic heads' variance and covariance maps for different degrees of vertical averaging 71

6.4. Sample pdf estimation for point and vertically averaged hydraulic heads 76

6.5. Sample pdf fitting procedure to Gaussian and α-stable models 80

7. DISCUSSION 88

7.1. Practical applications 88

7.2. Objective and novelty 88

7.3. Indicator simulations 91
7.3.1. Comparison of SISIM and TPS results 92
7.3.2. Providing guidelines 93
7.3.3. Consequences of using SISIM and/or TPS 95
7.3.4. When should be used one or another? Both? 97

7.4. Flow field simulations 99
7.4.1. Comparison of SISIM and TPS results 100
7.4.2. Providing guidelines 107
7.4.2.1. Vulnerability issues 109

8. CONCLUSIONS 110

8.1. Future work 111

9. ANNEXES / APPENDIXES 114

9.1. Publications 114

9.2. Dissemination activities 115
9.2.1. Conferences and workshops 115
9.2.2. Posters at international conferences 115
9.2.3. Oral presentations 116

9.3. Appendix to Chapter 7 117

10. REFERENCES 121

1. Introduction

The current Ph.D. thesis has been developed under the umbrella of the European Marie Curie ITN (Initial Training Network) IMVUL "*Towards improved groundwater vulnerability assessment*".

1.1. Aims

The aim pursued with this work is to improve our current knowledge in numerical modeling applied to hydrogeology, by means of conducting statistical analyses of the outcome of the procedures/workflows adopted and the application of the results to real field case studies.

The project we carried out is mainly focused on the use and comparison of two geostatistical techniques to produce heterogeneous aquifer simulations in order to simulate the flow field induced by a mean hydraulic gradient superimposed to the effect of a pumping well in a real double aquifer system. A posed problem of the kind is relevant to hydrogeology practitioners, especially to those related to groundwater vulnerability and its characterization and/or quantification. The actual system bears at surface level a natural and active springs' network which is threatened by anthropological activities such as water over abstraction, due to excessive pumping effects for agricultural (mainly) and industrial purposes. We did combine a stochastic approach with the inclusion of real hard data (lithological input from available boreholes) to condition the aforementioned geostatistical simulations. We created a reality-based numerical model to study the impact of the hydrofacies generation scheme and the effect of competing hydraulic stresses over a given environmental target parameter of our

choice: ***h*** (hydraulic heads). The output of a study of the kind we propose could be used to guide setting thresholds or limits in water abstractions, in order to control hazardous drawdowns that could lead to the drying up of a springs' network fed by a confined aquifer.

1.2. Objectives

In this dissertation, we perform a numerical Monte Carlo (MC) study based on a geological system whose heterogeneous structure mimics the one associated with an alluvial aquifer system located in northern Italy (Cremona province, Regione Lombardia) where abundant lithological and geological information are available. Our analysis considers a non-uniform flow scenario due to the superimposition of a base uniform (in the mean) flow and the action of a pumping well. Field-scale available lithological data are analyzed to characterize prevalent lithotype categories and the associated geological contact rules. The simulation domain is modeled as a composite medium with randomly distributed hydrofacies, each associated with a given hydraulic conductivity. Collections of conditional Monte Carlo realizations of the three-dimensional geomaterials distributions are generated by (*i*) a classical indicator-based approach (Sequential Indicator simulations, SISIM) and (*ii*) the Truncated Plurigaussian simulations (TPS) scheme, starting from available data which are employed as conditioning information. Afterwards we performed a statistical analysis (in terms of mean, variance, covariance function and probability distribution) of hydraulic heads as a function of (*i*) location in the domain and (*ii*) methodology of geological reconstruction of the system, highlighting the competing effect of the source term and boundary conditions. Since typical head observations are collected within screened boreholes, we explore the extent to which vertically averaging hydraulic heads can retain qualitative and quantitative information on the statistical behavior of point-wise head values.

1.3. Structure

The dissertation is organized as follows. We do start framing our research revising the previous scientific contributions by means of a review of the available literature in Chapter 2. Chapter 3 is devoted to illustrate the reader with the current information database related to the real field case study. There we describe the geological setup and present the previous studies/surveys carried out in the area. We point out the relevance of the chosen area in terms of groundwater vulnerability issues drawing the scenario where the numerical analysis is meant to be applied for. A description of the available lithological database is performed. Chapter 4 reports details about the methodology developed and employed. From modifying the available borehole database in order to simplify the naturally high heterogeneity of the hydrofacies system, through recalling some basic geostatistical concepts needed for our study, we introduce the two widely used geostatistical approaches employed to conditionally simulate (to hard data), in a MC framework, the large scale confined aquifer. We describe the hydrofacies simulation stage and the flow field simulations performed by means of the commonly used MODFLOW code. Finally we provide some guidelines on how we treated the output at different stages to allow reproduction of the results, bringing light to the procedure utilized to perform the posterior statistical analysis. Chapter 5 treats in detail the hydrofacies simulations approach adopted in our study while Chapter 6 deals with the description of the aquifer flow field simulations. A thorough discussion upon the obtained results is performed in Chapter 7, both for the geostatistical reconstruction of the aquifer system and the flow simulations. We end up with the major findings and conclusions, along with future work and potential research tracks that can be pursued. Annexes / Appendixes containing publications, dissemination activities and other extra material can be found at the end of this work. Before its end we enclose a list with scientific references.

1.4. Originality and principal outcome

The novelty of our study is rooted in the fact of investigating the relative impact of two different conceptualization and simulation techniques to characterize random hydrofacies spatial arrangement on the probabilistic distribution of hydraulic heads in three-dimensional aquifer systems, under non-uniform mean flow conditions of the kind that are associated with large scale field. This analysis is intimately tied to Probabilistic Risk Assessment (PRA) procedures and constitutes one of the steps which can be adopted in modern PRA applications based on the idea of decomposing the full problem (that might comprise several uncertainty sources, including those associated with hydrostratigraphic structure, aquifer recharge, boundary conditions, location and/or pumping/injection rate of wells) into sets of basic events. History matching and inverse modeling are out of our scope in the present study.

Amongst the main findings we would like to highlight that hydraulic heads deduced from TPS-based flow simulations reveal larger variability than their equivalents evaluated by a SISIM-based modeling strategy. This can be seen as a consequence of setting geological contact rules, as considered within a TPS simulation scheme, which can lead to an increased variability in the internal architecture of hydrofacies distributions within a relatively large-scale aquifer model of the kind we consider.

Due to the enhanced degree of variability displayed within the collection of simulations and to the occurrence of long-tailed ***pdfs***, reliance on a TPS scheme produces a broader range of possible drawdown values for the simulated groundwater system. As such, TPS-based results are associated with the most conservative (in terms of extreme values) drawdown estimates which can then be related to a given threshold probability of occurrence in the context of PRA protocols, where the target environmental metric is the piezometric drawdown.

2. Literature review

Heterogeneity is embedded in practically all life systems at almost every scale. This assumption also affects/includes geosciences and its related fields/disciplines. In particular we are interested in characterizing the natural heterogeneity that exists in groundwater systems, by means of Geostatistics and numerical simulations, specifically at a field scale. This is one of our objectives in order to improve the current knowledge in numerical modeling of water reservoirs and links to the more general aim of estimation and quantification of groundwater vulnerability in real/natural systems.

We decided to employ widely used and well-known, both by academics and practitioners, geostatistical and numerical tools to simulate a double aquifer system and its associated flow field when a pumping well is acting as a sink/forcing term in the system. The situation just described is compatible with actual field practices like water abstractions for agricultural, industrial or drinking water purposes. These stresses are applied to natural environments which react in turn, mostly having a negative impact on the available water resources and the surrounding natural environments. Sometimes the aforementioned stresses are pushed to certain limits that drive the system into a non-equilibrium state. Since these activities cannot cease due to civil/industrial requirements, a compromise needs to be met in order to protect the resources we are exploiting (and sometimes overexploiting).

What we propose is a stochastic approach conducted at a field scale, involving geostatistical and numerical analyses, in order to compare two methodologies and the joint information we can extract from their outcome. In other words, we compared two well-established geostatistical methods that treat in a different way the heterogeneity embedded in

natural systems, and the impact of the geostatistical simulation on the posterior flow field solution (and in particular, on the hydraulic heads). This allowed us estimating low order moment statistics of calculated hydraulic heads in order to forecast which method introduces more variability in the results and/or which method can be useful as a function of the context under study (extreme values analysis, worst case scenario, etc.). From a practical point of view, in stochastic hydrogeology, it is of great importance being able to put thresholds on water abstractions that might lower local/regional hydraulic heads leading towards a real menace to the available groundwater resources.

The present work is focused on the assessment of the impact on hydraulic head statistics of two geostatistically-based methodologies for the stochastic simulation of the spatial arrangement of hydrofacies in field scale aquifer systems. The relevance of an appropriate characterization of the probability distribution of hydraulic heads is critical in the context of Probabilistic Risk Assessment (PRA) procedures which are nowadays considered as viable procedures to estimate the risk associated with catastrophic events in environmental problems (Tartakovsky, 2013 and references therein). Application of PRA to actual settings typically requires the estimate of the probability density function (***pdf***) of a target Environmental Performance Metric (EPM, a terminology introduced by De Barros et al., 2012).

The study of the relative impact of different conceptualization and simulation techniques to represent random hydrofacies spatial arrangement on the probabilistic distribution of hydraulic heads in three-dimensional aquifer systems under non-uniform mean flow conditions of the kind that is associated with large scale field settings is still lacking. As highlighted above, this analysis is tied to Probabilistic Risk Assessment procedures and constitutes one of the steps which can be adopted in modern PRA applications based on the

idea of decomposing the full problem (that might comprise several uncertainty sources, including those associated with hydrostratigraphic structure, aquifer recharge, boundary conditions, location and/or pumping/injection rate of wells) into sets of basic events (e.g., Bolster et al., 2009; Jurado et al., 2012; Tartakovsky, 2013 and references therein).

Here we perform a numerical Monte Carlo study based on a geological system whose heterogeneous structure mimics the one associated with an alluvial aquifer system located in northern Italy, where abundant lithological and geological information are available. Our analysis considers a non-uniform flow scenario due to the superimposition of a base uniform (in the mean) flow and the action of a pumping well. Field-scale available lithological data are analyzed to characterize prevalent lithotype categories and the associated geological contact rules. The simulation domain is modeled as a composite medium with randomly distributed hydrofacies, each associated with a given hydraulic conductivity. Collections of conditional Monte Carlo realizations of the three-dimensional geomaterials distributions are generated by (*i*) a classical indicator-based approach and (*ii*) the TPS scheme, starting from available data which are employed as conditioning information. We present a statistical analysis (in terms of mean, variance, covariance function and probability distribution) of hydraulic heads as a function of (*i*) location in the domain and (*ii*) methodology of geological reconstruction of the system, highlighting the competing effect of the source term and boundary conditions. Since typical head observations are collected within screened boreholes, we explore the extent to which vertically averaging hydraulic heads can retain qualitative and quantitative information on the statistical behavior of point-wise head values.

2.1. Geostatistical simulations

Geostatistics can be roughly defined as the branch of Geology and/or Statistics that deals with the study of phenomena that vary over the spatial dimension. It was developed originally in the context of mining industry, to tackle problems that dealt with the spatial prediction of mineral ore grades. Its general approach led afterwards to its vast application in a wide range of settings across the geographical, geological, atmospheric, environmental, and epidemiological sciences (among others). Geostatistics mainly provides a set of probabilistic tools that help in understanding and modeling the spatial variability of a target variable of interest, bearing in mind the main motivation of predicting unsampled values of the aforementioned variable over areas/volumes where little/scarce information is provided. This process is also (well-) known as interpolation. It is necessary to soar to the work of Daniel Krige and other authors to find the origins of the discipline. They developed methods to calculate/estimate gold and uranium reserves in the Witwatersrand, in South Africa, during the decade of the 1950's. Their ideas were extended and formalized during the 1960's by the French statistician Georges Matheron, who coined the term Geostatistics.

The selection of a model through which one can describe the natural heterogeneity of a system is a key point in the analysis of the distribution of groundwater flow (and possibly transport) variables. The model choice strongly depends on the scale of investigation. At the large field scale, geological heterogeneity of sedimentary bodies can be represented and modeled from information on depositional facies distributions. Statistical grid-based sedimentary Facies Reconstruction and Modeling (FRM) methods can be employed to provide consistent representations of facies distribution and are amenable to include conditioning to hard and/or soft data. Falivene et al. (2007) provide an overview of the most widely used deterministic and stochastic FRM methods, including pixel-based methods

termed as sequential indicator simulation (SISIM), transition probability schemes (e.g., T-PROGS; Carle, 1999), multiple point simulation (Strebelle, 2002; Zhang et al., 2006; Wu et al. 2008), truncated Gaussian simulation (TGS) and truncated plurigaussian simulation (TPS).

Sequential indicator algorithms are widespread geostatistical simulation techniques that rely on indicator (co-) kriging. These have been applied to different datasets to study the influence of the random distribution of aquifer sedimentological facies on target environmental variables. In this context, Riva et al. (2006) present a synthetic numerical Monte Carlo study aimed at analyzing the relative importance of uncertain facies architecture and hydraulic attributes (hydraulic conductivity and porosity) on the probabilistic distribution of three-dimensional well catchments and time-related capture zones. The authors base their comparative study on a rich database comprising sedimentological and hydrogeological information collected within a shallow alluvial aquifer system. Riva et al. (2008, 2010) adopt the same methodology to interpret the results of a field tracer test performed in the same setting. These authors consider different conceptual models to describe the system heterogeneity, including scenarios where the facies distribution is random and modeled through a SISIM-based technique and the hydraulic properties of each material are either random or deterministically prescribed. Comparisons between the ability of different geostatistical methods to reproduce key features of field-scale aquifer systems have been published in the literature (e.g., Casar-González, 2001; Falivene et al., 2006; Scheibe and Murray, 1998, Dell'Arciprete et al., 2012). Lee et al. (2007) performed a set of Monte Carlo simulations to mimic a pumping test in an alluvial fan aquifer using the sequential Gaussian simulation method and the transition probability indicator simulation. Emery (2004) highlights limitations of SISIM upon examining the conditions under which a set of realizations is consistent with the input parameters.

Truncated Gaussian simulation enables one to condition simulations on prior information stemming from various sources while guaranteeing consistency between variogram and cross-variogram of the variables considered. The possibility of using a multiplicity of Gaussian functions to codify hydrofacies extends the potential of TGS and is the cornerstone of TPS (Galli et al., 1994). Later on, Le Loc'h and Galli (1997) extended the aforementioned reference. TPS allows taking into account complex transitions between material types and simulating anisotropic distributions of lithotypes, whereas TGS explicitly considers only sequentially ranked categories. The application of TPS usually aims at (*i*) assessing the uncertainty associated with the location of the internal boundaries demarcating geomaterials within the domain, and (*ii*) improving the geological constraints in the characterization of quantitative attributes such as mineral ore grades. TPS is typically employed to simulate geological domains in different contexts, including petroleum reservoirs and mineral deposits, spatial arrangement of hydrofacies in aquifers, or soil types at a catchment scale (e.g., Betzhold and Roth, 2000; Skvortsova et al., 2000; Fontaine and Beucher, 2006; Galli et al., 2006; Emery et al., 2008; Dowd et al., 2007; Mariethoz et al., 2009). More recently, a few publications brought open source codes/suites to use the TPS workflow in standard personal computers (Dowd et al., 2003; Xu et al., 2006 and Emery, 2007). The routines are available as FORTRAN and MATLAB codes.

2.2. Hydraulic head pdfs

In the groundwater literature, the functional format of probability distributions of solute travel/residence times, trajectories and concentrations has been extensively analyzed during the last years (Fiorotto and Caroni, 2002; Bellin and Tonina, 2007; Riva et al., 2008, 2010; Schwede et al., 2008; Enzenhoefer et al., 2012 amongst others). On the other hand, less attention has been devoted to study the probability distribution of hydraulic head (***h***) in

complex groundwater systems and under non-uniform (in the mean) flow conditions. These settings are crucial for the study of the (negative) consequences arising from events associated with the occurrence of ***h*** dropping below (or rising above) a given threshold. These basic events are critical for various goal-oriented risk assessment practices including, e.g., the protection of natural springs, ponds or the prevention of damages to underground infrastructures. They all constitute core requirements in the planning of groundwater abstraction procedures or during the designing of protection barriers. In this context, estimates of first and second (conditional or unconditional) statistical moments of ***h*** have been largely analyzed by means of analytical (e.g., Guadagnini et al., 2003; Riva and Guadagnini, 2009 and references therein) or numerical (e.g., Guadagnini and Neuman, 1999b; Hernandez et al., 2006) methods for bounded randomly heterogeneous aquifers under the action of pumping. Low-order (statistical) moments (i.e., mean and variance-covariance) of hydraulic heads in unbounded and bounded domains under uniform (in the mean flow) conditions have been investigated, amongst others, by: Dagan (1985), Rubin and Dagan (1988, 1989), Ababou et al. (1989), Dagan (1989), Osnes (1995), Guadagnini and Neuman (1999a, b). Even as these low-order moments have a considerable theoretical and practical interest, they are not directly suitable to PRA protocols where the behavior of the tails of the target variable distribution needs to be identified. This behavior can differ from the one dictated by the classically assumed Gaussian or lognormal distributions and can be influenced by the type of system heterogeneity, hydraulic boundaries and source/sink terms, as we discuss in this work.

Jones (1990) observed the non-Gaussian shape of heads' ***pdf*** close to pumping wells in a two-dimensional confined aquifer where the transmissivity is lognormally distributed and spatially correlated according to an exponential covariance model. Kunstmann and Kastens

(2006) modeled an aquifer in Gambach (Germany) under general non-uniform flow conditions as a two-dimensional, block-heterogeneous system, where transmissivity is homogeneous within each of five considered distinct zones. These authors noted that groundwater velocities could be well approximated by lognormal distributions while heads could be best described by long-tailed ***pdfs*** (such as the Weibull or the Gamma distributions). Nowak et al. (2008) presented a detailed numerical study centered on the analysis of statistical moments and ***pdf*** of heads and velocity components. Their work involved three-dimensional flow through realizations of randomly heterogeneous conductivity fields subject to uniform mean flow conditions. The authors noted that the shape of heads' ***pdf*** is similar to a Gaussian or a Beta distribution at locations which were respectively far or close to the Dirichlet boundaries. The longitudinal discharge components appeared to be well interpreted by a lognormal distribution while their transverse counterparts displayed long tails. Additional studies which are concerned with key statistics of groundwater fluxes under uniform (in the mean) flow conditions include the works of Englert et al. (2006) and Zarlenga et al. (2012).

3. Cremona field case study

In this section we describe the Cremona aquifer from a hydrogeological point of view.

3.1. Area under study

3.1.1. Location

The area subject of this study is the territory portion of the Pianura Padana valley bounded to the west and south by the river Adda (which runs North-South) to Crotta d'Adda, where it enters the river Po, and eastward from river Serio, which runs along the North-South direction until Montodine, where it flows into the river Adda.

In the absence of a clear identification of a hydrogeological boundary, the demarcation of the northern limit was evaluated in a manner consistent with other studies conducted in the aforementioned region. In particular, it was adopted the same northern boundary identified in a thesis project developed at the Politecnico di Milano by Rametta, (2008). That is located along the northern boundary running parallel to the coordinate Gauss-Boaga 5060000 North. The limits described above identify an area of approximately 785 km^2. This system will be identified later in terms of "the large scale model". **Figure 3.1.1.1** displays a sketch with the area under study.

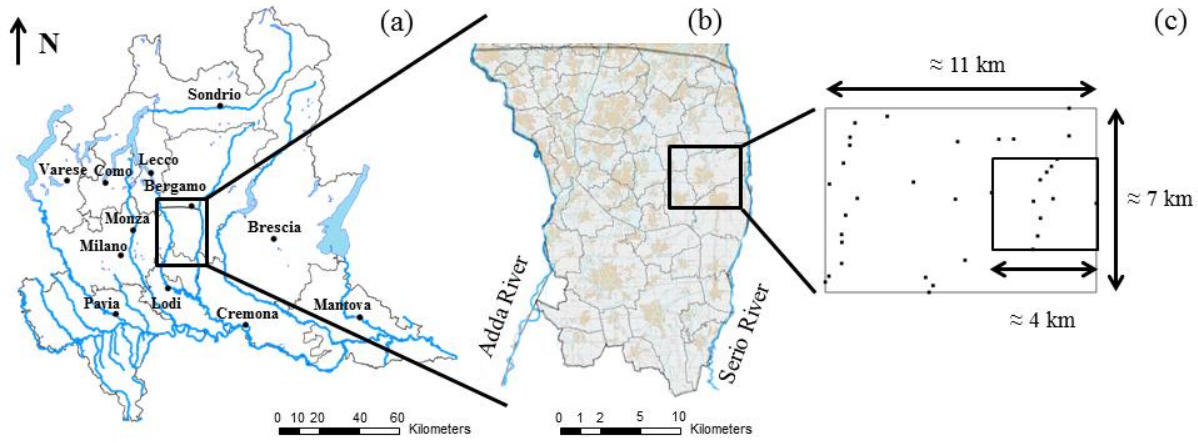

Figure 3.1.1.1: Sketch of the area from which sedimentological data are extracted including the location of (a) Regione Lombardia in Italy, (b) the large scale aquifer system studied by Bianchi Janetti et al. (2011) along with the sample area marked with a black rectangle, and (c) sub-domain where conditional lithofacies simulations are performed (delimited by a black rectangle) together with the local borehole network.

In this region was also identified a sample area. The location of it is shown schematically in **Figure 3.1.1.1**. The choice was made on the basis of considerable strategic importance of the area under consideration, due mainly to the following factors:

- Presence of numerous springs that feed a series of significant spring tails.
- Important interaction between surface water and groundwater. The contemporary analysis of the effect of major springs, a dense network of surface channels and pumping wells (which are used either for drinking water or irrigation purposes) requires modeling of a wide range of physical processes for describing the distribution of water flows in the area.

These elements make the problem interesting from a scientific point of view, because it requires the adoption of sophisticated modeling techniques. The problem is also relevant from an operational point of view, since the presence of interactions between different physical processes enhances the representativeness of the region to characterize the

phenomena that takes place in the whole range of fountains that develops in the West (eastern Pianura Padana).

3.1.2. Previous studies

Hydrogeological studies conducted by Maione et al. (1991) and Gandolfi et al. (2007) investigated, respectively, the portion of the province of Bergamo in the south of the Alps Orobie and the entire province of Cremona. These studies have provided an important source of data and a valuable source of prior knowledge of the area investigated.

The area surveyed by Maione et al. (1991) is located between the rivers Adda and Serio and bounded by the Alps and the northern outcrop line of fountains. The authors proposed a geological model which identifies two distinct aquifers: a shallow phreatic aquifer and a deep artesian aquifer, which flows beneath the surface without significant interaction with the former.

The model proposed by Gandolfi et al. (2007) which covers the entire province of Cremona, is bordered in the West by the river Adda, on the East by the Oglio river and in the South by the river Po. In the North, since there is a lack of natural water boundary that can be adopted as a closure model, was chosen the northern boundary along a line joining the rivers Adda and Oglio at a distance of several kilometers North of the administrative boundary of the province of Cremona. The conceptual model of the aquifer system shows a double system of groundwater flow with:

- A surface portion characterized generally by high transmissivity and large flow values supported by the surface trade with the hydrographical network. Recharge is due to infiltration from rainfall and water used for irrigation.

- A deeper portion characterized by a complex succession of geological bodies with different conductivities, which are essentially governed by the flow of water withdrawals for drinking water supply. Its flow values are well below the ones transiting the upper portion.

3.1.3. Hydrogeological structure

The available literature research and the collection of stratigraphic data were initially extended to the provinces of Bergamo and Cremona. At a later stage, attention was focused on the portion of land bounded by the paths of the rivers Adda and Serio.

The preliminary conceptual geological model of the area under investigation was constructed on the basis of the following information and documents:

- Maione et al. (1991): drawn from the study were 218 stratigraphic columns located in the provinces of Bergamo and Cremona and 15 reconstructed lithostratigraphic sections.
- Provincia di Cremona – Atlante Ambientale: in the study were used 464 stratigraphic columns located within the province of Cremona.
- Consorzio della Media Pianura Bergamasca (CMPB): we used 14 stratigraphic columns.
- Beretta et al. (1992): the study contains 29 reconstructed lithostratigraphic sections from the province of Cremona.

The analysis of the sections can schematically identify, within the territory examined, the presence of two overlapping aquifers within the Quaternary alluvial sequence of the Padano sedimentary basin filling. This fact allows considering two different aquifers.

Phreatic aquifer. It is located in the coarse clastic deposits ranging between the ground level and a clay level that is characterized by certain continuity at the investigation scale. The roof of the body with low hydraulic conductivity, named by Maione et al. (1991) "***A*** horizon", coincides with the clay level in the high plain which is present in the most superficial fluvio-glacial Valtellina complex (which separates the polygenic strain from the underlying calcareous strain). In the lowlands the delineation of the ***A*** horizon is more uncertain. In general it is represented by a clay layer being within the same alluvial deposit, following the criteria of Maione et al. (1991).

The superficial thickness consists of thick clastic continental deposits belonging to different sedimentary cycles that appertain to diverse geological periods. Nevertheless, they display a lateral continuity between them in terms of the hydraulic conductivity parameter. Within these, stand out the following:

- Polygenic conglomerate (fluvio-glacial Mindel) in the high plains.
- Fluvio-glacial gravels and sands (RISS-Wurm) that form the lowlands and the filling of the erosion furrows in the polygenic conglomerate.
- Recent alluvial gravels and sands deposited by rivers that cross the plain.

In the northern line of Canonica d'Adda - Ghisalba prevail the conglomeratic deposits, while in the southern portion dominate loose gravel and sand deposits. Within the aquifer thickness are intercalated layers of clay with variable planar/lateral continuity. Due to this fact, the aquifer may shift from ground conditions to local conditions of semi-confinement. The thickness of this aquifer ranges from 40 m to 80 m, along the main anisotropic direction of the system (North-South).

Confined aquifer. Below the level of clay which forms the basis of the aquifer water table surface, there is a succession formed by alternating coarse clastic sediments and clays whose degree of continuity and relative thickness of the deposits (displaying different grain size) is very variable. Inside the porous and/or fractured layers, confined by other layers of fine-grained sediments, artesian aquifers are based. The base of the sequence described, called "***B*** horizon" by Maione et al. (1991), consists of clay minerals with occasional inter-bedded (predominantly sandy) lithotypes.

The reconstructed sections show that the geological system has artesian aquifers of variable thickness depending on the geometry of the substrate. It is a range characterized by a significant thickness (170 m to 200 m) controlled by the alignment Osio Sopra-Osio Sotto, Levate-Verdellino, Comun Nuovo-Urgnano and in the area of Cologno al Serio. This thickening represents the filling of a morphological-tectonic graben. Going southwards of the identified structural sections, aligned with the SW-NE direction in accordance with the alignment Ghisalba-Treviglio, the complex artesian aquifer tends to decrease significantly (up to 30 - 40 m) with an increase in percentage of the clay-rich levels over the porous ones.

In the plain portion of the territory under study, the information that can be derived from stratigraphic data allows to outline the characteristics of the subsurface by means of the following lithostratigraphic units:

- Predominant gravel-sandy deposits whose continuity is interrupted by locally inter-bedded silt-clay lithotypes.
- Alternation of gravelly-sandy and silt-clay lithotypes.
- Predominant silty-clay deposits with occasional sand.
- Mainly fine deposits, sometimes of the silty-sandy type.

3.1.4. Wells / piezometers

Information concerning the presence of wells/piezometers comes from the following sources:

- Regione Lombardia: Programma di Tutela e Uso delle Acque – PTUA.
- Agenzia Regionale per la Protezione dell'Ambiente Lombardia - ARPA Lombardia.
- Consorzio di Bonifica della Media Pianura Bergamasca – CMPB.

Piezometric monitoring of the aquifer system in the region under consideration, can be done using information from a set of 761 observation wells. It is worthy to point out that a number of wells outside the large-scale model area were taken into account. This choice aims at achieving greater consistency in order to track the reference piezometric maps, particularly on the rivers which shape the limits of the superficial area influenced by the groundwater flow model.

Information on the measurements of the land surface at the individual wells is associated by means of using heterogeneous techniques. Among them, are included:

- GPS measurements.
- Interpolation from the base of the Regional Technical Cartography.
- Topographic lines.

Unfortunately, it was not possible to trace the detailed description of the origin of these values for each well. A first empirical test of the reliability of the allowances provided, was determined by estimating the values of the land surface at the wells of interest from the Digital Elevation Model DTM40.

The reliability of the data reported is of fundamental importance for a proper definition of the piezometric level in the region. In fact, the measure monitored at all points of observation is not the piezometric level, but rather the depth to the water table with respect to the ground level. The piezometric level has been rebuilt, for each well/piezometer, as the difference between the values of water table depth and the land surface.

The water table depth data from ARPA, registered monthly or bimonthly, covers a time span between 1999 and 2006, while the database provided by the CMPB covers a longer period which goes from 1989 to 2007. The measurement campaigns conducted by CMPB are carried monthly or every two months. The water table depth data recorded by the Politecnico di Milano (and reported within the PTUA) refers to three different surveys conducted in April 1994, November 1996 and March 2003.

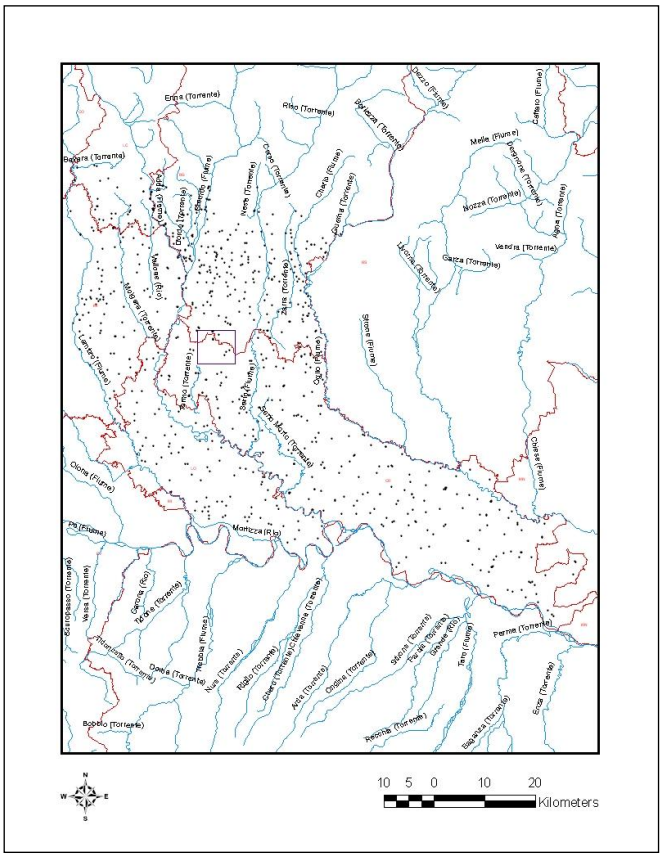

Figure 3.1.4.1: Location of the wells in which the piezometric level is currently monitored (Guadagnini, L. et al., 2008).

3.1.5. Springs

The intricate drainage network that characterizes the study area is largely fed by a great number of springs, typical hydrogeological items of the northern side of the Pianura Padana. Within the area delimited by the large-scale model there are a total of 161 spring heads (depicted in **Figure 3.1.5.1**). The location of the aforementioned springs is derived from the following sources:

- Protection Program and Water Uses, Lombardia region (2006).
- www.atlanteambientale.it, province of Cremona.

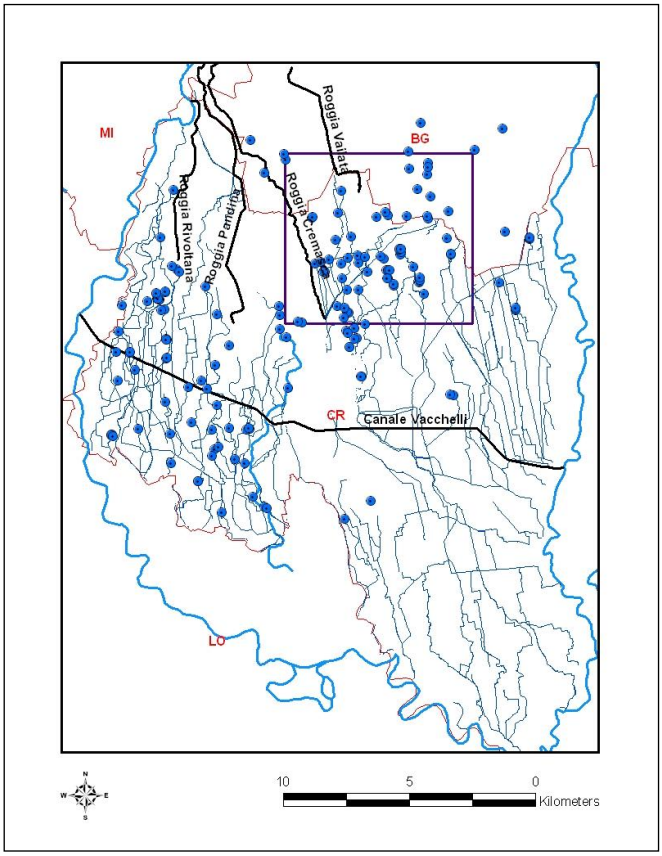

Figure 3.1.5.1: Location of the spring heads (Guadagnini, L. et al., 2008).

The typical morphology of these hydrogeological structures is depicted in the following images (**Figure 3.1.5.2**).

While the two top pictures represent the typical planar section (top left) and vertical cross-section (top right) of a spring, the bottom diagram illustrates the Pianura Padana system from the highest area located in the North (Alps) to its distal zones. It can be noted here that, as it is observable through our borehole database, exists a transition from coarser materials in the northern boundary towards finer materials (when we approach the distal parts of the alluvial system).

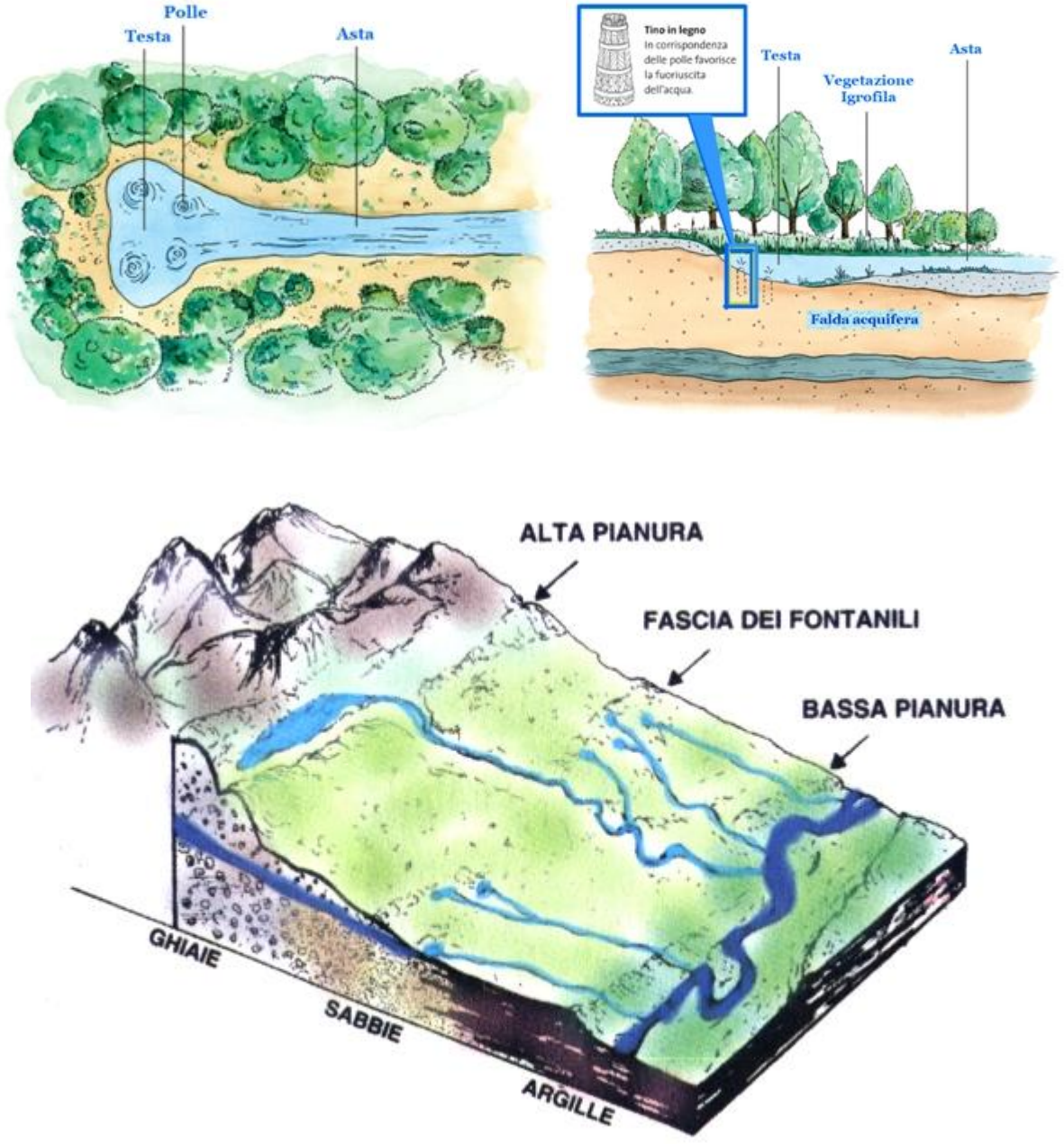

Figure 3.1.5.2 : Source: http://www.comune.capralba.gov.it/parco/territorio/fascia/index.aspx#/-1/, http://www.cooperativadelsole.it/?p=446.

3.2. Reference information database

Implementing a flow model within a real aquifer system requires the structuring of an information database that should contain a complete set of data necessary to understand, with the greatest degree of detail possible, the geological architecture of the porous medium and the hydrological processes that govern the flow field in the area under study. This database should be structured in an organic and functional way, to:

- Allow rapid access to the information of interest.
- Ensure the ability to update quickly and effectively the data collection.
- Guarantee the ability to interact with the mathematically formulated model.

A rough outline that could describe how the reference information database was implemented can be divided into the following stages:

- Collection of raw data from the different agencies responsible for monitoring the quantities of interest.
- Data selection for the region studied.
- Analysis and processing of data in order to evaluate its significance at different temporal and spatial scales.
- Structuring the reference information base.

In **Table 3.2.1** we present an extract of the already re-worked lithological database. The information contained in the table below is compartmented in columns displaying, amongst other fields: the well code (corresponding to the original database and map vertical cross-sections); the three-dimensional UTM coordinates; identified strata thickness; its relative depth expressed in *m.a.s.l* (meters above sea level); the detailed lithological description and its indicator category.

Codice	X (m)	Y (m)	Z (m)	Quota (m.s.l.m)	Livello stratigrafico	Spessore (m)	Profondita (m)	Descrizione Dettagliata	L1	L2	L3	Categoria
min	**1534718.60**	**5036420.00**	**105.00**	**-123.69**	---	**0.30**	**0.50**	---	---	---	---	---
max	**1557725.54**	**5064758.56**	**270.00**	**270.00**	---	**145.51**	**305.22**	---	---	---	---	---
37	1539941.32	5054573.75	222.00	222.00	1	2.7	2.7	Argilla e Limo	A	L	---	1
37	1539941.32	5054573.75	222.00	191.50	2	30.5	33.2	Ghiaia	G	---	---	3
37	1539941.32	5054573.75	222.00	159.30	3	32.2	65.4	Conglomerato (Ghiaia Cementata)	C	---	---	4
37	1539941.32	5054573.75	222.00	157.70	4	1.6	67	Ghiaia	G	---	---	3
37	1539941.32	5054573.75	222.00	152.20	5	5.5	72.5	Conglomerato (Ghiaia Cementata)	c fess.	---	---	5
37	1539941.32	5054573.75	222.00	150.90	6	1.3	73.8	Argilla e Limo	A	L	---	1
37	1539941.32	5054573.75	222.00	145.90	7	5	78.8	Conglomerato (Ghiaia Cementata)	C	---	---	4
37	1539941.32	5054573.75	222.00	144.40	8	1.5	80.3	Argilla e Limo	A	L	---	1
37	1539941.32	5054573.75	222.00	137.40	9	7	87.3	Conglomerato (Ghiaia Cementata)	C	---	---	4
37	1539941.32	5054573.75	222.00	132.90	10	4.5	91.8	Ghiaia	G	---	---	3
37	1539941.32	5054573.75	222.00	125.30	11	7.6	99.4	Conglomerato (Ghiaia Cementata)	c fess.	---	---	5
37	1539941.32	5054573.75	222.00	121.00	12	4.3	103.7	Argilla e Limo	A	L	---	1
37	1539941.32	5054573.75	222.00	118.90	13	2.1	105.8	Ghiaia	G	---	---	3
37	1539941.32	5054573.75	222.00	113.90	14	5	110.8	Argilla e Limo	A	L	---	1

Table 3.2.1: This database sample displays the rich geological data record build up aiming to obtain the necessary hard data for our simulation phase process, i.e. the variogram analysis and the a posteriori geostatistical (conditional) simulations.

The total drilled depth information used in the area under study is slightly over 13.5 km (data belongs to the CMPB). For our purpose of quantifying the existing volumetric proportions of the five re-classified lithotypes, and therefore finding a hint to establish the final indicator values, we used the information coming from a bulk set of 144 wells. We chose to keep constant the indicator volumetric proportions across the three-dimensional space. We know that it is not a 100% realistic assumption but it helps to keep simpler, yet valid, the problem under analysis.

We did carry a statistical analysis over some key features including the ones presented in **Table 3.2.2**, in order to bring light to the modeling problem and be able to find proper constraints for solving the geostatistical and the flow field simulations. For instance, knowing the minimum well depth, its maximum and the mean, allowed us to set the boundaries in the vertical direction for our numerical domain. We used, for our numerical simulations, the vertical geological cross-sections along the N-S direction (namely S3, S4 and S5) as detailed in the study from Guadagnini, L. et al. (2008). Along the W-E direction we used the S10 and S11. The total borehole depth used as conditioning data adds up to almost 3.6 km, i.e. a whole set of 35 wells. The minimum thickness recorded in the borehole dataset is 0.5 meters. We did use this information to further discretize our remaining hard data.

Well depth [m]	F1 vol. (%)	F2 vol. (%)	F3 vol. (%)	F4 vol. (%)	F5 vol. (%)	TOTAL (%)
3557.30	43.62	1.75	22.31	21.23	11.08	100.00

	F1	F2	F3	F4	F5
min thickness [m]	0.50	1.53	0.50	0.50	1.00
MAX thickness [m]	59.03	19.98	39.11	46.77	128.83

Table 3.2.2: The top table displays the total drilled depth used to condition the numerical simulations and estimate the volumetric facies proportions (kept constant across the full domain). The bottom table shows the minimum and maximum thicknesses for every hydrofacies expressed in meters [m].

LEGEND	
A+G	argilla + ghiaia
A+L	argilla + limo
A+F	argilla + fossili
Asup.	argilla superficiale
A+Lt	argilla + limo + turba
C	Conglomerate
Cf	Conglomerate fessurato
G	ghiaia
G+A	ghiaia + argilla
S	sabbia
Sc	sabbia cementata
AR	arenaria
T	terreno

TOTAL						
F1-F1	**F1-F2**	**F1-F3**	**F1-F4**	**F1-F5**		**Transitions**
10.53	1.97	22.37	26.10	11.62		456.00
F2-F2	**F2-F3**	**F2-F4**	**F2-F5**			**Check (%)**
0.00	1.10	0.66	0.00			100.00
F3-F3	**F3-F4**	**F3-F5**				
1.32	14.91	3.51				
F4-F4	**F4-F5**					
2.19	3.51					
F5-F5						
0.22						

F1	**A+G, G+A, A+L, A+F, A+Lt, Asup, T**
F2	**S**
F3	**G**
F4	**C, AR, Sc**
F5	**Cf**

Table 3.2.3: The top left table represent the main lithotype classes found in the sample area under study, while the bottom left table displays the re-categorized hydrofacies and the original categories that were included in each one. The top right table is presented to show a key finding that helped to establish the lithotype rule for the Truncated Plurigaussian simulations. There we illustrate (in percentage values) the existing 456 transitions between the different geomaterials. This has nothing to do with probability transitions. We wanted to investigate qualitatively and quantify the amount of times a facies appears next to the other remaining facies.

3.3. Regional vulnerabilities

In the Cremona region the pollutants are not only the most worrying issue. Thanks to the springs' existence, a rich environment is developed on the ground surface. All the activities that take place surrounding the springs' area commit an overexploitation of the aquifers in the zone under study. We refer mainly to agricultural practices, water pumping for drinking purposes and industrial use, etc. Those actions produce non-equilibrium in the system, provoking the decrease in the water level in the springs and their influence zone.

3.4. Final remark

We would like to point out some choices that we made at this stage and that affect the latter steps of our research.

The restructured geological database containing the borehole information from different sources allowed us to estimate the volumetric proportions of the final five regrouped hydrofacies. Not only that, we could infer the crucial lithotype rule needed to run the Truncated Plurigaussian simulations scheme. In addition, we determined (after consulting surface lithological maps corresponding to the area under study) the main anisotropy directions (along the N-S, W-E and vertical) and characteristic lengths of the geological structures. As in the vast majority of studies of this kind, our available vertical hard data resolution is much higher than its horizontal counterpart.

We decided to reduce the complex heterogeneity embedded in our natural groundwater system by means of reclassifying the existent lithotypes into five hydrogeologically meaningful hydrofacies. We chose to keep the problem simple by setting stationary hydraulic conductivity values in the aforementioned indicator lithotypes.

4. Methodology

In the following we focus on the workflow we employed to pursue the goals stated in the introduction of this dissertation.

4.1. Modifying the geological database

We introduced the actual geological database in Chapter 3, in order to show where the conditioning data for our geostatistical simulations comes from. As previously stated we got a few tenths of borehole records that gave us a hint of the inherent highly heterogeneous nature of the geological materials found in the area under study. To be able to tackle this extra (natural) complexity in an efficient computational way, and in order to get results in a limited amount of time, we decided to re-categorize the existent geological database. We proceeded as follows:

LEGEND	
A+G	argilla + ghiaia
A+L	argilla + limo
A+F	argilla + fossili
Asup.	argilla superficiale
A+Lt	argilla + limo + turba
C	conglomerato
Cf	conglomerato fessurato
G	ghiaia
G+A	ghiaia + argilla
S	sabbia
Sc	sabbia cementata
AR	arenaria
T	terreno

F1	**A+G, G+A, A+L, A+F, A+Lt, Asup, T**
F2	**S**
F3	**G**
F4	**C, AR, Sc**
F5	**Cf**

Table 4.1.1: Original lithotypes found in the area under study (left) and the re-classified categories (right).

Therefore, by reducing the original lithological classes resulting from previous surveys, we simplified the original problem and improved its computational tractability (in terms of computing effort and time). The new categories or indicators were described as:

- F1: fine materials.
- F2: sands.
- F3: gravels.
- F4: conglomerates.
- F5: fractured conglomerates.

As a way of computing the final volumetric proportions for each indicator, to be used as an input in the geostatistical simulations, we took the newly reclassified values for the different vertical (N-S and W-E) cross-sections and computed the corresponding percentages. The results were the following:

Well depth [m]	F1 [%]	F2 [%]	F3 [%]	F4 [%]	F5 [%]	TOTAL [%]
3557.30	43.62	1.75	22.31	21.23	11.08	100.00

Table 4.1.2: Total borehole depth and estimated volumetric proportions from hard data source.

Initially we were tempted to remove the geomaterial indicator F2 (corresponding to the sandy materials found in the system) due to its low contribution to the final volumetric proportions percentage. Finally we decided to keep it as it was and analyze the impact on the final geostatistical simulations. By keeping the hydrofacies class F2 not only we preserved in a better way the original heterogeneity inherent to the double aquifer groundwater system, but we were able to study the impact on the flow field simulations of a less representative facies. This was possible because we decided to embed into every geomaterial category a steady value of the hydraulic conductivity (***K***) for each indicator class, i.e. a constant (in time) value of ***K***.

We do contemplate the possibility of carrying on with the idea of suppressing the F2 hydrofacies in future studies, derived from the current research project.

4.2. Recalling geostatistical concepts

There exist various basic manuals about Geostatistics either for beginners and practitioners in industry not familiar with the field (Clark, 1979), being mainly focused on the mining industry. Kitanidis (1997) presents an introduction to Geostatistics along with some applications in hydrogeology. "An introduction to applied Geostatistics" is probably the most complete of those references (Isaaks and Srivastava, 1990).

Here we are not interested in delivering a complete geostatistical introduction, since they already exist, but we would rather make explicit which concepts derived/coming from Geostatistics we used for our research work. We used the term Geostatistics in the European sense of the "Theory of the Regionalized Variables" developed by G. Matheron and co-workers at Fontainebleau (1970's). We made use of the simplest function that characterizes any geostatistical study: the semivariogram. The definition of a semivariogram (γ) arises out of the notion of continuity and relationship due to position. It is a graph (and/or formula) describing the expected difference in value between pairs of samples (bearing a target property of interest) with a given relative orientation. In the following we present its mathematical expression:

$$\gamma = \frac{1}{2n}\sum[g(x) - g(x+h)]^2$$

Where ***n*** are the sample pairs, ***g*** are the functions (properties under study) and ***h*** is the fixed distance between the sampled positions. In our study we mostly dealt with vertical and horizontal (omni-directional) indicator semivariograms computed from the available conditioning indicator data.

4.3. Indicator variogram calculation

Before going through calculating the indicator variograms, we did need to generate further conditioning data by refining (along the vertical direction) the available indicator values. The information contained in the geological database spreadsheet, as usual in borehole/core interpretation, made explicit where the appearance of a given lithotype started/ended. We performed that a priori step in seeking an improvement of the subsequent semivariogram analysis by introducing further more points in the variogram estimation. In order to achieve this, we used an existing in-house built FORTRAN routine (named STRAT). The aforementioned routine performed a data refinement along the vertical by, namely, replicating the available data points every 0.5 meters (when necessary). That generated quite a decent amount of conditioning data, sufficient to accept as valid the posterior results. In any case it is worthy to note that as in almost geostatistical study, the information/resolution obtained along the vertical direction was much higher than that along the horizontal plane. This fact will inevitably condition our results but it is unavoidable from a technical point of view, since it depends on the available data that we have used from previous field studies/surveys. This is a common drawback faced by practitioners of all kind, but does not invalidate the results obtained as long as it is recognized and accepted as a limitation of the approach. In fact, this might lead to inaccurate results, introducing further uncertainty on the final outcome.

For the statistical analysis that we wanted to carry out we needed to compute the vertical and horizontal indicator semivariograms. That was made with the purpose of estimating the ranges (and correlation lengths) of the hydrofacies semivariogram functions. The resulting variogram ranges estimated at this step will act as input information for the geostatistical simulations along with the volumetric proportions estimated previously. We

departed from our modified (extended) indicator conditioning dataset. We did use the available computational tools provided for this purpose by the GSLIB manual (program ***gamv***, Deutsch and Journel, 1997). We did perform various types of variogram estimations (mainly omni-directional and along the main anisotropy directions). Those calculations were supported by the available geological information coming from previous studies and superficial lithological maps. We found and determined that the main anisotropy directions were along the N-S, W-E and the vertical direction. Finally we only considered, for posterior fitting with an exponential variogram model, horizontal omni-directional and vertical variograms.

An exponential semivariogram model was chosen (after performing a RSME analysis) for fitting the directional semivariograms. For the purpose of this rather simple data treatment (even though the dataset was pretty vast) and its statistical analysis, we employed common available software packages (such as text and spreadsheet editors).

4.4. SISIM vs TPS (and the geostatistical simulations)

Among the vast range of FRM methods, following the classification in Falivene et al. (2007), we decided to employ 2 different well-known and widely-spread geostatistical indicator pixel-based methods. Those allowed us to compare the effect of the embedded geological heterogeneity in the simulations and the posterior effect on the hydraulic head ***pdfs***, after solving the flow field problem in a multi-realization context. Pixel-based methods work assigning a facies to grid cells according to the facies occurrence ***pdf***, which is computed for each grid cell. These methods allow direct conditioning by hard and/or soft data. Categorical or indicator methods are based on transforming each facies category to a new property, defined as the occurrence probability of the facies, and building the ***pdf*** at each

grid cell as the combination of the reconstruction or modeling of these new properties (e.g. Journel and Alabert, 1989).

A number $\boldsymbol{N}$ = 1000 of three-dimensional realizations of hydrofacies distributions were generated with TPS and SISIM schemes. Indicator-based conditional simulations are performed via the software SISIM (Deutsch and Journel, 1997). TPS simulations are based on the algorithms and codes presented by Xu et al. (2006) and Emery (2007). This number has been found sufficient to support the validity/correctness of our analyses/work (results regarding this can be found in Chapter 5). For the purpose of our analysis and for reason related to computational costs, the numerical simulations are performed within a model domain whose extent corresponds to the sub-domain identified in **Figure 3.1.1.1**. The estimated computational effort, in terms of time has been approximately 2 weeks.

At this point we would like to emphasize that we carried out our simulations at a field scale, since the available borehole database allowed for this kind of analysis. The lithological and geological information available in this region were employed as conditioning data for our aquifer system model. The Cartesian grid adopted for the hydrofacies simulations comprises 74 × 86 elements, respectively along the N–S (y) and W–E (x) directions. The grid spacing is set to $\Delta x = \Delta y = 50$ m, resulting in a simulation domain with a planar extent of 3700 × 4300 m^2. Since one of the objectives of this study is to analyze the way the vertical variability of hydraulic heads is impacted by facies distribution, boundary conditions and/or source terms without considering the effect of the particular geometry of the bottom of the aquifer, we adopt in the following a constant thickness B = 100 m which is representative of an average width of the system in the area. We discretize B into 50 layers of uniform thickness Δz = 2 m for the purpose of our computations. Therefore the total amount of nodes was 74 × 86 × 51, adding up to a total of 324,564 cells.

We decided to use SISIM (in its SGeMS implemented version) in first instance since it is a common geostatistical tool among practitioners and academics, due to its:

- Reliability and robustness.
- Easy implementation.
- Low computing requirements in terms of time and equipment.

We did use 5 categories with its computed volumetric proportions obtained from the available conditioning hard data (see point 4.1 for further details). We opted for using a ***Full IK*** option since we had information and estimated indicator variograms for every single facies (horizontal omni-directional and vertical). Details of the estimated empirical semivariograms can be found in Chapter 5.

We then chose to use the TPS approach. As stated previously, this is an extended version of the Truncated Gaussian method. The main difference with respect to SISIM lies in the lithotype rule. By means of this tool we are given the chance of including further geological information from our area under study, constraining which contacts are allowed between the different hydrofacies. This restriction implies a higher degree of realism at the geostatistical simulation stage. We did use the borehole database as conditioning data for both SISIM and TPS. In addition we used surface lithological maps to work out the main anisotropy directions. We found that the system was developed following the actual rivers course, along the N-S direction. We identified elongated geological bodies along that direction, and spreading along the W-E. The third main direction is set along the vertical direction. We took characteristic measures of those outcropping geological units along with information coming from previous surveys carried out in that specific area. Last but not least, we performed a counting check in percentage of contacts among the different identified

hydrofacies. This gave us an expected hint about the actual system that we kept and accounted for during the simulations stage: the fine materials were spread everywhere and were in contact with all the geomaterials. On the other hand, the coarser hydrofacies were in touch one to another following a grain size hierarchical relationship, i.e. sands in touch with gravels, gravels with conglomerates and conglomerates with fractured conglomerates. Details on the resulting lithotype rule can be found in Chapter 5.

In the following, we describe the procedure used to perform the TPS simulations. We did use the online available MATLAB routines enclosed in Emery (2007).

We initially worked out the thresholds for the 2 underlying Gaussian random fields, linked to the lithotype rule. Then we used another MATLAB routine to calculate the indicator simple and cross-variograms associated with the proposed truncation rule, the estimated volumetric facies proportions and the Gaussian variograms. The calculation is based on expansions of the indicator function into Hermite polynomials (see Emery, 2007; Eqs. (3) – (7)). A graphical comparison between the resulting indicator variograms and the empirical ones (derived from the available hard data) allowed us determining the variogram models of the Gaussian random fields.

We employed two different methodologies that will allow us to fully compare (since both methodologies are variogram-based) the impact on the actual flow field simulations influenced by the way that the heterogeneity of the real aquifer system has been embedded in each of them. In the SISIM case due to the variographic analysis only, and in the TPS-based simulations by means of the variogram analysis and the lithotype rule.

4.5. Flow field simulations using VMOD

The numerical solution of the grid associated with flow (and eventually transport) can and in some cases should be finer than the one adopted for the generation of the hydrofacies. In particular, accurate numerical solution of flow requires a fine grid close to source/sink terms such as wells.

We did use the output hydrofacies indicator realizations from both geostatistical simulation methods as a base grid to perform the flow field simulations. We decided at this stage to refine the actual grid in the planar direction. As a result the new lateral cell extent was set to $\Delta x' = \Delta y' = 25$ m. The discretization in the vertical direction was kept as it was with $\Delta z' = \Delta z = 2$ m. Finally, the total amount of nodes in the grid is 1,298,256.

This is not associated with downscaling. We generated values of a property that are representative of a given volume (or block) and, as such, are constant within the volume itself, even if this volume (cell) is subdivided for an accurate solution of the flow problem. The assignment of the data (which in our case is just hydrofacies category) to the finer grid employed for flow, has been accomplished by subdividing into 4 columns that replicate the original data. A similar strategy for the setting of the numerical grid associated with the flow problem has been adopted in previous works (e.g., Riva et al., 2006, 2008, 2010).

This straightforward way of extrapolating data into the refined grid is shown in **Figure 4.5.1**. We used the new grid to populate the various indicator categories with constant hydraulic conductivity values. We took this option in order to simplify the numerical modeling process. We did not have availability of hard hydraulic conductivity data with a level of discretization which was nearly comparable with that of the lithological information we employed in the simulations. There is typically conceptual uncertainty associated with the

selection of a model which can represent the heterogeneity of an aquifer at different scales of observation. Here, we are interested in an observation window which encompasses horizontal and vertical scale lengths of the order of 4000 m and 100 m, respectively. At these scales the distribution of lithotypes in the system is a key driver for the distribution of groundwater flow quantities. On the other hand, the spatial heterogeneity of hydraulic parameters within a given lithotype is relevant at smaller scales of observations as seen, for example, in the works of Winter et al. (2003), and Riva et al. (2006, 2008, 2010). Treating both sources of uncertainty (i.e., uncertainty in the location of the boundaries between different materials and in the distribution of attributes within each material) can be performed, e.g., in a composite medium framework, along the lines of the references cited above. Here, we are indeed adopting a composite medium approach where facies distribution is uncertain and hydraulic attributes are deterministically known.

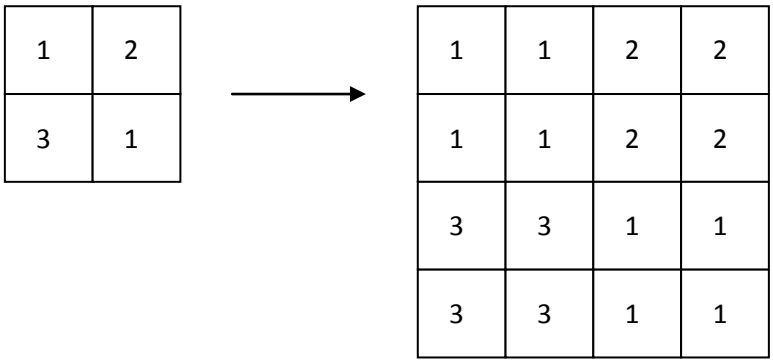

Figure 4.5.1: Extrapolation model for the flow field simulations.

Firstly we created the basic numerical scenario in Visual MODFLOW (VMOD; McDonald and Harbaugh, 1988). We generated the new (refined) numerical grid and loaded it into VMOD with its stationary and isotropic hydraulic conductivity "***K***" (see **Table 4.5.1**) field values for each hydrofacies category. We then included a sink term and located it approximately in the middle of the domain, i.e. a fully penetrating pumping well acting at

-3,000 m^3/day. This can be seen as a simplification of the real problem in which one or various pumping wells (water abstractions) exist and work close to each other. The pumping rate was distributed along the vertical direction among the different cut materials. That was possible by means of an in-house FORTRAN routine that worked editing the pumping well input file for VMOD, distributing the total pumping rate among the different materials and proportionally to the ***K*** value of each intersected geomaterial class. Therefore, higher pumping rates were acting over the most conductive materials. That helped in avoiding high gradients in the numerical model that may end up leading to numerical problems/instabilities in the final solution. We performed steady state simulations.

We then used as constant head boundary conditions in the northern and southern edges, mean values of real hydraulic head recordings in the area under study, i.e. a fix value of 172.5 meters and a fix value of 145 meters respectively. On the western and eastern edges in addition to the bottom of the model, we set no-flow boundaries. Results of the flow field simulations for both SISIM and TPS methods are enclosed in Chapter 5.

Class	K [m/d]
F1	1.120e-007
F2	1.790e-005
F3	7.160e-004
F4	9.090e-005
F5	6.050e-003

Table 4.5.1: K values for the flow simulations, based on the values used by Bianchi Janetti et al. 2011.

4.6. Workflow for treating the output from the multi-realization scheme

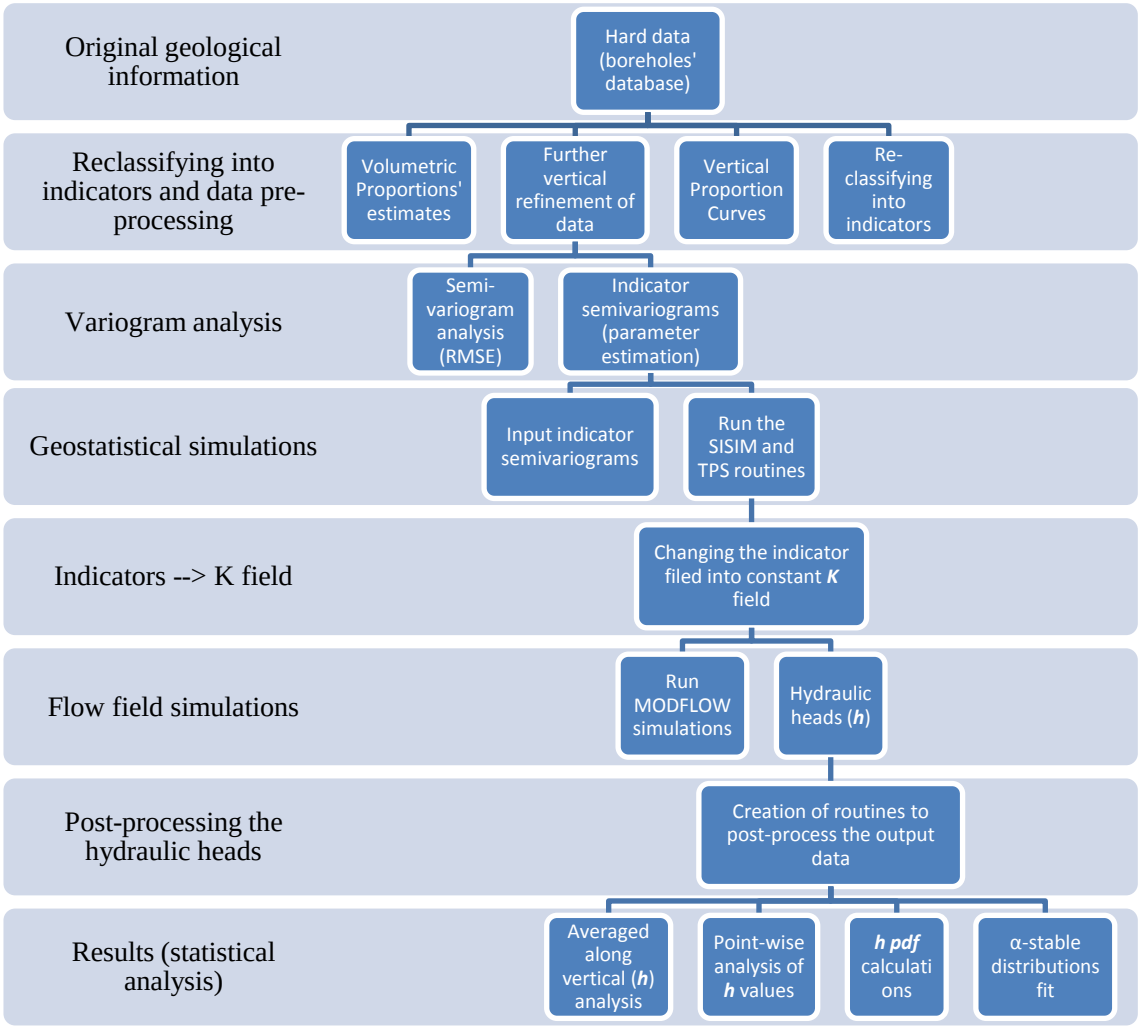

5. Aquifer system simulations

In this section we deal with the details of the subchapters that we covered in the methodology or Chapter 4.

5.1. Modifying the geological database

Initially we performed some statistical analyses regarding the frequency of appearance of a given lithotype, or the expected amount of lithotypes found in each well, for the different geological vertical cross-sections studied in the area of interest. In the following Table (**5.1.1**) we gathered the amount of lithotypes found in each well, classified per geological vertical cross-sections (along the N-S and the W-E directions).

	Well	Lithotypes (nº)	A+G	A+L	C	Cf	G	G+A	Sc	S	AR	T	A+F
S3	**348**	5	0.05	0.35	0.20	0.20	0.20	---	---	---	---	---	---
	349	6	0.05	0.30	0.20	0.05	0.30	---	0.10	---	---	---	---
	350	5	0.10	0.30	0.05	0.25	0.30	---	---	---	---	---	---
	111	7	0.14	0.36	0.07	0.07	0.21	0.07	---	0.07	---	---	---
	7	5	0.09	0.41	0.14	---	0.23	0.14	---	---	---	---	---
	6	4	---	0.40	0.10	---	0.40	---	---	---	0.10	---	---
	8	4	0.10	0.40	---	---	0.40	---	0.10	---	---	---	---
	331	4	---	0.33	---	---	0.33	0.17	---	---	---	0.17	---
	332	3	---	0.25	0.25	0.50	---	---	---	---	---	---	---
	328	5	---	0.29	0.14	---	0.29	0.14	---	---	---	---	0.14
	333	4	---	0.25	0.25	---	0.25	---	---	---	0.25	---	---

	Well	Lithotypes (nº)	A+G	A+L	C	Cf	G	G+A	Sc	S	AR	T	Asup.
S4	**340**	6	---	0.23	0.29	0.13	0.29	---	0.03	---	0.03	---	---
	304	5	---	0.20	0.40	---	0.10	0.20	---	0.10	---	---	---
	54	3	---	0.40	0.20	---	0.40	---	---	---	---	---	---
	50	3	0.33	0.33	0.33	---	---	---	---	---	---	---	---
	51	6	---	0.18	0.18	---	0.35	---	0.06	0.18	---	---	0.06
	52	6	0.11	0.11	0.22	---	0.22	0.22	---	---	---	0.11	---

	Well	Lithotypes (nº)	A+G	A+L	C	Cf	G	G+A	Sc	S	AR	T	A+F
S5	**341**	5	---	0.28	0.17	0.22	0.31	0.03	---	---	---	---	---
	342	5	---	0.30	0.20	0.20	0.20	0.10	---	---	---	---	---
	124	2	---	0.33	---	---	0.67	---	---	---	---	---	---
	123	4	---	0.25	---	---	0.25	0.25	---	---	0.25	---	---
	117	7	0.06	0.25	0.25	0.13	0.19	0.06	0.06	---	---	---	---
	118	7	0.03	0.43	0.20	0.11	0.09	0.06	0.09	---	---	---	---
	129	3	---	0.40	0.40	---	0.20	---	---	---	---	---	---
	120	4	0.09	0.36	0.18	---	0.36	---	---	---	---	---	---
	125	2	0.50	---	---	---	0.50	---	---	---	---	---	---
	121	5	---	0.27	0.27	---	0.18	0.18	0.09	---	---	---	---

	Well	Lithotypes (nº)	A+G	A+L	C	Cf	G	G+A	Sc	S	AR	T	A+F
S10	**354**	5	---	0.33	0.26	0.11	0.26	---	0.04	---	---	---	---
	307	3	0.27	0.27	0.45	---	---	---	---	---	---	---	---
	344	4	---	0.17	0.25	0.17	0.42	---	---	---	---	---	---

	Well	Lithotypes (nº)	A+G	A+L	C	Cf	G	G+A	Sc	S	AR	T	A+Lt
S11	**110**	7	0.11	0.32	0.25	0.07	0.18	0.04	---	---	---	---	0.04
	257	5	0.08	0.33	0.33	0.17	0.08	---	---	---	---	---	---
	303	6	---	0.30	0.20	---	0.20	---	---	0.10	---	0.10	0.10
	122	7	---	0.29	0.14	0.21	0.14	0.07	---	---	---	0.07	0.07
	119	4	0.25	0.25	0.25	---	0.25	---	---	---	---	---	---

Table 5.1.1: In the tables overlying this caption we present the 5 geological cross-sections considered in our study, as well as the boreholes located on those sections (that were included in the area under study), the lithotype counter for each well and the percentage of each original geomaterial.

As stated previously, we performed an indicator recategorization in order to simplify the real highly heterogeneous geology inherent to the double aquifer system under study. The underlying Table (**5.1.2**) contains a sample of the procedure followed in order to achieve that objective.

Well	Re-classified categories	Depth [m] at 167 (m.a.s.l.)	L1	L2	Indicators
349	Argilla e Limo	4.97	A	L	**1**
349	Argilla con Ghiaia	9.54	A	G	**1**
349	Ghiaia	11.68	G	---	**3**
349	Sabbia Cementata	14.96	S	---	**4**
349	Conglomerato (Ghiaia Cementata)	23.56	C	---	**4**
349	Ghiaia	25.12	G	---	**3**
349	Argilla e Limo	27.17	A	L	**1**
349	Sabbia Cementata	31.16	S	---	**4**
349	Conglomerato (Ghiaia Cementata)	36.92	C	---	**4**
349	Argilla e Limo	44.05	A	L	**1**
349	Ghiaia	49.27	G	---	**3**
349	Argilla e Limo	51.70	A	L	**1**
349	Ghiaia	58.69	G	---	**3**
349	Argilla e Limo	62.35	A	L	**1**
349	Conglomerato (Ghiaia Cementata)	65.11	C	---	**4**
349	Ghiaia	66.25	G	---	**3**
349	Conglomerato (Ghiaia Cementata)	67.34	c fess.	---	**5**
349	Ghiaia	72.75	G	---	**3**
349	Argilla e Limo	76.70	A	L	**1**
349	Conglomerato (Ghiaia Cementata)	81.04	C	---	**4**

Table 5.1.2: We did use the conversion established in Table 4.1.1, to obtain the final indicator values (last column on the right). Here we also show the main lithologies identified at different depths, from a reference topographic height of 167 meters above sea level (m.a.s.l.).

5.2. Variogram analysis and indicator variogram model fitting results

A detailed geospatial analysis of the indicator-based variables is performed and three principal anisotropy directions are identified (North-South, N-S; West-East, W-E; and vertical). This finding is consistent with field observations and lithological interpretations for the area where, e.g. the river network (and therefore the depositional trends) is aligned along the N-S direction. **Table 5.2.1** summarizes the parameters of the exponential indicator variograms which are estimated on the basis of their empirical counterparts and are adopted for the SISIM simulations. The selection of the exponential model has been based on the least square criterion and standard analysis of cross-validation errors (details not reported).

Lithology class	Sill	Ranges [m] – SISIM (N-S / W-E / Vertical)
F1	0.246	1830 / 1280 / 37
F2	0.017	700 / 470 / 20
F3	0.173	1240 / 910 / 34
F4	0.167	860 / 670 / 20
F5	0.098	1220 / 900 / 36

Table 5.2.1: Indicator variogram model parameters estimated for the five hydrofacies and for the SISIM technique. A zero nugget is estimated for all models.

An exponential model is also selected to characterize the structure of the spatial dependence of the two underlying Gaussian fields employed in the TPS method. The parameters of the variograms of these fields are estimated through the iterative procedure presented by Emery (2007).

This procedure is based on an analytical relationship (see (3) – (6) in Emery, 2007) between the correlograms of the two Gaussian fields (G1 and G2) and the indicator variograms which are derived from the available data and employed in the SISIM-based simulation strategy. This analysis leads to estimating the range values of 900 m and 600 m, respectively along N-S and W-E directions, for both Gaussian fields. Vertical ranges of 19 m and 36 m are estimated for G1 and G2, respectively. As an example of the quality of the results obtained, **Figure 5.2.1** to **5.2.5** depict selected directional sample indicator variograms associated with facies F1 to F5 together with the corresponding calibrated models adopted for the SISIM and TPS simulation techniques. It is noted that the available data density contributes to render estimates of horizontal ranges which are subject to more uncertainty than their vertical counterparts.

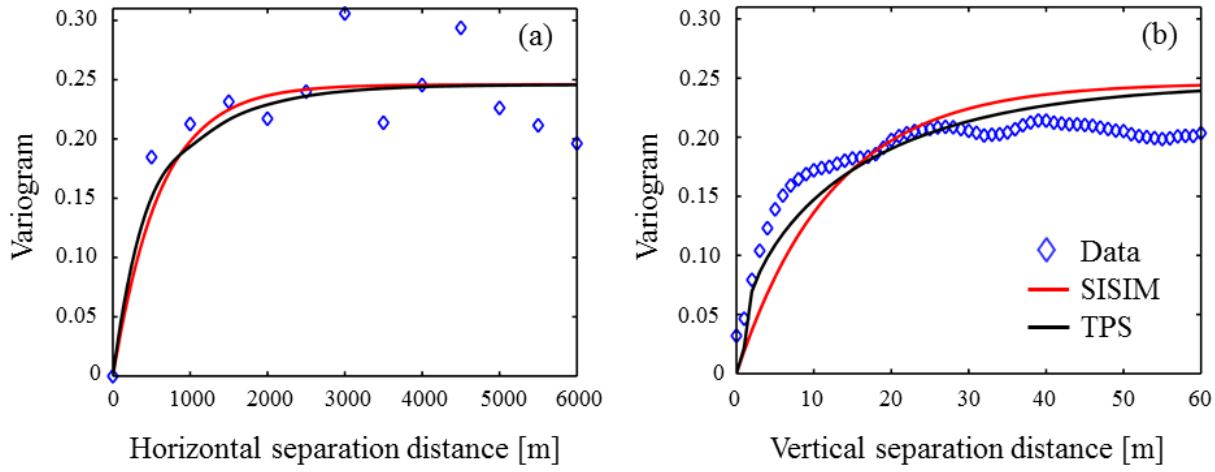

Figure 5.2.1: Experimental (symbols) and modeled (SISIM and TPS) variograms for facies F1 along (a) N-S and (b) vertical directions.

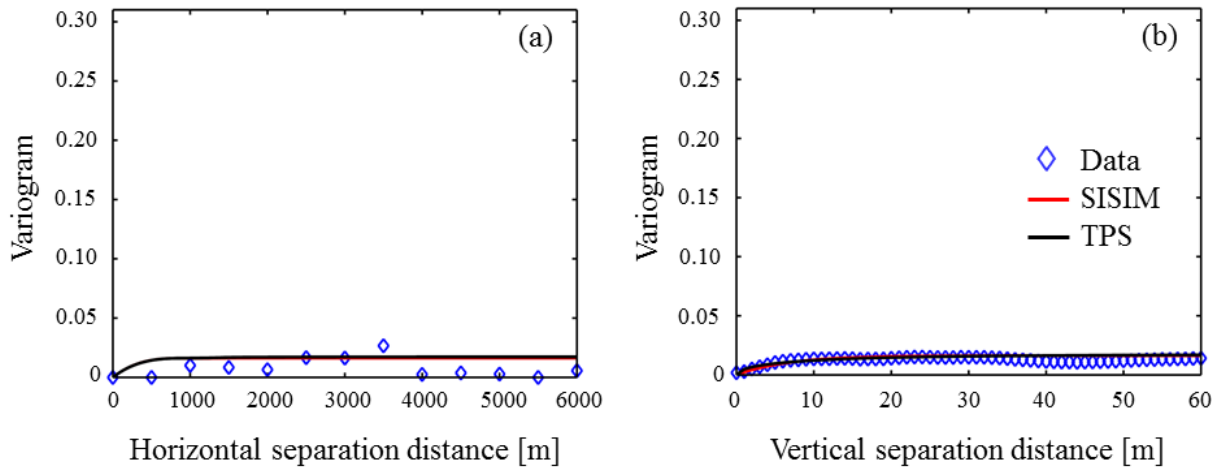

Figure 5.2.2: Experimental (symbols) and modeled (SISIM and TPS) variograms for facies F2 along (a) N-S and (b) vertical directions.

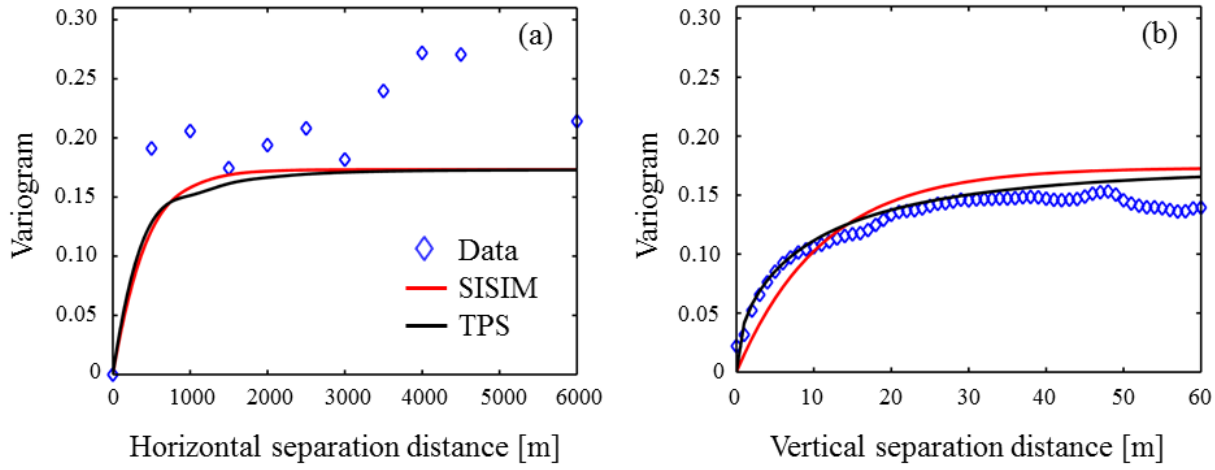

Figure 5.2.3: Experimental (symbols) and modeled (SISIM and TPS) variograms for facies F3 along (a) N-S and (b) vertical directions.

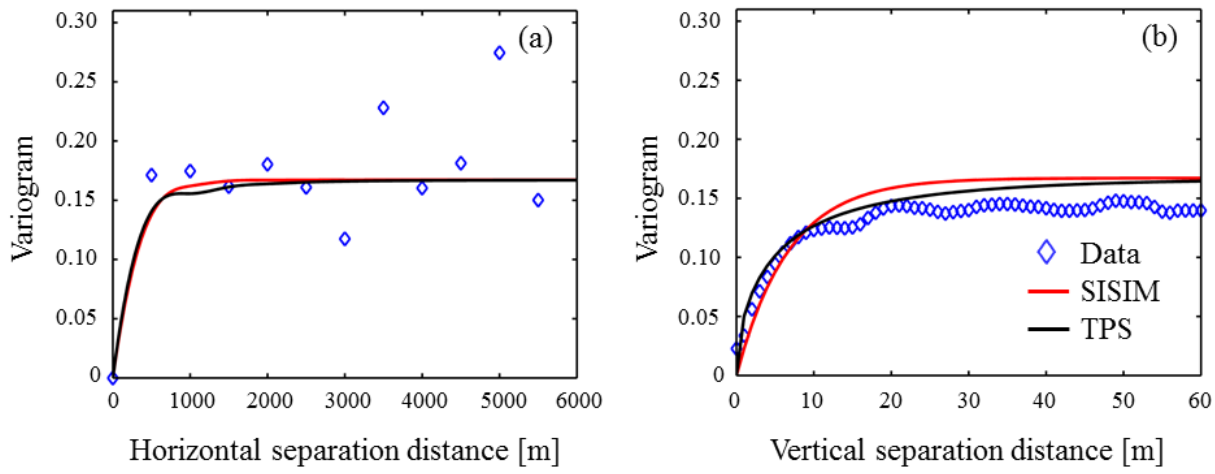

Figure 5.2.4: Experimental (symbols) and modeled (SISIM and TPS) variograms for facies F4 along (a) N-S and (b) vertical directions.

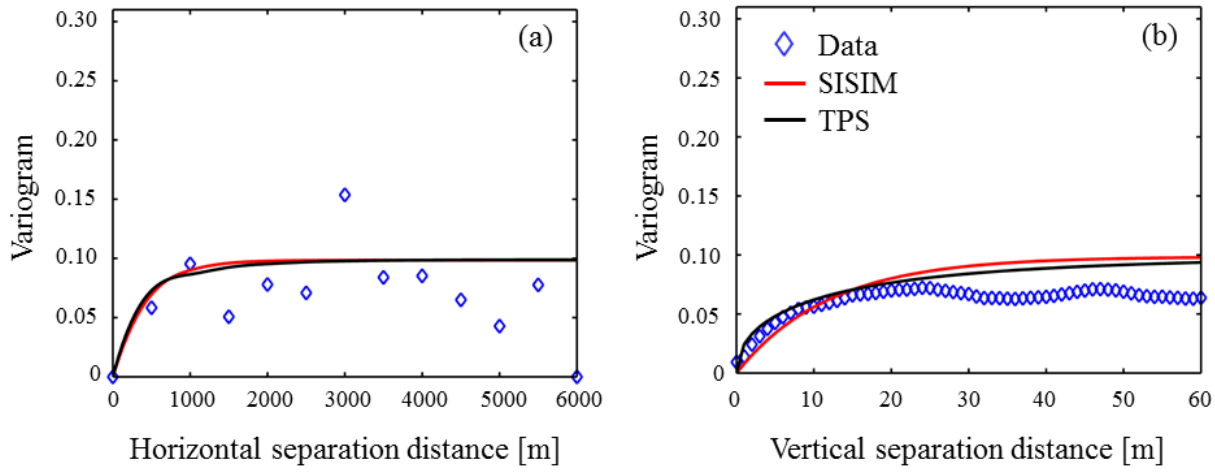

Figure 5.2.5: Experimental (symbols) and modeled (SISIM and TPS) variograms for facies F5 along (a) N-S and (b) vertical directions.

The shape of the variograms near the origin is linked to the regularity of the boundaries between mineralogical domains (Emery, 2007). In particular, the exponential variogram model is smoother than the spherical at the origin and is associated with more regular boundaries. In contrast, the spherical model increases linearly (close to the origin) and entails a more erratic boundary between the simulated domains.

5.3. Description of representative results

We would like to start this subchapter by showing the final hard data set (**Figure 5.3.1**), to get a first impression on how these data will condition the double aquifer system variogram analysis and afterwards the geostatistical MC simulations.

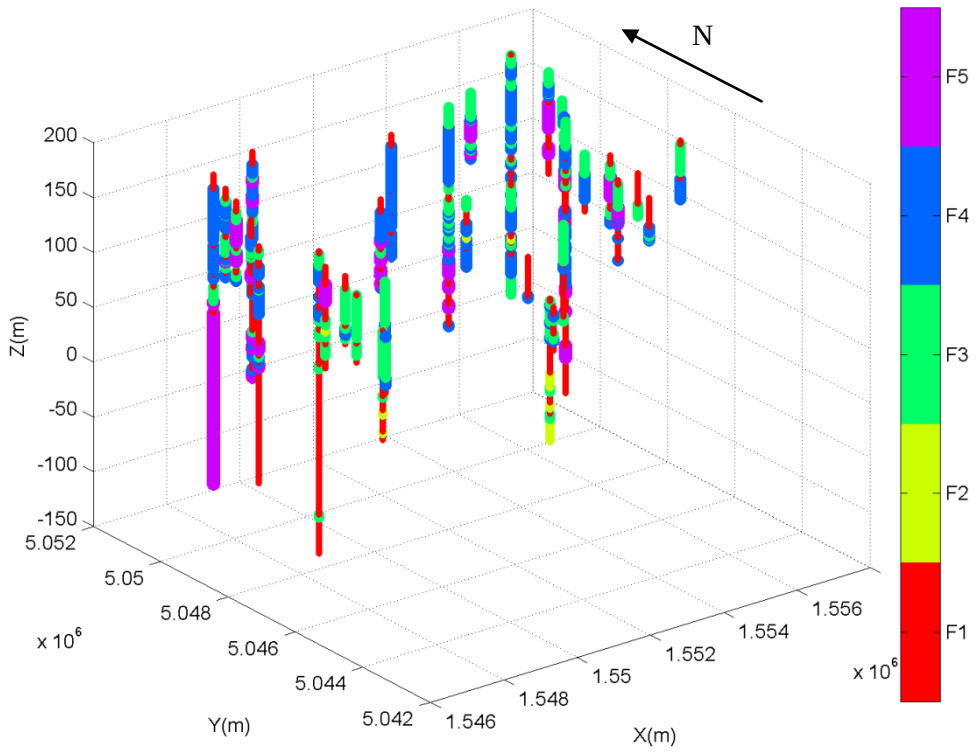

Figure 5.3.1: The three-dimensional plot of all the reclassified borehole geological information (hard data) helps in rendering visible the double aquifer system structure. It displays, weighting as a function of the indicator values, the five different hydrofacies in depth. The coordinates correspond to the real geographical coordinates. This does not correspond with the simulated area.

We did calculate the vertical proportion curves of our groundwater system from the available geological data (see **Figure 5.3.2**), i.e. we checked how the proportions of the different identified (and reclassified) geomaterials change in the vertical direction (in depth). That is made explicit in the following plots.

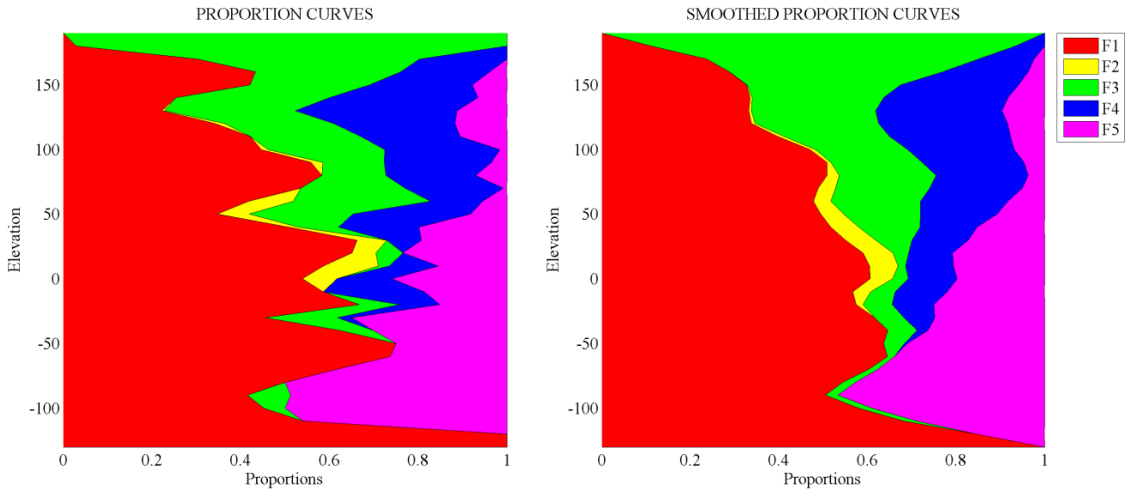

Figure 5.3.2: The left plot displays the raw proportion curves calculated in depth whereas the right plot shows the smoother proportion curves along the vertical direction (smoothing factor = 2). Elevation is expressed in meters. These proportions are assumed to be stationary across the full area under study, including the final smaller simulated domain.

The hard data coordinates, the corresponding indicator values, the bench height and the smoothing factor were used as input. The bench height corresponds to the actual vertical discretization length in order to calculate the vertical proportions. The smoothing factor is a set value (input) that allows calculating a moving average over the benches located above and below the bench under consideration.

5.3.1. Qualitative analysis of heterogeneity' reproduction for SISIM and TPS

Apart from the statistical analyses we carried out in other sections, we also would like to present a closer look to the qualitative results obtained through the two collections of MC simulations.

In **Figure 5.3.1.1**, we do show two representative realizations obtained by means of the TPS and SISIM methods. Both hydrofacies reconstruction methods reproduce the anisotropy pattern detected in the system, along with the natural slope of the real geological setup (set at 0.5º). However, TPS (*a*) renders an improved continuity of sedimentary structures, which are elongated along the N-S direction, consistent with observations from surface lithological maps. We can see that the realization corresponding to the SISIM results (*b*) displays a more patchy scenario, which in turn will impact on the posterior flow field simulation. The imposed lithotype rule on the TPS model is honored.

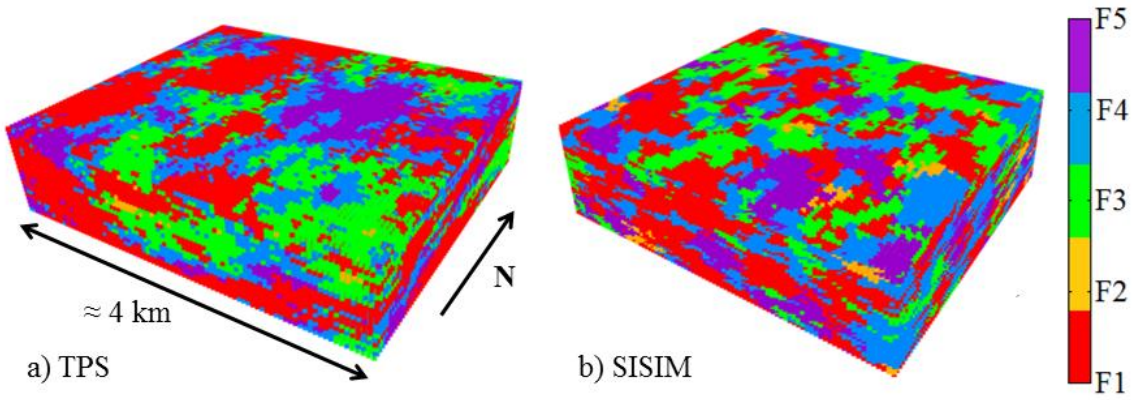

Figure 5.3.1.1: Selected realizations of hydrofacies distributions obtained by means of (a) TPS and (b) SISIM. The size of the represented blocks is 3.7 km × 4.3 km × 0.1 km. Vertical exaggeration is set to 10× for ease of illustration.

5.3.2. Statistical analysis of SISIM and TPS output volumetric proportions

This subchapter is devoted to illustrate some of the statistical results obtained from the analysis of the raw geostatiscal simulations, corresponding to the two employed methodologies.

We firstly studied the range/spread of values, realization per realization, and for each hydrofacies. The wider range of output values that TPS introduced, which will impact on the following stages of this work, is possible to be identified in **Figure 5.3.2.1**. However, SISIM shows more compact behavior around its input volumetric proportion although its distribution of possible outcomes is not centered at that value. Contrarily, TPS results do show a bigger spread, but centered on the input volumetric proportion value.

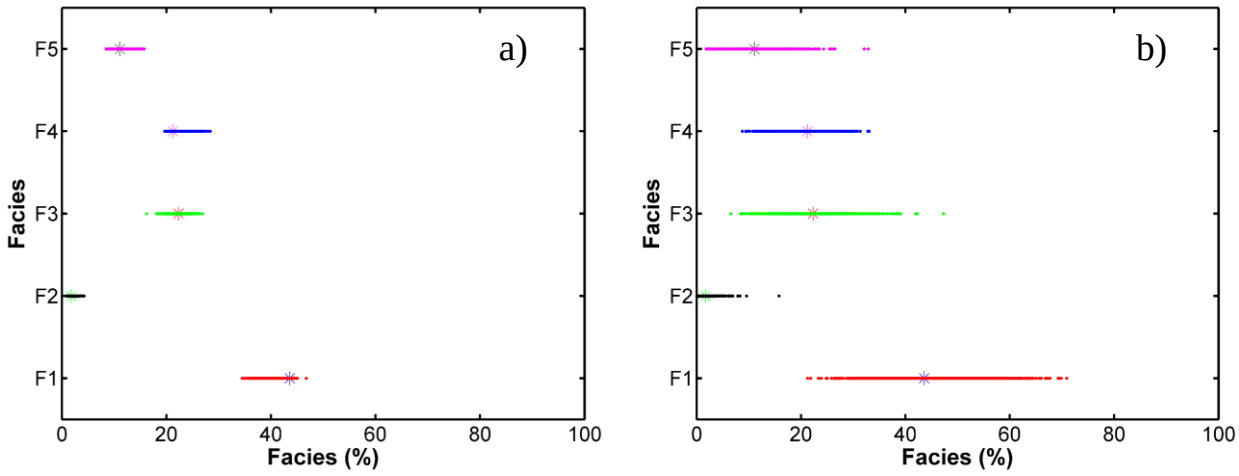

Figure 5.3.2.1: On the X axis we plot the (%) obtained for each realization (series of colored dots), as a function of each indicator class (Y axis). We plot the results corresponding to the SISIM (a) and the TPS (b) methods. Star symbols mark the expected input volumetric proportion, imposed by the real geological database.

We then explored the convergence of the sample mean (%) and the standard deviation (%) throughout the simulations and for each method (see **Figure 5.3.2.2**). Results corresponding to the SISIM technique seem to converge faster for both metrics. In terms of the sample mean, the SISIM results converge faster to a value slightly different to that used as input volumetric proportion, as per the TPS results converge more slowly but to a closer value to that used as input.

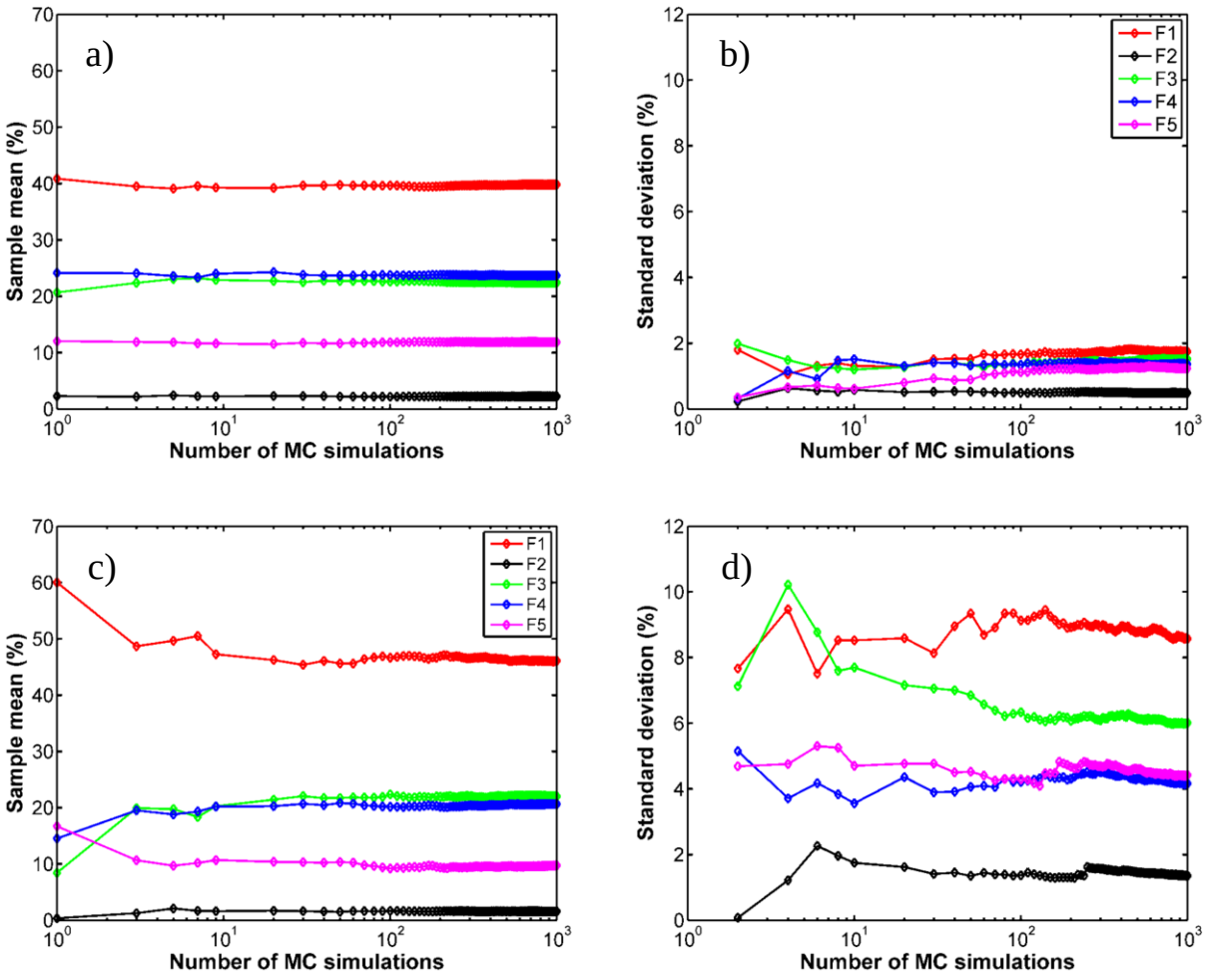

Figure 5.3.2.2: Dependence of sample (a, c) mean and (b, d) standard deviation of the volumetric proportions of hydrofacies F1, F2, F3, F4 and F5 on the number of Monte Carlo realizations for the SISIM- (a, b) and TPS-based (c, d) generation schemes.

We plot the following Figures (**5.3.2.3** and **5.3.2.4**) in order to better visualize and further understand the spread of volumetric proportions (%) throughout the simulation process. The bin classes used to build up the histograms have been calculated as follows: the minimum and maximum values for each hydrofacies histogram correspond to those imposed by the set composed of the 1000 simulations, for both SISIM and TPS. Then, each bin differs from the next in one full point of (%).

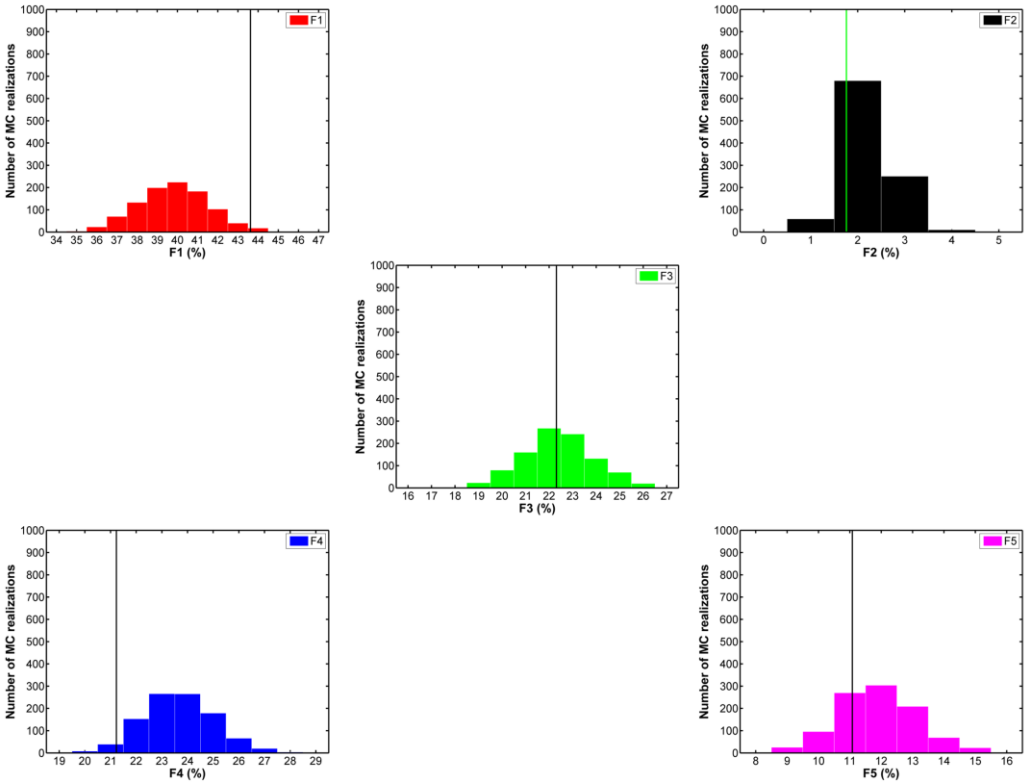

Figure 5.3.2.3: Histograms depicting the volumetric proportions obtained from the full set of 1000 SISIM simulations. The vertical lines do show the position of the input volumetric proportion calculated from the geological database.

The histograms show typical Gaussian distributions of the output volumetric proportion (%) values although SISIM fails to reproduce (in the mean) the input volumetric proportions for 3 of the hydrofacies. The less abundant lithotype (F2) seems to be the best reproduced.

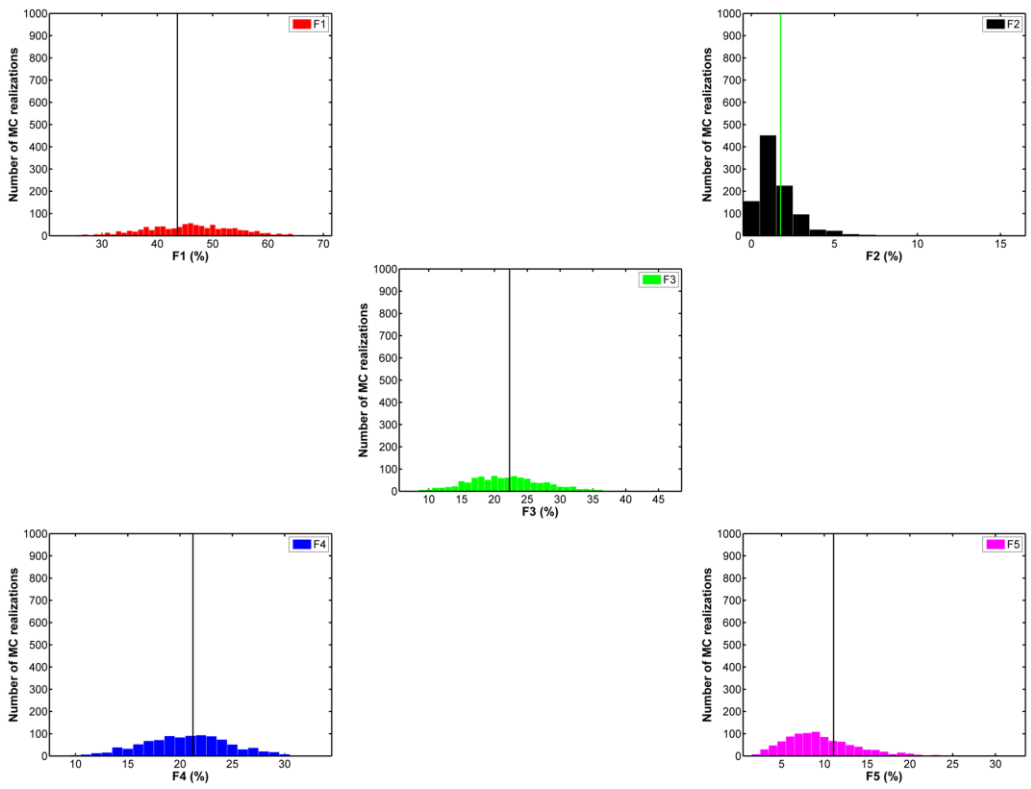

Figure 5.3.2.4: Histograms depicting the volumetric proportions obtained from the full set of 1000 TPS simulations. The vertical lines do show the position of the input volumetric proportion calculated from the geological database.

The histograms show typical Gaussian distributions of the output volumetric proportion (%) values, rather flat compared to the SISIM counterparts. That higher variability of the output has a direct impact on the flow field simulations and the resulting hydraulic head distributions (which will be analyzed later on).

TPS results, conversely to SISIM, reproduce (in the mean) quite accurately the input volumetric proportions for 4 of the hydrofacies. Only F5, the fractured conglomerates (second less abundant indicator after F2, the sands), show a slightly skewed behavior towards the left in the (%) distribution.

We found that introducing a tolerance respect the original input volumetric proportions, we could gain information respect its over and underestimation as a function of the generation scheme (**Figure 5.3.2.5**). We set a tolerance of ±10% for the most abundant hydrofacies F1, followed by a ±5% for F3 and F4, whereas a ±2.5% and a ±0.5% were set for F5 and F2 respectively.

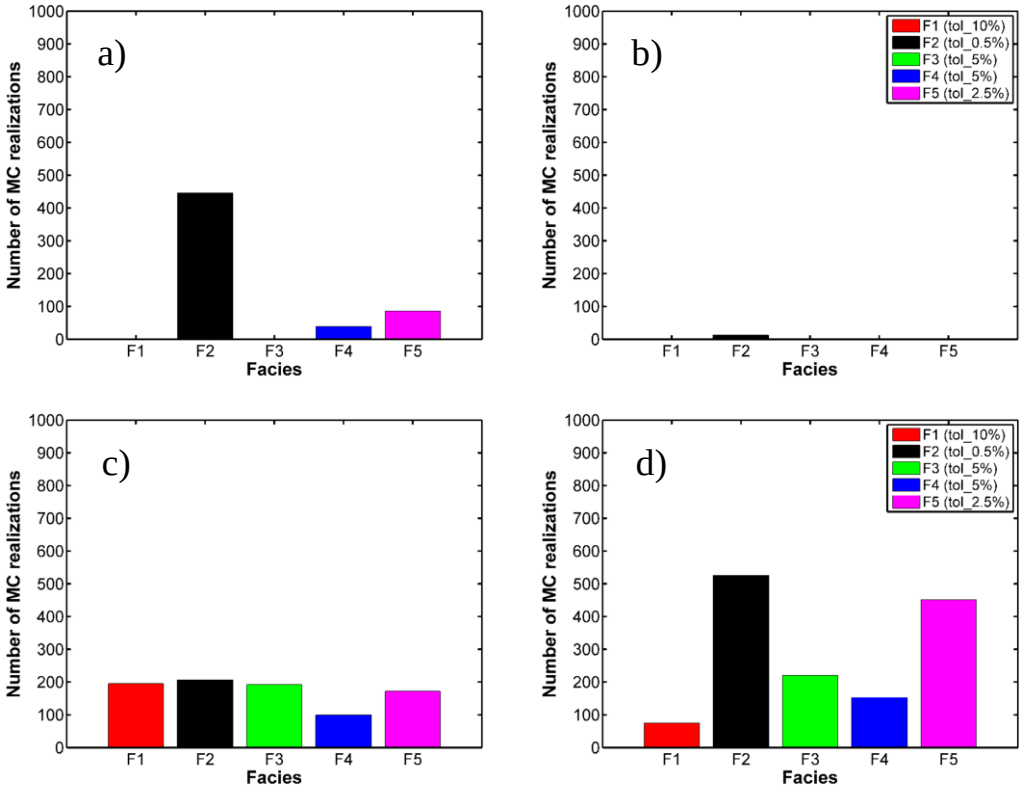

Figure 5.3.2.5: Charts showing the amount of MC simulations that whether over (a, c) and/or underestimated (b, d) the input volumetric proportions, for both SISIM (a, b) and TPS (c, d).

SISIM tends to overestimate the input volumetric proportions when the indicator is less abundant, but almost no underestimation (for those tolerances) is found in our results. On the other hand, TPS tends to overestimate evenly throughout the different indicator classes while tends to underestimate more the input volumetric proportions of those less abundant simulated geomaterials (i.e. F2 and F5).

5.3.3. Variogram calculations from output simulations (SISIM and TPS) checking input parameters honoring

We employed well established software(s) (Deutsch and Journel (1997) for SISIM; algorithms and codes presented by Xu et al. (2006) and Emery (2007) for TPS). We performed tests on the ability of those codes to properly generate multiple system realizations. **Table 5.3.3.1** lists the material volumetric proportions inferred from the available data and employed in the simulation process together with the sample average and standard deviation of the volumetric proportions calculated for each facies and for both simulation methods.

Hydrofacies	Input hydrofacies proportions	μ_{SISIM}	σ_{SISIM}	μ_{TPS}	σ_{TPS}
F1	43.6%	39.8%	1.7%	46.1%	8.6%
F2	1.8%	2.2%	0.5%	1.6%	1.4%
F3	22.3%	22.4%	1.5%	22.0%	6.0%
F4	21.2%	23.7%	1.4%	20.6%	4.3%
F5	11.1%	11.9%	1.2%	9.7%	4.4%

Table 5.3.3.1: Input and simulated volumetric proportions for the five hydrofacies. Average (μ_i; i = SISIM, TPS) and standard deviation (σ_i) of the volumetric proportions are calculated for each facies on the basis of N = 1000 realizations.

On these bases, we judge our results to be of acceptable quality. A corresponding check has been performed on the variogram along the vertical direction calculated from selected realizations.

As an example, we present these results in **Figure 5.3.3.1** for ten selected realizations of the SISIM- and TPS-based generations and facies F4. We think the results are of acceptable quality. It can be noticed that for the chosen sample of 10 MC simulations, the SISIM-based results tend to overestimate the indicator semivariogram model.

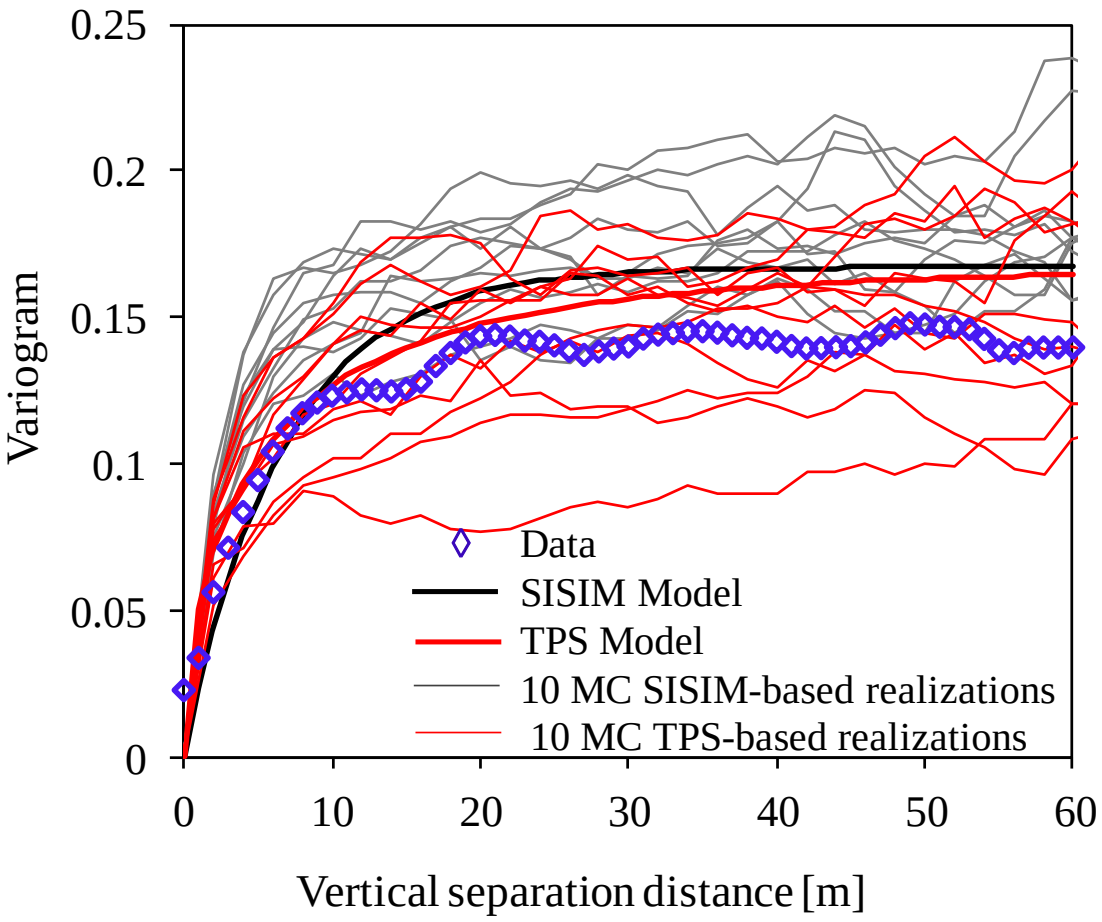

Figure 5.3.3.1: Experimental (symbols) and numerical SISIM-based and TPS-based spatial variograms for facies F4 along the vertical direction.

5.3.4. Sample Log*K* fields for mean (μ) and variance (σ^2), from SISIM and TPS

Finally, we present in this subchapter a collection of results regarding the sample mean and variance of the Log***K*** fields obtained from the performed geostatistical simulations. As mentioned in previous chapters, we imposed for each simulated indicator class a constant ***K*** value.

We wanted to study the impact of the reconstruction method, including the effect of the conditioning data, on the average Log***K*** field. What the following plots tell us is valuable information to better understand the results of the flow field simulations (see Figures **5.3.4.1** and **5.3.4.2**).

These plots show vertical cross-sections along the N-S and the W-E directions, with the sample mean and variance of the corresponding Log***K*** fields obtained from the 1000 realizations and acquired with each simulation method. The vertical scale has been exaggerated 25 times in order to improve the visualization of the outcome, though distortion of the geological structures is introduced (unavoidable). It is important to remark at this point, that any of these vertical cross-sections intersects any actual conditioning borehole data.

Regarding the SISIM results, we can see that persistent clusters of the equivalent to fine materials (F1) are found at the northern and southern subdomains. That suggests that we are close to some of the actual conditioning boreholes and that SISIM embeds this influence in its final outcome.

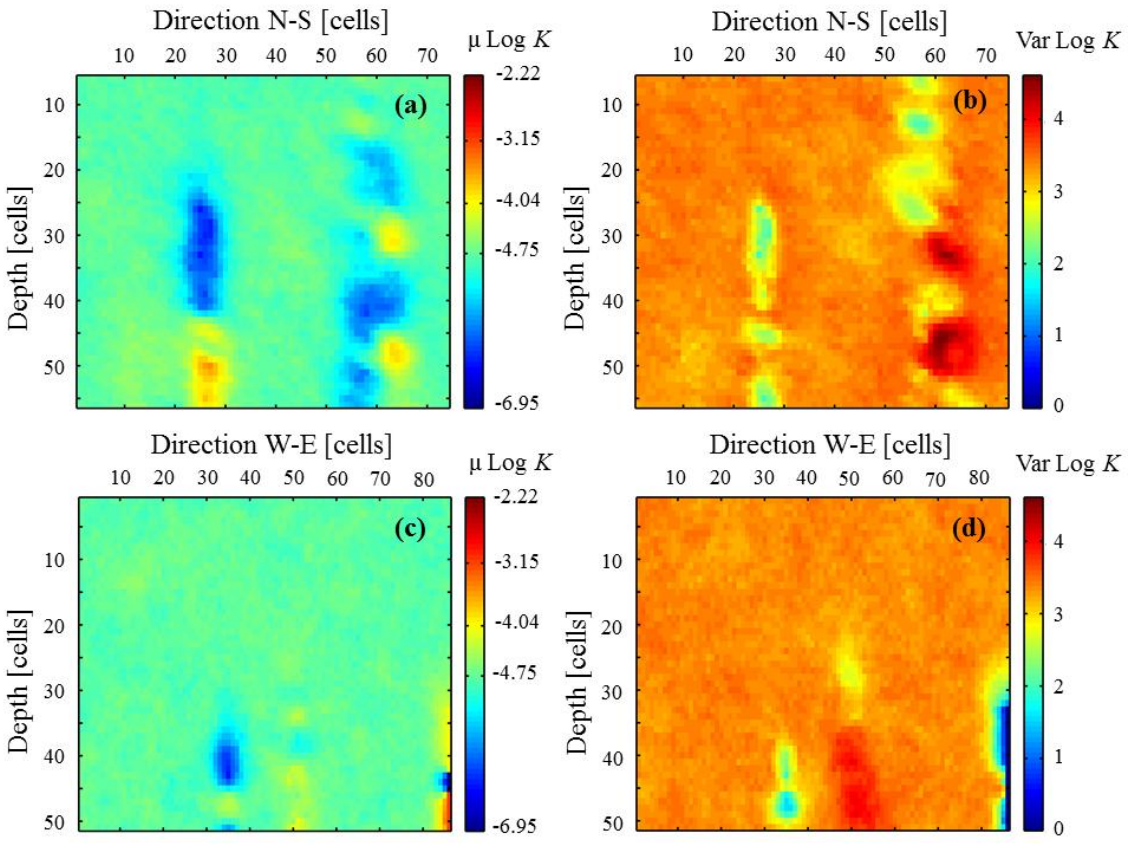

Figure 5.3.4.1: SISIM-based vertical distributions of sample (a), (c) mean and (b), (d) variance of the decimal logarithm of hydraulic conductivities, Log*K*, obtained along the two cross-sections represented in Figs. 5.3.4.1 (a, b). Vertical exaggeration is set to 25× for ease of visualization. "μ" stands for mean and "Var" for variance.

In contrast, the mean Log***K*** field obtained through the TPS method shows a more homogeneous field, in terms of its statistical output, along the N-S direction. Contrarily, along the W-E direction, the effect of a close conditioning data borehole does impact on the sample Log***K*** field. The effect of that single well throughout the collection of simulations seems to be smoothed allowing its impact to travel further than its SISIM counterparts.

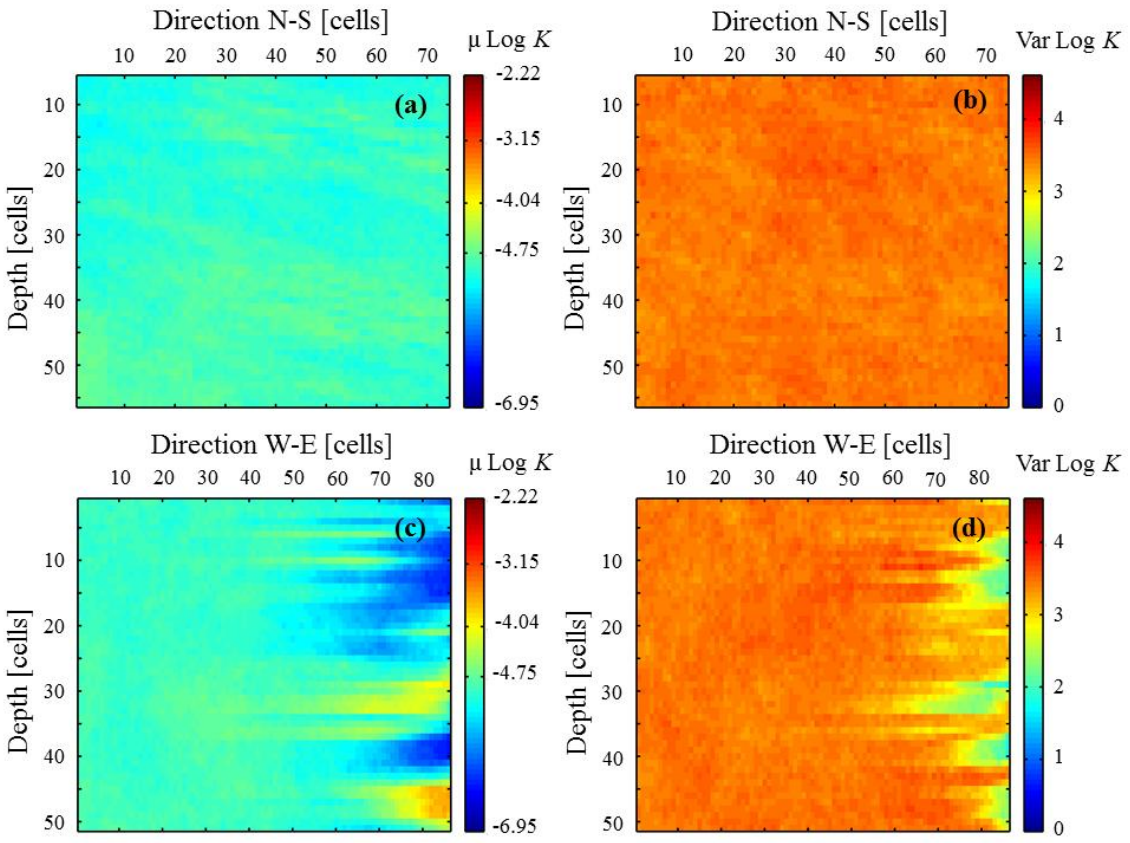

Figure 5.3.4.2: TPS-based vertical distributions of sample (a), (c) mean and (b), (d) variance of the decimal logarithm of hydraulic conductivities, Log*K*, obtained along the two cross-sections represented in Figs. 5.3.4.2 (a, b). Vertical exaggeration is set to 25× for ease of illustration. "μ" stands for mean and "Var" for variance.

6. Flow field simulations

In this chapter we describe the most relevant results regarding the flow simulations performed by means of MODFLOW, over the two sets of 1000 of geostatistical MC realizations obtained with SISIM and TPS schemes.

6.1. Stating the problem: modeling details and procedure

The generated sample of stochastic realizations of (conditional) three-dimensional hydrofacies distributions are employed to simulate a steady-state convergent flow scenario due to pumping. The flow problem is solved through the code MODFLOW (McDonald et al., 1988). Noting that at the large field scale of investigation the spatial arrangement of lithotypes is a key driver for the distribution of groundwater flow quantities, we adopt here a composite medium approach (Winter et. al., 2003) where the spatial location of facies is uncertain and their hydraulic attributes are deterministically known.

In **Table 6.1.1** we set the values for hydraulic conductivity $\boldsymbol{K}_{Fi}$ associated with facies F_i (i = 1, ..., 5). These values are inferred from the results of geostatistical inverse modeling of the large scale groundwater system studied by Bianchi Janetti et al. (2011) and are used here for consistency. Values have been kept isotropic in the three-dimensional space and do not vary inside each indicator, i.e. $\boldsymbol{K}$ only changes from F_i to F_j but not in the same hydrofacies class or indicator.

	K_x / K_y / K_z [m/s]
F1 (Fine materials)	1.12×10^{-7}
F2 (Sands)	1.79×10^{-5}
F3 (Gravels)	7.16×10^{-4}
F4 (Conglomerates)	9.09×10^{-5}
F5 (Fractured conglomerates)	6.05×10^{-3}

Table 6.1.1: Hydraulic conductivity values inferred from the results of the numerical inverse modeling carried out by Bianchi Janetti et al. (2011). The values have been kept isotropic for the current numerical study.

Statistical analysis of calculated hydraulic heads is performed in terms of low-order moments (mean and co-variance) and probability density functions (***pdfs***) by considering point and vertically averaged values. The latter are evaluated along segments of thickness ΔB = 10 m, 20 m and 100 m (i.e., corresponding to 1/10 *B*, 1/5 *B*, and *B*, the complete thickness of the domain), to simulate completely and partially screened borehole readings.

6.1.1. Numerical grid

The numerical mesh employed for the flow simulations (**Figure 6.1.1.1**) is built by further refinement of the hydrofacies generation grid along the horizontal directions, resulting in a regular horizontal grid spacing of $\Delta x' = \Delta y' = \Delta x / 2 = 25$ m. The vertical discretization grid adopted for the flow simulations coincides with the one adopted for the hydrofacies generation procedure, i.e. $\Delta z' = \Delta z = 2$ m. A fully penetrating pumping well is located approximately at the center of the domain. We enclose **Figure 6.1.1.2** to aid in visualization of the full area under study, the numerically simulated domain and the hard data.

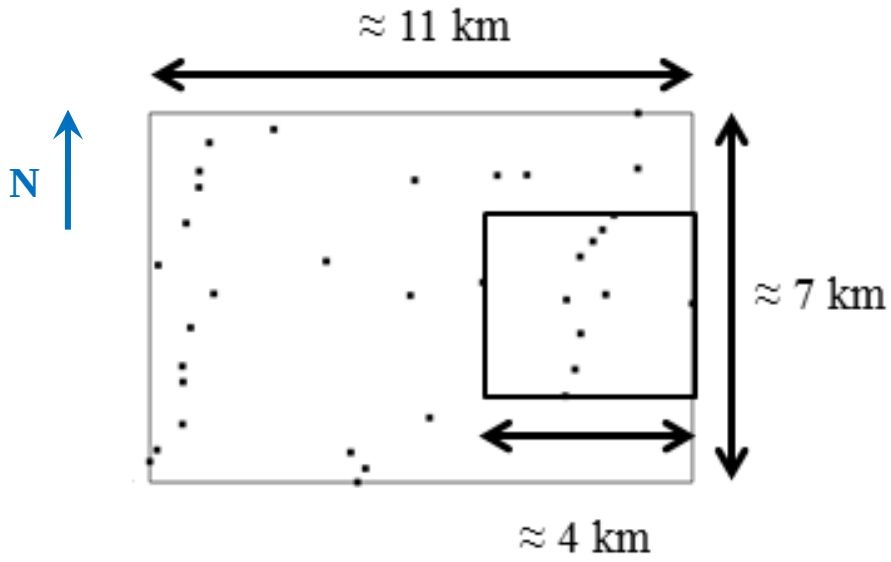

Figure 6.1.1.1: Sketch representing the full area under study and the sub-area used for the numerical simulations (solid black square). In the vertical direction the representative depth/thickness has been set to *B* = 100 meters. Dots represent the available conditioning hard data (borehole logs).

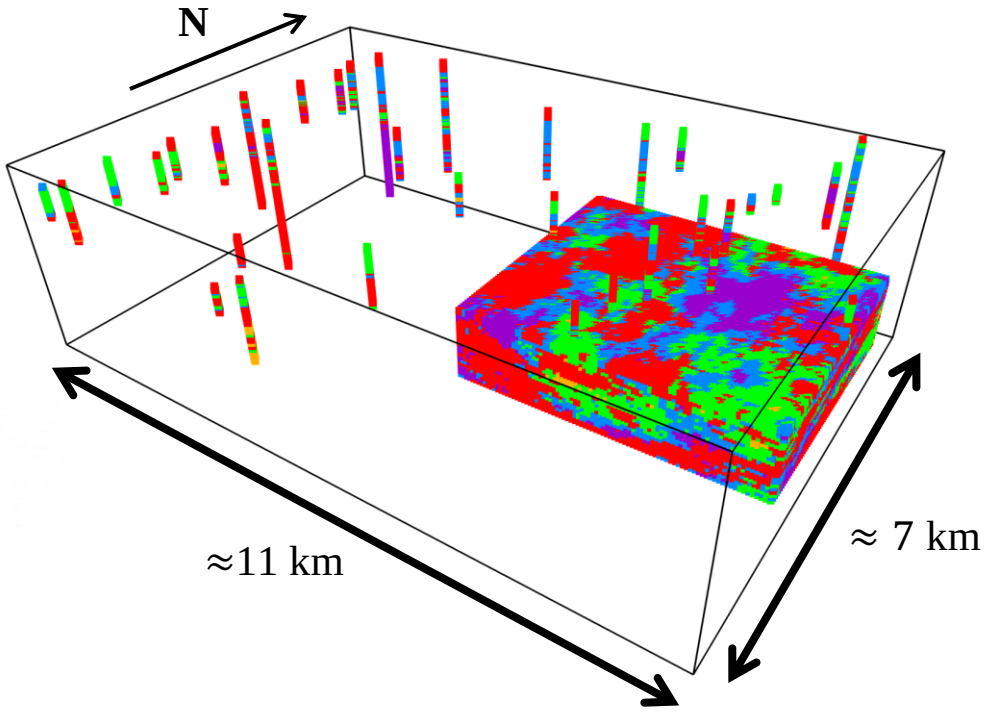

Figure 6.1.1.2: Three-dimensional view of the full area under study and the sub-area used for the numerical simulations, along with a selected TPS realization and the whole set of conditioning borehole data. Vertical scale has been exaggerated 25× for ease of visualization.

6.1.2. Boundary conditions

A total pumping rate of 3,000 m^3/day is imposed and subdivided among the well blocks, proportionally to the hydraulic conductivity of each block. Uniform heads of 172.5 m and 145 m are respectively imposed on the northern and southern edges of the domain to mimic typical average values of regional hydraulic gradients observed in the area (≈ 0.7%). No-flow conditions are imposed along the eastern, western, top and bottom boundaries. The results of the three-dimensional flow modeling are taken to simulate sets of drawdown responses monitored at a set of vertical observation boreholes. These enable one to compare the effect of the stochastic simulation schemes on the response of the system, in terms of hydraulic head statistics.

6.2. N-S and W-E ensemble average drawdown maps

After running the flow field simulations we needed to post-process the generated output files in order to extract the hydraulic head data from the full set of MC scenarios computed via SISIM and TPS.

We then decided to explore the evolution of the hydraulic heads along the identified main planar anisotropy directions, i.e. the North-South (N-S) and West-East (W-E). To illustrate our recurrent sampling points, located along the central N-S and W-E vertical cross-sections, we enclose the following sketch (**Figure 6.2.1**) where some representative locations are depicted.

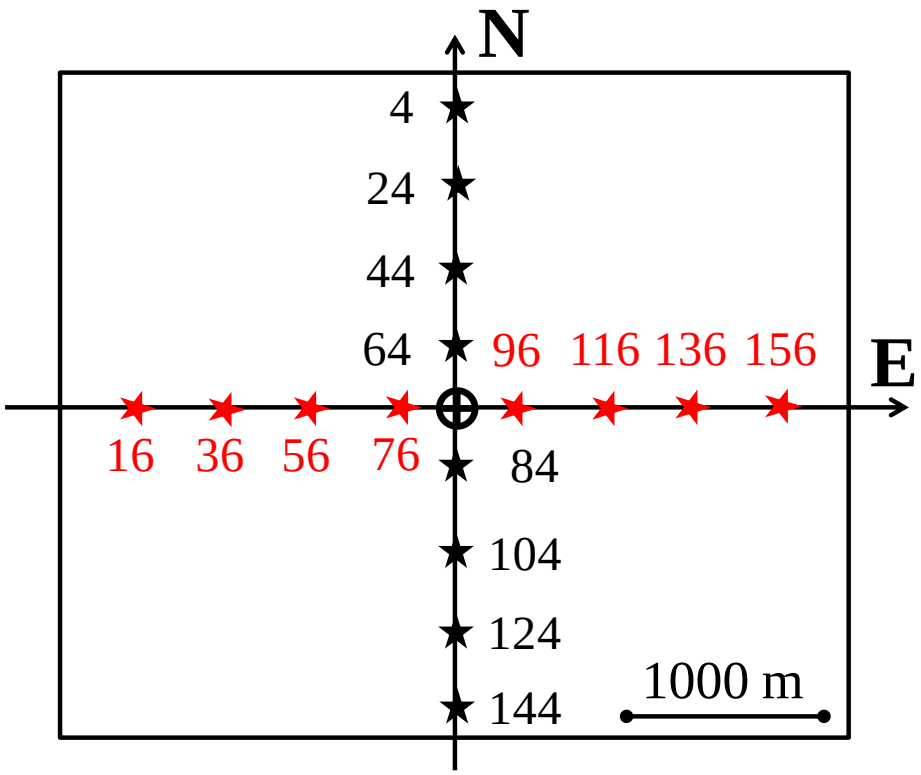

Figure 6.2.1: Sketch representing the simulated sub-area used for the numerical simulations. In it are highlighted by star symbols, along the N-S and the W-E directions, key locations analyzed in terms of the hydraulic head output. The pumping well location is marked with a black solid circle.

We computed the vertical sample mean of the hydraulic heads, for both SISIM and TPS, along the N-S and the W-E directions. Moreover, we computed the ensemble mean along different vertical segments reproducing potential field records in screened boreholes. Below these lines, representative results are shown. We firstly present the results corresponding to the averaging over the full thickness, for both SISIM and TPS, in **Figure 6.2.2**.

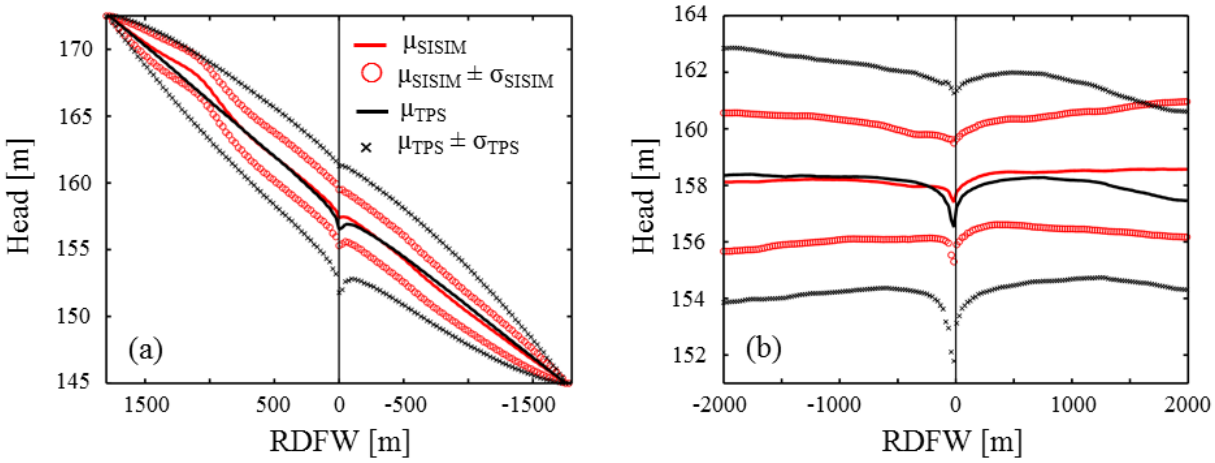

Figure 6.2.2: Space dependence of Monte Carlo-based sample mean (μ) of hydraulic heads calculated through SISIM and TPS. Results are reported in terms of radial distance from the well (RDFW) and are associated with vertical averaging of heads over the entire thickness of the domain along the (a) N-S and (b) W-E directions. Intervals of width corresponding to one standard deviation (σ) around the corresponding sample means are also reported.

It is observed that on the northernmost part of the domain the computed hydraulic heads are consistently higher for the SISIM output. The existing oscillation is an effect of the persistent fine material clusters described in the previous chapter. TPS counterparts do show a higher variance throughout the entire domain. Biggest drawdowns are always associated with the TPS results.

Figure 6.2.2 illustrates the spatial distribution along selected cross-sections of the sample mean hydraulic heads calculated for both simulation methods. Results are reported in terms of radial distance from the well (RDFW; positive for points located North or East of the pumping well and negative otherwise) and are obtained by vertical averaging point heads over the complete domain thickness (Figs. 6.2.2.a, b). In **Figure 6.2.3** we present the same results for the upper (Fig. 6.2.3.a, c) and lower (Fig. 6.2.3.b, d) 20 m screened segments. Intervals of width corresponding to one standard deviation are reported to provide an indication of the extent of the sample variability induced by the generation method.

Regardless the width of the selected vertical integration segment, it is noted that hydraulic head values are highest for SISIM in the northern and eastern subregions of the simulation domain. On the other hand, TPS renders largest average values in the southern and western parts of the system.

The largest drawdown at the well is always obtained from the TPS method. TPS yields the largest sample standard deviation of hydraulic heads, consistent with the results illustrated in **Table 5.3.3.1**. The observed behavior can be related to the differences in the internal structure of the hydrofacies and hydraulic conductivity distributions generated with the two selected methodologies.

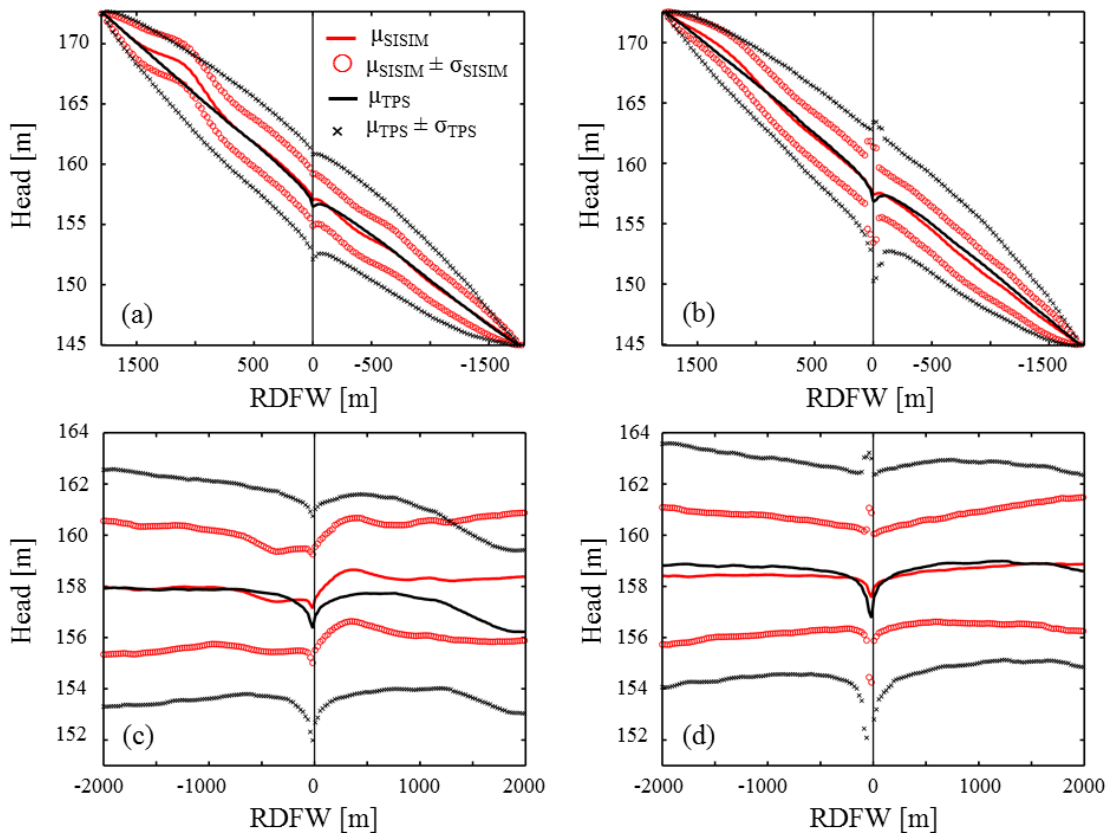

Figure 6.2.3: Space dependence of Monte Carlo-based sample mean (μ) of hydraulic heads calculated through SISIM and TPS. Results are reported in terms of radial distance from the well (RDFW) and are associated with vertical averaging of heads over the upper 20 m screened segments along the (a) N-S and (c) W-E directions and with averaging over the lower 20 m screened segments along the (b) N-S and (d) W-E directions. Intervals of width corresponding to one standard deviation (σ) around the corresponding sample means are also reported.

6.3. Hydraulic heads' variance and covariance maps for different degrees of vertical averaging of the results

In a further step in our research work, we decided to study the behavior of the variance and the covariance matrices of point and vertically averaged hydraulic heads. We started with the pointwise analysis of hydraulic heads' variance.

Figure 6.3.1 shows the vertical distribution of the variance of point values of ***h*** at various relative distances from the well along the N-S (Fig. 6.3.1.a) and the W-E (Fig. 6.3.1.b) directions and calculated from the SISIM-based simulations. Vertical profiles obtained at points located at the same radial distance from the well (see also Figs. 6.3.1.c and 6.3.2.c for the planar location of control points) are reported with the same color. Images of the covariance matrices of point values of heads at different depths along verticals taken at selected control locations complement the set of results (Figs. 6.3.1.d-i). **Figure 6.3.2** depicts the corresponding quantities associated with TPS-based simulations.

With reference to the SISIM-based scenario, the variance of point values of ***h*** forms non-uniform vertical profiles which are almost symmetric around the intermediate depth of the system (z = 50 m, Figs. 6.3.1.a, b). Differences between values of variance at the top and bottom of the aquifer are mainly related to the conditional nature of the simulations. The largest values of variance occur at locations close to the well and to the impervious boundaries (including the top and the bottom of the aquifer). Head variance tends to decrease and its vertical profile to become more uniform with increasing relative distance from the extraction well (measured along the mean flow direction). This result is similar to what observed by Guadagnini et al. (2003) on the basis of their analytical solution of flow moment equations for bounded three-dimensional Gaussian (normal) Log***K*** fields under mean radial

flow conditions. Note that along the W-E direction the variance tends to first decrease and then to increase with distance from the well and reaches a local maximum at the no-flow boundaries. The qualitatively observed increase in the correlation between hydraulic head values at mid locations along the vertical which is observed in Fig. 6.3.1(d) and the wavy behavior noted for the vertical distribution of variance values in Fig. 6.3.1(a), are consistent with the persistence of clusters of fine materials in the area stemming from the SISIM generation method (Fig. **5.3.4.1**).

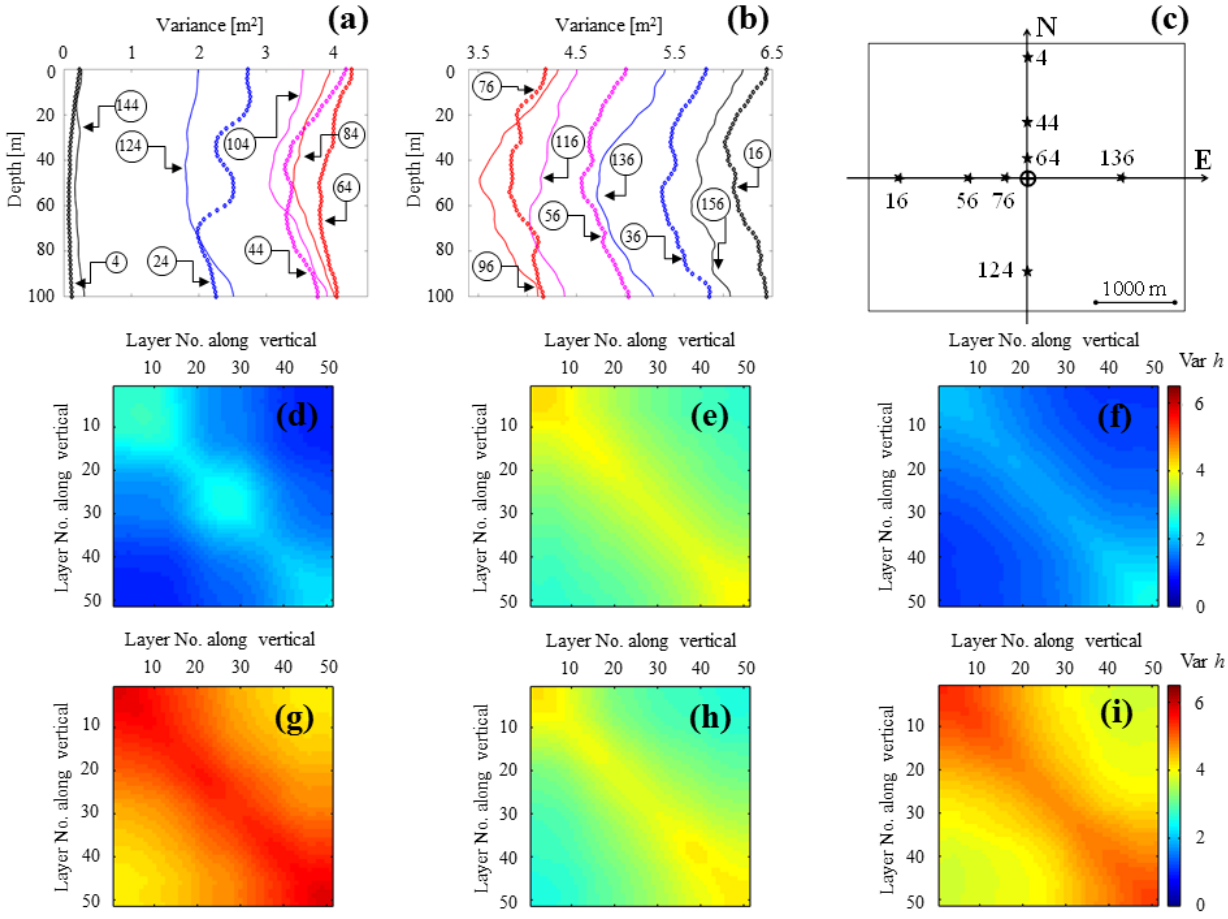

Figure 6.3.1: (a), (b) Vertical distributions of the variance of point values of hydraulic heads at different planar control points (marked by circled numbers) and calculated from the SISIM-based simulations. Planar location of some of the control points is illustrated in (c) as a guidance. Covariance matrices of point values of hydraulic heads at different depths (along the vertical direction) taken at the control points (d) 24, (e) 64, (f) 124, (g) 36, (h) 76, and (i) 136.

The variance distributions associated with the TPS method are typically characterized by a reduced vertical variability at locations along the N-S direction (see Fig. 6.3.2.a) and generally display larger values than those associated with SISIM-based results (compare Figs. 6.3.1.a and 6.3.2.a). Moving along the W-E direction (see Fig. 6.3.2.b), it is noted that the variance associated with locations at the bottom of the system is consistently larger than that related to points close to the top. These effects are due to the imposed contact rules between hydrofacies. These rules tend to reproduce the natural dip of the geological structures in the system and increase the possibility of occurrence of vertical fluxes.

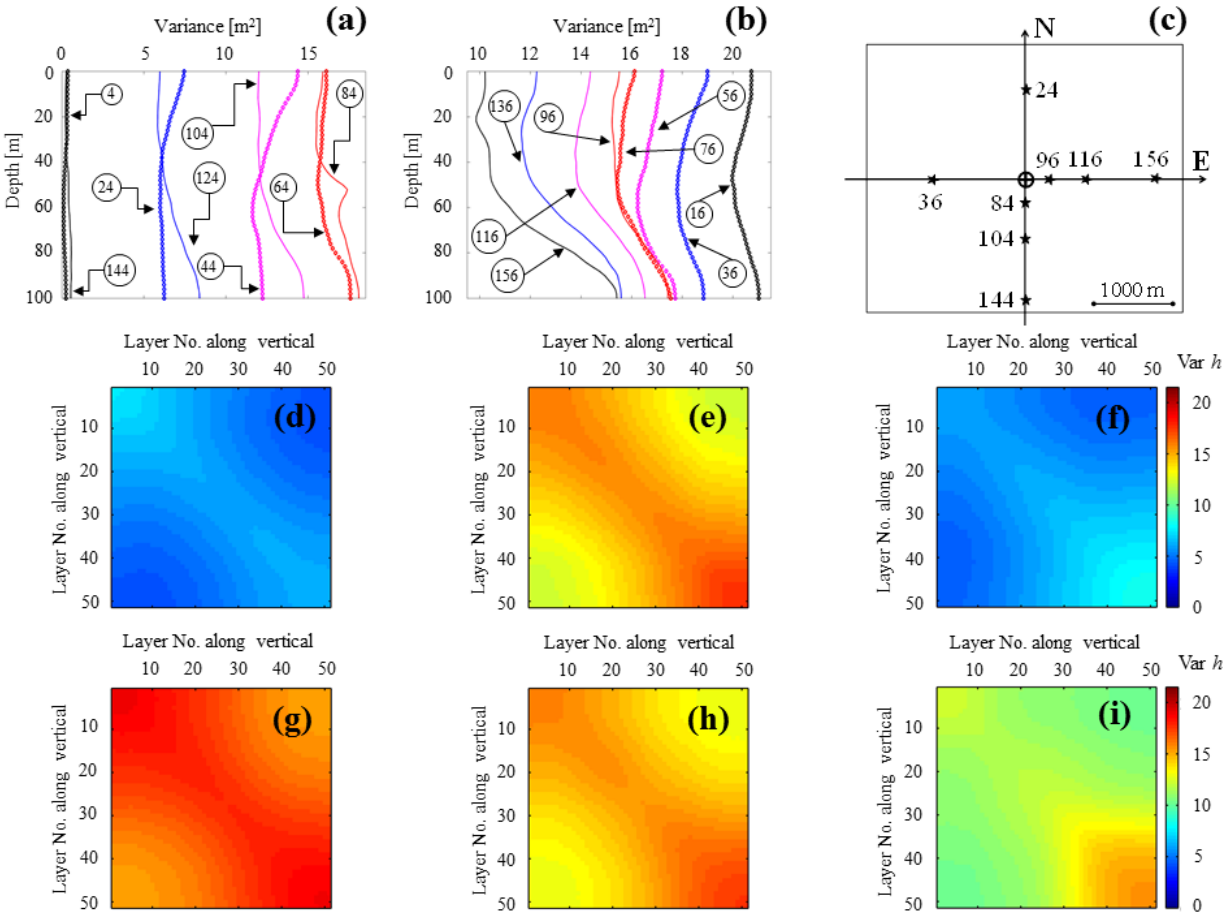

Figure 6.3.2: (a), (b) Vertical distributions of the variance of point values of hydraulic heads at different planar control points (marked by circled numbers) and calculated from the TPS-based simulations. Planar location of some of the control points is illustrated in (c) as a guidance. Covariance matrices of point values of hydraulic heads at different depths (along the vertical direction) taken at the control points (d) 24, (e) 64, (f) 124, (g) 36, (h) 76, and (i) 136.

Examples of quantitative results on the effect that vertical averaging of hydraulic heads along different depth intervals can have on the vertical correlation structure are reported in **Figure 6.3.3**. The figure displays SISIM-based covariance matrices of hydraulic heads at different depths (along verticals) taken at three selected control points along the N-S and W-E directions and corresponding to two different degrees of refinement of the vertical averaging thickness, i.e. ΔB = 20 m (Figs. 6.3.3.a-c, g-i) and 10 m (Figs. 6.3.3.d-f, j-l). Despite the loss of resolution and information along the vertical direction due to spatial averaging, the main representative features and patterns observed for point values based covariances (see Figs. 6.3.1.d-f) remain visible. The same observation can be made for TPS-based simulations, see **Figure 6.3.4**.

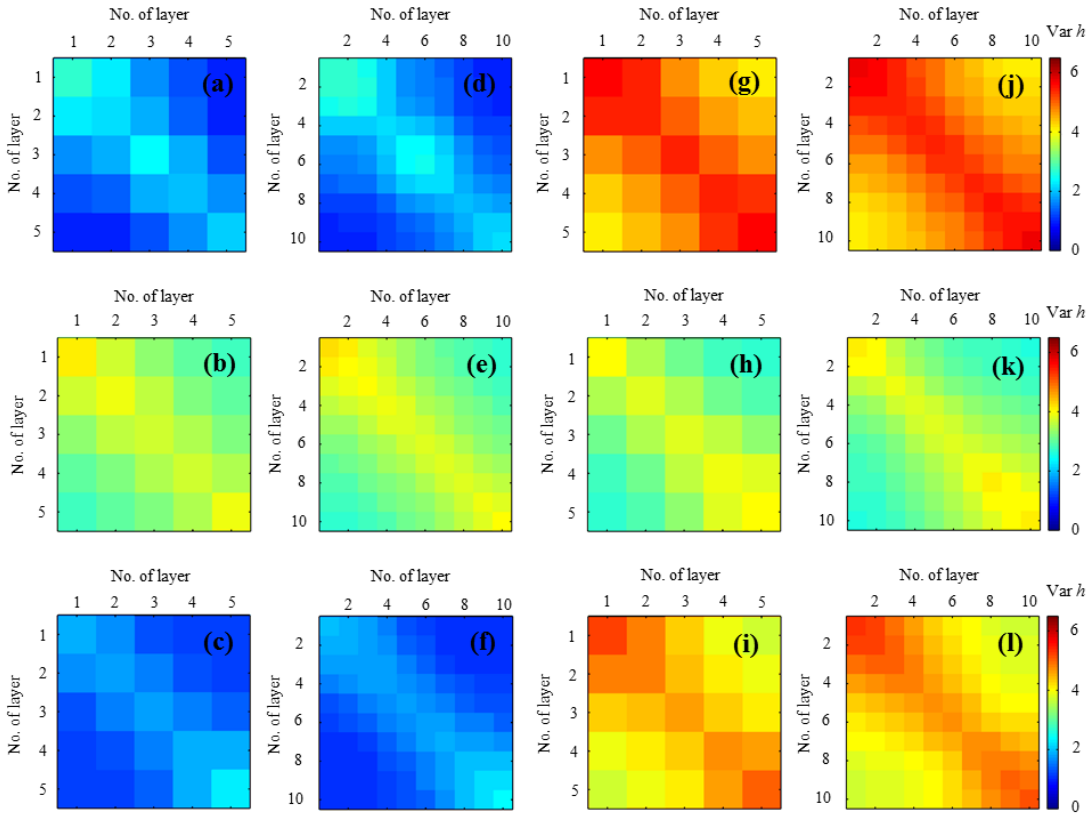

Figure 6.3.3: SISIM-based covariance matrices of hydraulic heads at different depths along verticals taken at selected control points (a, d) 24, (b, e) 64, (c, f) 124, (g, j) 36, (h, k) 76 and (i, l) 136 (see Figure 6.2.1 for location of control points). Results correspond to two different degrees of refinement of the vertical averaging thickness, i.e., ΔB = 10 m (Figs. 6.3.3.d-f, j-l) and ΔB = 20 m (Figs. 6.3.3.a-c, g-i). Horizontal and vertical axes represent the layer numbering associated with each averaging interval.

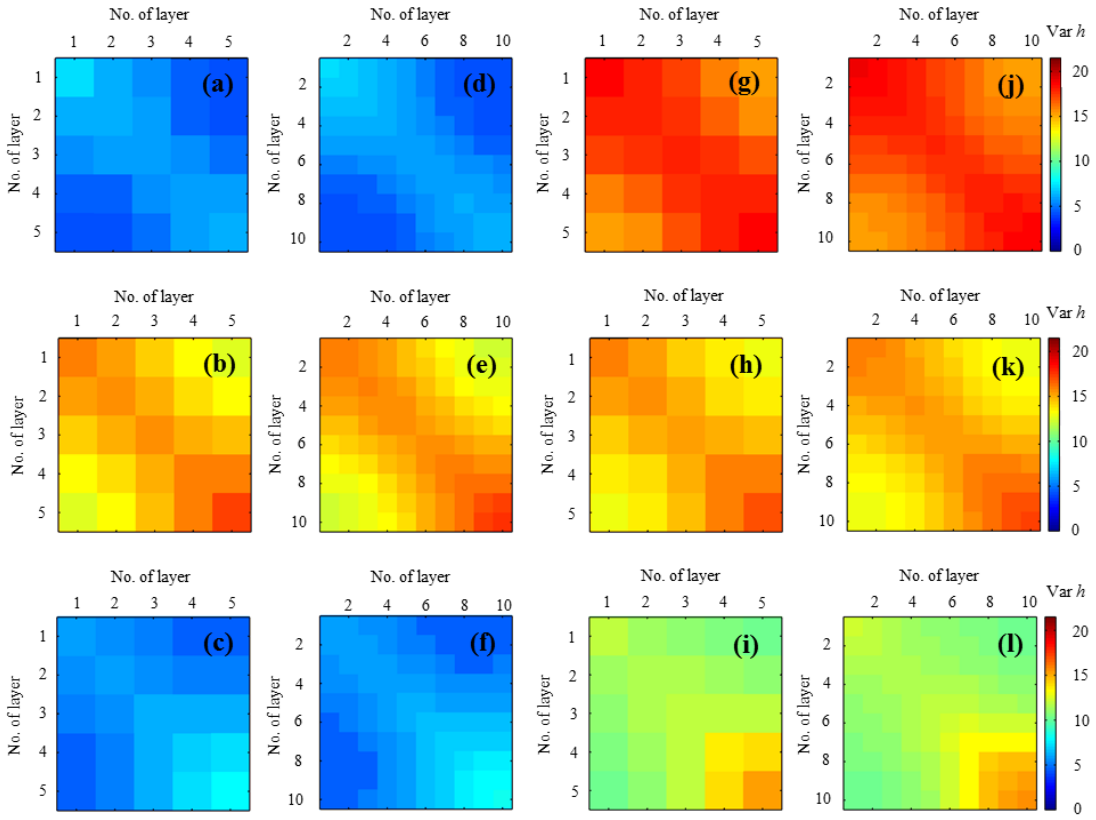

Figure 6.3.4: TPS-based covariance matrices of hydraulic heads at different depths along verticals taken at selected control points (a, d) 24, (b, e) 64, (c, f) 124, (g, j) 36, (h, k) 76 and (i, l) 136 (see Figure 6.2.1 for location of control points). Results correspond to two different degrees of refinement of the vertical averaging thickness, i.e., ΔB = 10 m (Figs. 6.3.4.d-f, j-l) and ΔB = 20 m (Figs. 6.3.4.a-c, g-i). Horizontal and vertical axes represent the layer numbering associated with each averaging interval.

6.4. Sample pdf estimation for point and vertically averaged hydraulic heads

Figure 6.4.1 depicts the N-S and W-E spatial dependence of the sample ***pdf*** of hydraulic heads averaged over the whole aquifer thickness and calculated through the SISIM- and TPS-based reconstruction methods. The SISIM-based setting appears to be associated with the largest peakedness of the empirical distributions. Visual inspection of sample ***pdfs*** suggests that a Gaussian model might not always be appropriate to characterize the observed behavior. These ***pdfs*** are sometimes characterized by heavy tails, for which, e.g. an α-stable distribution might be an appropriate interpretive model. On this basis, hydraulic head values calculated at different locations in the system and averaged along vertical segments of various thicknesses are examined by (*a*) assuming that they derive from an α-stable distribution, (*b*) estimating the parameters of these distributions and (*c*) analyzing the degree to which the calibrated distributions fit the numerical results.

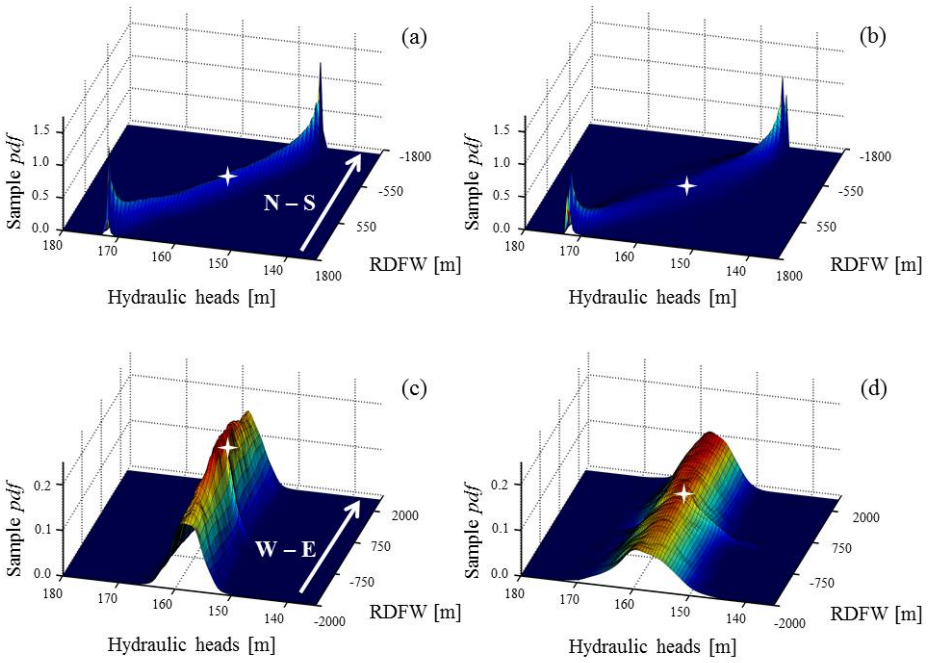

Figure 6.4.1: Spatial distribution of the sample pdf of vertically integrated hydraulic heads calculated through the (a), (c) SISIM- and (b), (d) TPS-based reconstruction methods along the N-S and W-E directions. RDFW stands for Relative Distance From Well (in meters). White stars mark the location of the pumping well.

In **Figure 6.4.2** we report the results obtained for the top 20 meters averaged vertical segment, both for SISIM and TPS methods. Qualitatively we observe that the shapes of the ***pdfs*** does not change substantially, remaining more or less Gaussian along the W-E direction and close to the pumping well, while close to the imposed head boundary conditions the peakedness of the hydraulic head distributions increases towards its limit value.

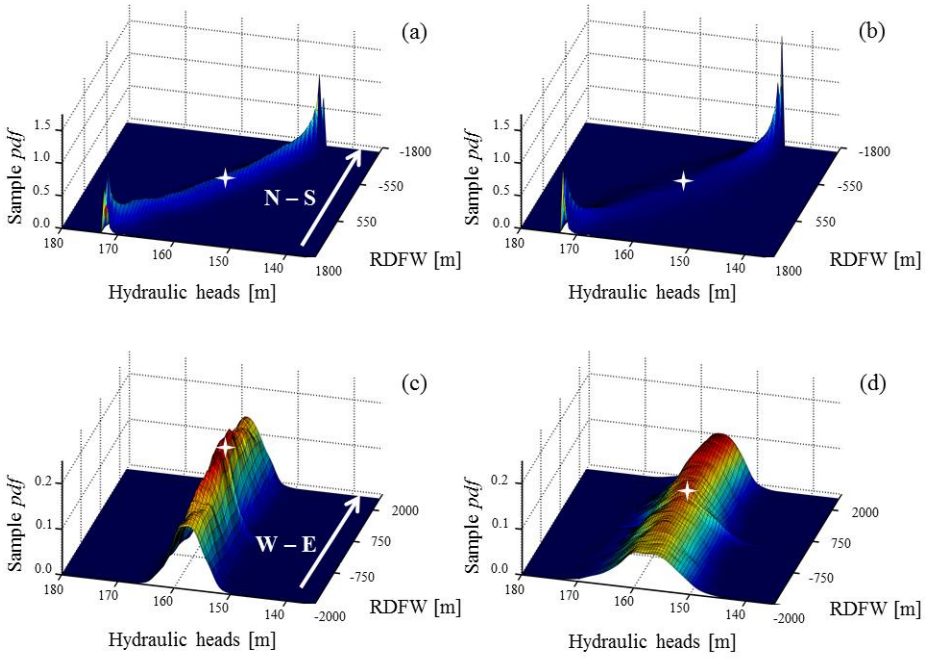

Figure 6.4.2: Spatial distribution of the sample pdf of vertically integrated hydraulic heads over the top 20 meters and calculated through the (a), (c) SISIM- and (b), (d) TPS-based reconstruction methods along the N-S and W-E directions. RDFW stands for Relative Distance From Well (in meters). White stars mark the location of the pumping well.

A statistical analysis is performed at selected locations, to test the influence of the averaging procedure along the vertical direction on the simulation results. As an example, **Figure 6.4.3** illustrates the variability along the vertical of SISIM-based hydraulic head sample ***pdfs*** calculated on the basis of the MC simulations at control point 24 (located in the northern part of the domain, at about 600 m from the prescribed hydraulic head boundary and 1250 m from the well) and for the different averaging intervals considered, i.e. point values (Fig. 6.4.3.a), ΔB = 10 m (Fig. 6.4.3.b) and ΔB = 20 m (Fig. 6.4.3.c).

The influence of the northern (prescribed head) boundary condition is notable on the skewness and on the (left) heavy tail of the distributions. The pointwise and vertically averaged values of ***h*** share some notable statistical properties. All sample distributions appear to be reasonably fitted by an α-stable model which is negatively skewed (i.e., $\hat{\beta} \approx -1.0$) and with $\hat{\alpha}$ values ranging between 1.6 and 1.8. The same analysis performed at points lying in the southern part of the system provides qualitatively similar results, with sample ***pdfs*** being fitted by positively skewed ($\hat{\beta} \approx 1.0$) α-stable distributions.

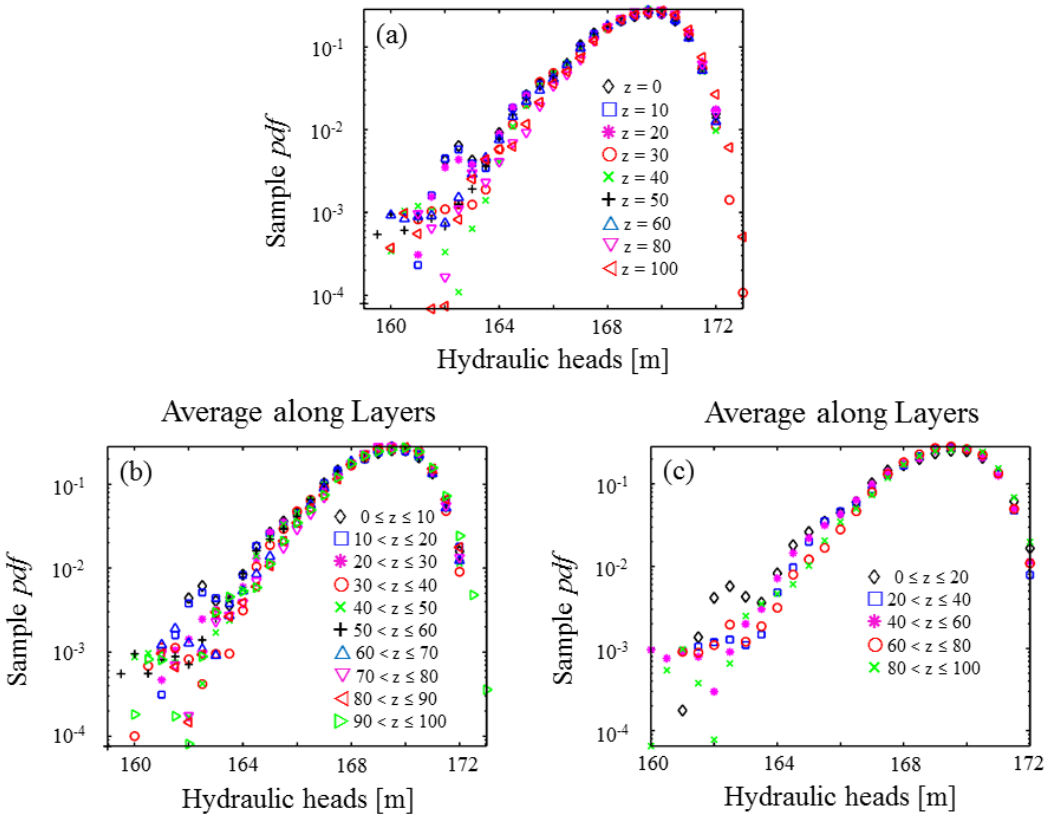

Figure 6.4.3: Vertical distribution of SISIM-based hydraulic head sample pdfs calculated at control point 24 (see Figure 6.2.1) and for the different averaging intervals considered, i.e. (a) point hydraulic head values, and head values vertically averaged along coordinate z with (b) Δ*B* = 10 m and (c) Δ*B* = 20 m.

TPS-based results (**Figure 6.4.4**) display a similar behavior albeit characterized by generally longer tails (with estimates $\hat{\alpha} \approx 1.5$). The tails of the hydraulic heads ***pdfs*** along the N-S direction become increasingly evident for both simulation schemes, and hence best interpreted through an α-stable distribution, as the distance from the pumping well increases and the (deterministic Dirichlet) boundaries are approached.

The observed similarities between the shapes of the sample ***pdfs*** of pointwise and vertically averaged heads suggests the possibility of capturing the key features of the statistical behavior of ***h*** by means of vertically integrated observations.

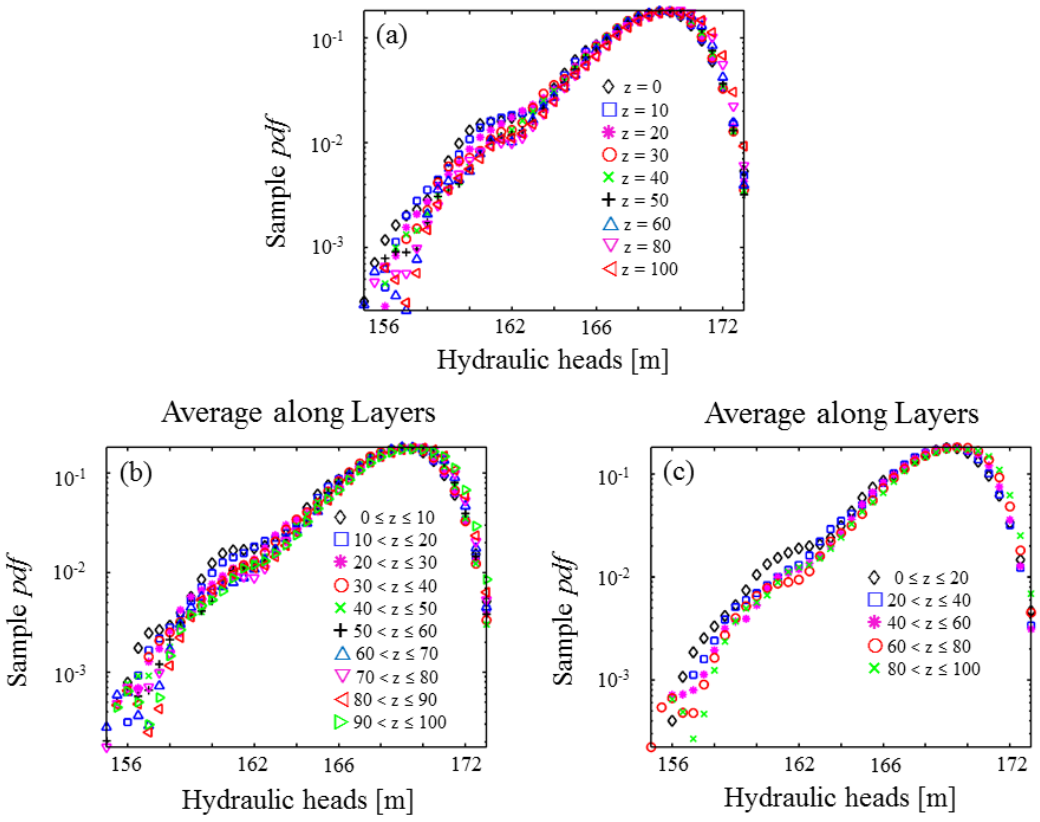

Figure 6.4.4: Vertical distribution of TPS-based hydraulic head sample pdfs calculated at control point 24 (see Figure 6.2.1) and for the different averaging intervals considered, i.e. (a) point hydraulic head values, and head values vertically averaged along coordinate z with (b) ΔB = 10 m and (c) ΔB = 20 m.

6.5. Sample pdf fitting procedure to Gaussian and α-stable models

In the following Tables (**6.5.1** to **Table 6.5.4**) we enclose the results obtained for both SISIM and TPS flow field simulations. We used the available code from Nolan (2001) that allows calculating the Gaussian (normal) and the α-stable best fits (in a ML, Maximum Likelihood framework) for the hydraulic heads' ***pdfs***. It is important to remark here that the Gaussian model is a specific case of the α-stable distribution, i.e. when the stability index parameter α = 2.

	Piezometer	FIT	α	β	μ	σ	Skewness	Kurtosis
SISIM	24	Normal	2.0	0.0	168.21	1.305	-0.973	5.095
		STABLE	1.80	-1.0	168.21	1.305	-0.973	5.095
	44	Normal	2.0	0.0	164.14	1.675	-0.351	3.240
		STABLE	1.90	-1.0	164.14	1.675	-0.351	3.240
	64	Normal	2.0	0.0	160.19	1.841	-0.130	3.221
		STABLE	1.99	-0.682	160.19	1.841	-0.130	3.221
	84	Normal	2.0	0.0	156.43	1.765	0.150	2.882
		STABLE	2.0	-0.897	156.43	1.765	0.150	2.882
	104	Normal	2.0	0.0	152.58	1.649	0.432	3.050
		STABLE	2.0	-0.234	152.58	1.649	0.432	3.050
	124	Normal	2.0	0.0	148.94	1.239	0.664	3.495
		STABLE	2.0	-0.922	148.94	1.239	0.664	3.495

Table 6.5.1: Full vertically averaged SISIM results obtained via the STABLE code (Nolan, 2001), for selected points along the vertical N-S cross-section, including the Gaussian and the α-stable fit. Skewness and kurtosis values are also reported.

	Piezometer	FIT	α	β	μ	σ	Skewness	Kurtosis
SISIM	**36**	Normal	2.0	0.0	158.21	2.216	0.103	2.654
		STABLE	2.0	-0.999	158.21	2.216	0.103	2.654
	56	Normal	2.0	0.0	158.14	2.040	0.100	2.774
		STABLE	2.0	-0.805	158.14	2.040	0.100	2.774
	76	Normal	2.0	0.0	157.97	1.835	0.018	2.915
		STABLE	2.0	-0.877	157.97	1.835	0.018	2.915
	96	Normal	2.0	0.0	158.33	1.827	-0.016	2.898
		STABLE	2.0	-0.609	158.33	1.827	-0.016	2.898
	116	Normal	2.0	0.0	158.45	1.924	0.023	2.851
		STABLE	2.0	-0.842	158.45	1.924	0.023	2.851
	136	Normal	2.0	0.0	158.53	2.088	-0.047	2.862
		STABLE	2.0	-0.820	158.53	2.088	-0.047	2.862

Table 6.5.2: Full vertically averaged SISIM results obtained via the STABLE code (Nolan, 2001), for selected points along the vertical W-E cross-section, including the Gaussian and the α-stable fit. Skewness and kurtosis values are also reported.

	Piezometer	FIT	α	β	μ	σ	Skewness	Kurtosis
TPGS	**24**	Normal	2.0	0.0	168.17	2.338	-1.185	5.018
		STABLE	1.6	-1.0	168.17	2.338	-1.185	5.018
	44	Normal	2.0	0.0	164.10	3.326	-0.469	3.012
		STABLE	1.865	-0.99	164.10	3.326	-0.469	3.012
	64	Normal	2.0	0.0	160.02	3.829	-0.104	2.682
		STABLE	2.0	-0.115	160.02	3.829	-0.104	2.682
	84	Normal	2.0	0.0	156.30	3.900	0.057	3.683
		STABLE	1.99	0.531	156.30	3.900	0.057	3.683

	104	Normal	2.0	0.0	152.98	3.405	0.739	3.757
		STABLE	1.80	1.0	152.98	3.405	0.739	3.757
	124	Normal	2.0	0.0	149.29	2.410	1.496	6.692
		STABLE	1.60	1.0	149.29	2.410	1.496	6.692

Table 6.5.3: Full vertically averaged SISIM results obtained via the STABLE code (Nolan, 2001), for selected points along the vertical N-S cross-section, including the Gaussian and the α-stable fit. Skewness and kurtosis values are also reported.

	Piezometer	**FIT**	**α**	**β**	**μ**	**σ**	**Skewness**	**Kurtosis**
TPGS	**36**	Normal	2.0	0.0	158.31	4.131	0.140	2.635
		STABLE	2.0	-0.001	158.31	4.131	0.140	2.635
	56	Normal	2.0	0.0	158.29	3.947	0.126	2.625
		STABLE	2.0	0.0	158.29	3.947	0.126	2.625
	76	Normal	2.0	0.0	158.00	3.839	0.067	2.590
		STABLE	2.0	-0.010	158.00	3.839	0.067	2.590
	96	Normal	2.0	0.0	158.00	3.818	0.108	2.706
		STABLE	2.0	0.690	158.00	3.818	0.108	2.706
	116	Normal	2.0	0.0	158.28	3.681	0.131	2.755
		STABLE	2.0	0.695	158.28	3.681	0.131	2.755
	136	Normal	2.0	0.0	158.15	3.431	0.080	2.745
		STABLE	2.0	-0.410	158.15	3.431	0.080	2.745

Table 6.5.4: Full vertically averaged TPS results obtained via the STABLE code (Nolan, 2001), for selected points along the vertical W-E cross-section, including the Gaussian and the α-stable fit. Skewness and kurtosis values are also reported.

Figures **6.5.1** and **6.5.2** respectively show the N-S and W-E spatial evolution of the ***pdf*** of hydraulic heads obtained after averaging heads along the whole aquifer thickness (Figures 6.5.1.a-c) or over the top 25 m segment (Figures 6.5.1.d-f) and on the basis of the SISIM methodology. Empirical hydraulic head ***pdfs*** are interpreted by considering the Gaussian and the α-stable models. Each plot in Figures 6.5.1 and 6.5.2 reports the Monte Carlo sample distribution and corresponding ML fits for the Gaussian and α-stable distributions. The corresponding results associated with the TPS method are depicted in Figures **6.5.3** and **6.5.4**.

The tails of the hydraulic heads' ***pdfs*** along the N-S direction become increasingly evident for both simulation schemes, and hence best interpreted through an α-stable distribution, as the distance from the pumping well increases. At locations close to the fixed head boundaries, the distribution is skewed towards values which are representative of the inner portion of the domain. This behavior is observed for both types of vertically averaged information.

Conversely, the ***pdfs*** of vertically averaged heads along the W-E direction appear to be well interpreted by a symmetric distribution such as the Gaussian model, regardless the thickness of the vertical averaging segment and the generation model adopted. These features could be related to the prescribed boundary conditions which introduce fewer constraints (through the Monte Carlo realizations) to the heads computed along the W-E direction.

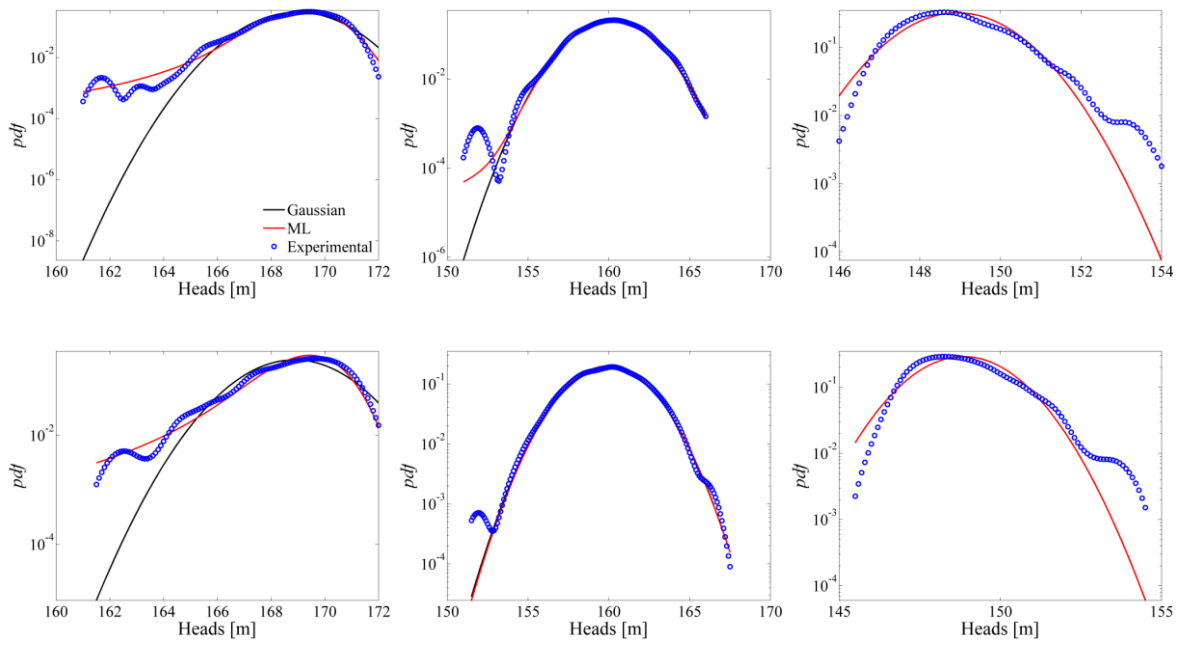

Figure 6.5.1: SISIM-based pdfs of vertically averaged (over the full thickness of the domain) hydraulic heads at control points (a) 24, (b) 64, and (c) 124 (see Figure 6.2.1). Corresponding results related to hydraulic heads vertically averaged along the top 25 meters of the domain are also reported for control points (d) 24, (e) 64, and (f) 124. ML fits for the Gaussian and α-stable distributions are also reported.

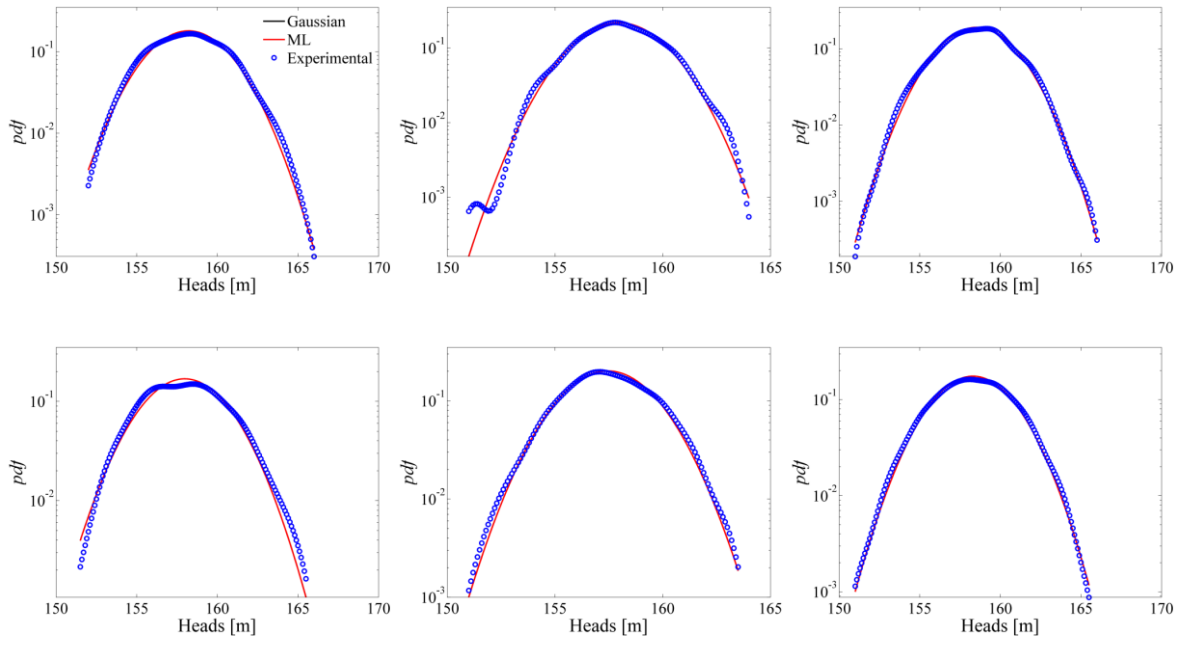

Figure 6.5.2: SISIM-based pdfs of vertically averaged (over the full thickness of the domain) hydraulic heads at control points (a) 36, (b) 76, and (c) 136 (see Figure 6.2.1). Corresponding results related to hydraulic heads vertically averaged along the top 25 meters of the domain are also reported for control points (d) 36, (e) 76, and (f) 136. ML fits for the Gaussian and α-stable distributions are also reported.

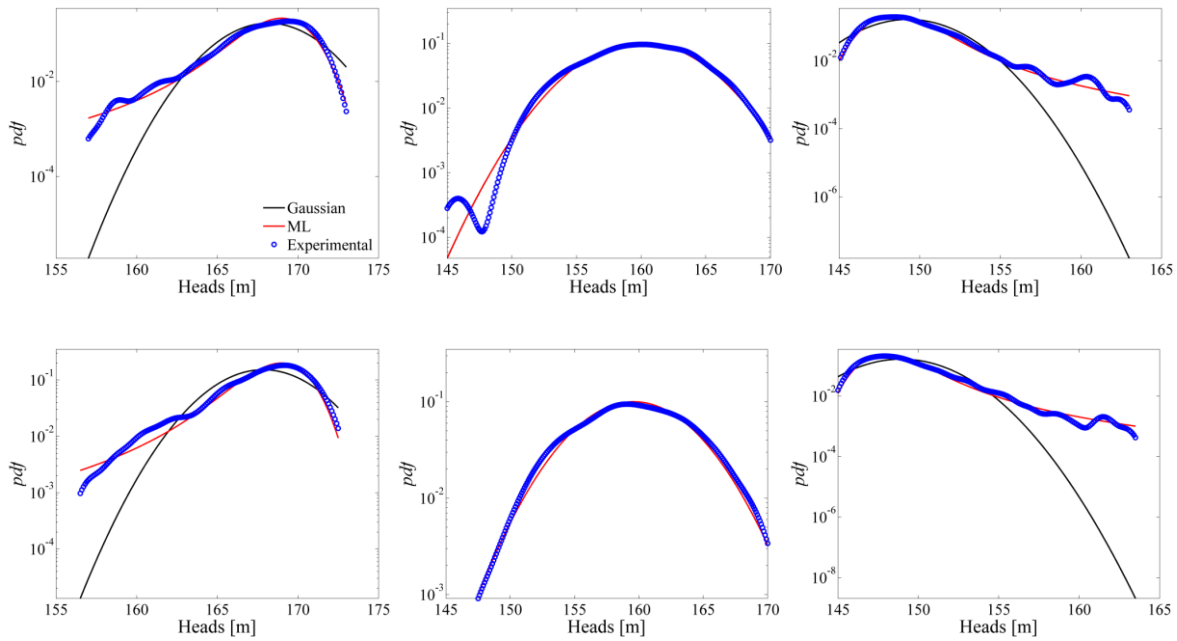

Figure 6.5.3: TPS-based pdfs of vertically averaged (over the full thickness of the domain) hydraulic heads at control points (a) 24, (b) 64, and (c) 124 (see Figure 6.2.1). Corresponding results related to hydraulic heads vertically averaged along the top 25 meters of the domain are also reported for control points (d) 24, (e) 64, and (f) 124. ML fits for the Gaussian and α-stable distributions are also reported.

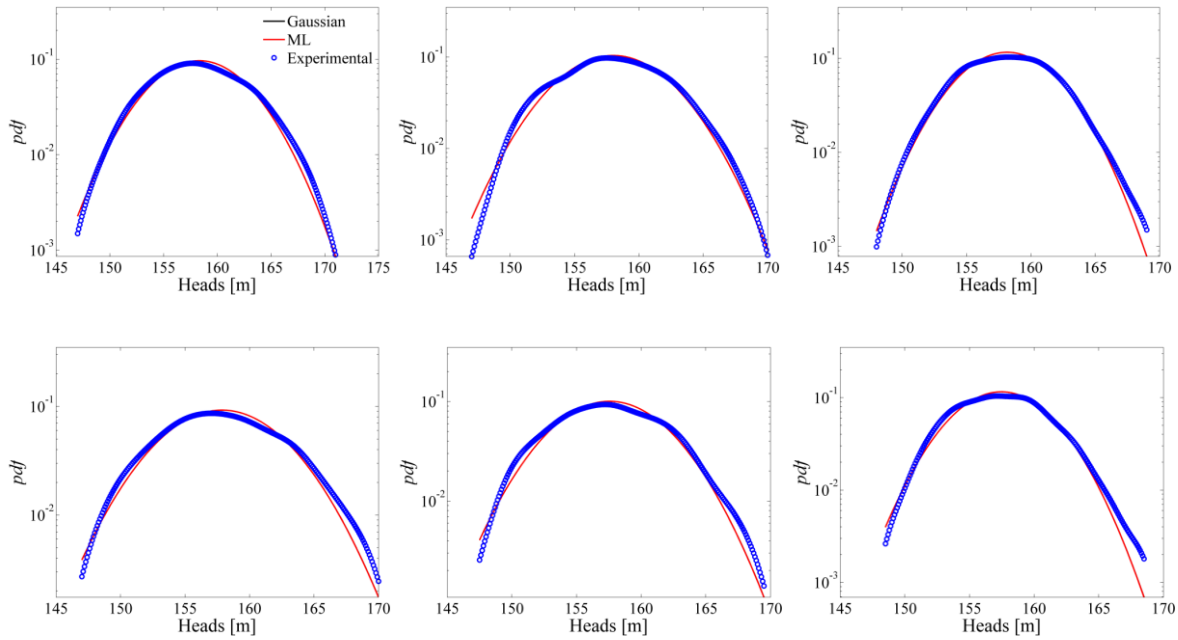

Figure 6.5.4: TPS-based pdfs of vertically averaged (over the full thickness of the domain) hydraulic heads at control points (a) 36, (b) 76, and (c) 136 (see Figure 6.2.1). Corresponding results related to hydraulic heads vertically averaged along the top 25 meters of the domain are also reported for control points (d) 36, (e) 76, and (f) 136. ML fits for the Gaussian and α-stable distributions are also reported.

Figure 6.5.5.a reports the N-S spatial dependence of $\hat{\alpha}$ estimates associated with the sample distributions of vertically averaged (over the complete thickness of the domain) hydraulic heads for both the SISIM- and TPS-based results. In general, we note that the tails of the head distributions are longer (i.e., $\hat{\alpha}$ is smaller) for TPS- than for SISIM-based simulations and decrease as the distance from the prescribed (deterministic) head boundaries increases. For large distances from these boundaries or close to the pumping well the distributions tend to become Gaussian (i.e., $\hat{\alpha}$ = 2.0). At locations close to the fixed head boundaries, the distribution is skewed towards values which are representative of the inner portion of the domain.

Conversely, the ***pdfs*** of vertically averaged heads along the W-E direction appear to be well interpreted by the Gaussian model (i.e., $\hat{\alpha} \approx 2.0$), regardless the thickness of the vertical averaging segment and the generation model adopted. The prescribed flux boundary conditions introduce less constraints (through the Monte Carlo realizations) to the heads computed along the W-E direction and the shape of the sample head distributions is not significantly modified when approaching the boundaries.

Figure 6.5.5.b reports the N-S spatial dependence of $\hat{\sigma}$ estimates obtained for the distribution of vertically averaged hydraulic heads for both the SISIM- and TPS-based results. Since the scale parameter σ is linked to the (ensemble) variability of the variable (in particular its square value is equal to half the variance when α = 2.0), we observe an increase of $\hat{\sigma}$ with the distance from the fixed head boundaries. Consistent with the analysis presented above, $\hat{\sigma}$ is significantly larger for the TPS-based results than for their SISIM counterparts.

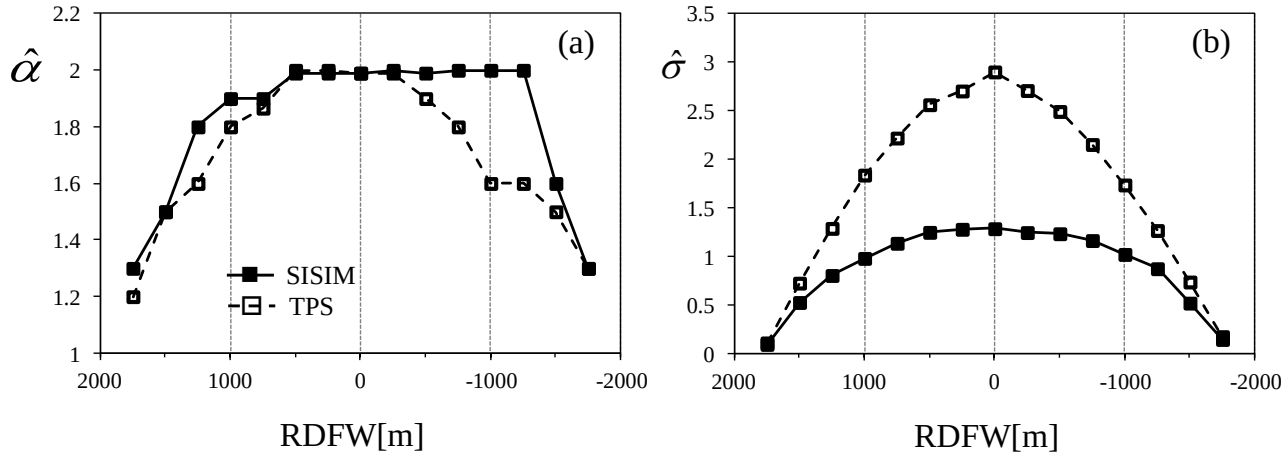

Figure 6.5.5: Estimates of (a) stability index ($\hat{\alpha}$) and (b) scale parameter ($\hat{\sigma}$) of hydraulic heads integrated along the full aquifer thickness versus RDFW (Relative Distance From Well) along the N-S direction.

7. Discussion

In this section we present the discussion of the results of the two previous chapters, regarding the geostatistical and the flow field simulations. We do this in order to come up with some conclusions and a better insight of the combined information acquired from the joint analysis of both methodologies' output.

7.1. Practical applications

Our results provide a basic component which can be employed to quantify a hydraulic head threshold that might be dangerous for a given location (for instance, an overabstraction that leads to a pronounced lowering of piezometric head). Probability distributions of hydraulic heads calculated through different stochastic reconstruction methodologies, provide a way of comparing and quantifying the uncertainty stemming from competing conceptual system models and associated with the estimation of the hydraulic head thresholds that might endanger the equilibrium of protected natural areas.

7.2. Objective and novelty

We aim at analyzing the way hydraulic heads probability distributions (in terms of functional form and parameters) are affected by the two reconstruction methods adopted for the aquifer system, i.e. embedding or not a conceptual model of facies contact. We do so by considering a convergent flow which, to the best of our knowledge, has not been analyzed in this context and is of critical importance in environmental applications of the kind described above.

Low-order (statistical) moments (i.e., mean and variance-covariance) of hydraulic heads in unbounded and bounded domains under uniform (in the mean flow) conditions have been investigated, amongst others, by: Dagan (1985), Rubin and Dagan (1988, 1989), Osnes (1995), Ababou et al. (1989), Dagan (1989), Guadagnini and Neuman (1999a, b). Our intent, in the bibliographic research, was to provide a review of the works dealing with the analysis of the probability density of hydraulic heads, with specific reference to the non-uniform (in the mean) flow configuration we analyzed. There are not too many works dealing with this specific issue. Indeed, this is a strong point of our study and it confirms the novelty of our analysis.

The target Environmental Performance Metrics (EPMs) we consider are (*a*) point and (*b*) vertically integrated hydraulic heads. The latter are the quantities which can be typically observed under field conditions, e.g. through screened boreholes, and for instance can be linked to water levels in natural springs which are fed by confined aquifers. The joint impact of heterogeneity model and vertical averaging under the combination of natural and forced flow regimes has not been addressed previously. We have approached this work by taking the point of view that the basic question is not which model is best, but how the models compare and what they tell us jointly about the physical quantities and process of interest, i.e. the probability distribution of hydraulic heads. This is the most that can be done in the absence of independent physical data or, possibly, in the presence of a very limited set of observations on the state variable. Of course, model identification is a very relevant and delicate subject, but goes beyond the scope of the present study. For a deeper insight to this specific issue we redirect the reader to the works published by Riva et al. (2010, 2011), Panzeri et al. (2013) and Bianchi Janetti et al. (2012).

We reiterate that we are interested in the comparison between outcomes associated with two competing models and we do think this to be a relevant aspect. Thorough understanding and quantification of the influence of a model on the variability of a system response can also be considered as a first step in a detailed model identification analysis. We think that such a comparison is of relevance, especially in the presence of (statistically) non-stationary hydraulic parameter distributions and non-uniform flow conditions of the kind we analyze here. The study we perform can be framed in the context of probabilistic risk assessment (PRA) of hydrogeological scenarios, thus facilitating uncertainty quantification associated with incomplete knowledge of the geological architecture of the system.

Albeit model calibration studies in the context of a truncated plurigaussian framework have been presented in the past (e.g., Mariethoz et al., 2009) our objective here is different, as we pose ourselves the question: "*How does the adoption of two simulation strategies embedding different system conceptualizations impact the statistics of the state variable field in a representative field scale aquifer model?*". The outcome of such a study is potentially relevant in intrinsic vulnerability studies, where one is interested in quantifying the probability associated with given hydraulic head values at target locations in the system as a function of the conceptual uncertainty associated with the geological model. This is more than a sensitivity study on the effect of facies distribution because it includes the effect of different modeling choices, based on the expertise of the groundwater flow modeler and field geologist.

7.3. Indicator simulations

When assessing model reliability against controlled synthetic test cases under different conditions, studies presented in the literature are mainly based on realistic images where the level of realism is difficult to quantify, as it can be assessed only in qualitative way. Therefore, given the purpose of our analysis, we preferred considering an actual set of lithological information which is associated with an observation window which is representative of a field scale setting. In our specific case, we think we have at our disposal a reasonably abundant data set, as compared to typically available information content of this kind for the investigated scale. We further note that we employed the available data not only for estimation of volumetric proportions or variogram assessment, but also to analyze the actual hierarchy of the system architecture in the area and, therefore, for the selection of the reconstruction methodology. When model performance needs to be assessed, then we agree that the best option is always to start from hypothetical settings, where a ground truth is clearly defined.

However, we are not aware of a comparative study of the kind we propose in the manuscript in presence of a non-uniform flow field. Indeed, this is an environmentally relevant scenario and we decided to analyze the (random) variability of the response of the system with two relatively simple and well-known techniques which are commonly employed for aquifer simulation. As such, we decided to compare the effects of the two techniques by observing the impact of the system conceptualization, as embedded in the lithotype rule, when all other inputs are kept constant.

7.3.1. Comparison of SISIM and TPS results

From a qualitative point of view it can be noted that TPS renders an improved continuity of sedimentary structures, which are elongated along the N-S direction, consistently with observations from surface lithological maps. Both methods reproduce the anisotropy pattern detected in the system.

Along the N-S direction the SISIM method yields persistent clusters characterized by small ($\approx 10^{-7}$ m/s) and large ($\approx 10^{-4}$ m/s) conductivity values while the TPS-based results are associated with a relatively uniform ($\approx 10^{-5}$ m/s) $\boldsymbol{K}$ distribution and a large Log$\boldsymbol{K}$ variance.

A key difference between the fields of Log$\boldsymbol{K}$ sample variance, obtained with the two methods, lies in the relatively uniform distribution of persistently large values which is visible in the TPS results. This is opposed to the outcome of SISIM simulations, which are associated with a spatially heterogeneous pattern (alternating low and large variance values). The effect of the conditioning data on the spatial persistence of variance values is different for the two methodologies, due to the geological constraints imposed in the TPS procedure through the adopted contact rules. These results are consistent with the spatial pattern which can be detected for single realizations of hydrofacies distributions.

Both simulation methods are conditional on the same dataset. Both techniques are variogram-based and are directly comparable. Comments about the merits of the truncated plurigaussian generation technique as opposed to a sequential indicator simulation are available in, for instance, Mariethoz et al. (2009) and in the **Introduction** of this manuscript. This points out the worth and value of numerical studies of the kind we perform, to understand the type of variability which is imprinted to the system response (in terms of key

statistics of hydraulic heads) by adopting or neglecting conceptual knowledge about the geological setup of an aquifer.

7.3.2. Providing guidelines

GEOLOGICAL SETUP AND AQUIFER SIMULATIONS

The thickness of the aquifer system is not constant across the area under study where the borehole network associated with the lithological data is set. The domain we adopt in our simulations is extracted from the real aquifer system and its thickness was selected to include its key features observed in the field. In other words, since one of the objectives of this study is to analyze the way the vertical variability of hydraulic heads is impacted by facies distribution, boundary conditions and/or source terms (without considering the effect of the particular geometry of the bottom of the aquifer), we adopt in the following a constant thickness B = 100 m which is representative of an average thickness of the system in the area.

We start by noting that we did not have availability of hard hydraulic conductivity data with a level of discretization which was nearly comparable with that of the lithological information we employed in our study. There is typically conceptual uncertainty associated with the selection of a model which can represent the heterogeneity of an aquifer at different scales of observation. Here, we are interested in an observation window which encompasses horizontal and vertical scale lengths of the order of 4000 m and 100 m, respectively. At these scales the distribution of lithotypes in the system is a key driver for the distribution of groundwater flow quantities. On the other hand, the spatial heterogeneity of hydraulic parameters within a given lithotype is relevant at smaller scales of observations as seen, for example, in the works of Winter et al. (2003) and Riva et al. (2006, 2008, 2010). Treating both sources of uncertainty (i.e., uncertainty in the location of the boundaries between

different materials and in the distribution of attributes within each material) can be performed, e.g., in a composite medium framework, along the lines of the references cited above. Indeed, we are adopting a composite medium approach where facies distribution is uncertain and hydraulic attributes are deterministically known.

VERTICAL PROPORTION CURVES

To simplify the problem under study we decided to keep invariant the hydrofacies distribution along the vertical direction. We did generate our indicator fields by imposing that the global proportion of a given facies does not vary among realizations. The pattern of the vertical distribution of facies proportions varies across realizations, as an effect of the conditioning on the available data. We estimated the vertical distribution of facies proportions from the complete available dataset. The material proportions are not uniform along the vertical. Therefore, albeit not specifically set in the generation procedure, there is a vertical variability of facies proportions due to the conditioning effect. We further note that the introduction of spatially variable material proportions can be accomplished, for example, along the lines of Mariethoz et al. (2009) or Yarus et al. (2012) and the references therein.

VARIOGRAM ANALYSIS

With reference to the functional format of the variogram structure, we start from the premise that nature is heterogeneous and physical properties are correlated in space. This has been abundantly recognized in the literature (e.g., De Marsily, 1986; Dagan and Neuman, 1997; Zhang, 2002). Unfortunately in most cases, available data are not good enough to discern the variogram underlying a correlated random field, especially along the horizontal direction (for scales of the kind we investigate). Then the variogram provides information about the sill and (with more difficulty and uncertainty) the range. Interpretation of this

information is the task of the modeler. While one could (in principle) fit a pure nugget to available data, it is very common to adopt models that incorporate spatial correlations (either finite or distributed on a hierarchy of scales) and small scale variability (i.e., a nugget effect). Therefore, we feel that the choice of a purely random distribution of categories (i.e., geomaterials) is not properly representative of actual fields, which should not (in general) be considered as a purely random process, due to the nature of depositional processes. Since this is known in the literature, we prefer not to add further particular comments on this aspect in the manuscript.

For the SISIM approach we computed the experimental indicator variograms with a GSLIB routine. Then, we performed an RMSE analysis to make a decision upon the best semivariogram model to use as input in the geostatistical simulations, for every lithotype. On the other hand, we adopted an iterative procedure to infer the variograms for the truncated plurigaussian simulations procedure, which is based on the work (and routines) presented by Emery (2007). This allowed us to infer the parameters of the variograms of the two Gaussian fields (G1 and G2) that ensure compatibility with the indicator variograms describing the geostatistical structure of the facies, as derived by the available field data. As such, SISIM and TPS methodologies are directly comparable.

7.3.3. Consequences of using SISIM and/or TPS

HONORING THE INPUT VOLUMETRIC PROPORTIONS

The apparent inability of the two methods to reproduce exactly the target volumetric proportions of hydrofacies for each realization of the collection, might be related to the low relative proportion (which is < 2.3%) between the conditioning data ($\approx 7.5 \times 10^3$) and the high number of simulated values ($\approx 3.25 \times 10^5$). This is specifically critical for the horizontal

direction where, as typically observed in practical applications, the spacing between data locations is larger than that associated with the vertical direction. However, the results listed in **Table 5.3.3.1** (Chapter 5) can be considered satisfactory for the purposes of our synthetic study. A significant relative error (≈ 20%) can be observed only for the SISIM-based reconstruction of the less abundant hydrofacies (F2). In general, the average volumetric proportions based on TPS results are closer to the input values than the SISIM-based counterparts.

Here we are referring to the reproduction of the material proportion in an ensemble (or multi-realization) sense. Considering the results listed in **Table 5.3.3.1** (Chapter 5), we find that our simulated fields satisfactorily represent the overall observed facies proportions in the multi-realization context, albeit not exactly for each realization. We wanted to point out that the ratio between conditioning-to-simulation points is among the important factors that control the simulated facies proportions. We based this observation on the work by Dell'Arciprete et al. (2012), who noted that (sic): "*a critical parameter in conditional simulations is the ratio between the number of conditioning data and the number of simulated cells*". These authors tested the effect of three different densities of conditioning points for the same case study. They observed that the facies proportions were correctly reproduced for conditioning-to-simulation points' ratio of about 10% whereas some discrepancies were observed if this ratio is lowered by about one order of magnitude (e.g., 1.7%).

HARD DATA CONDITIONING

Figures **5.3.4.1** and **5.3.4.2** (Chapter 5) aim at depicting the way the spatial heterogeneity of hydraulic conductivity is represented by the two simulation methods, in terms of spatial distribution of mean and variance of Log$\boldsymbol{K}$.

Hard data are accounted for when performing the geostatistical simulations. Note that no data are available in the vertical cross-sections displayed in the aforementioned figures. We selected these types of cross-sections to show the way the impact of conditioning points propagates in space for the two generation methodologies we employed. The SISIM-based scenario is associated with a more pronounced impact of the nearby conditioning points than TPS-based results are. This is explained by the different treatment of the heterogeneity that both methodologies embed. SISIM renders more "*salt and pepper*" features than TPS does. TPS displays a more correlated structure of the heterogeneity. This is also reflected by the different values of the variogram ranges which are estimated for the two methods.

7.3.4. When should be used one or another? Both?

There is no a more valid or unique answer to this "*ill-posed*" question. A fairly neutral answer would be, "*depends on the purpose of your own study*". What is invariant, a priori, is the initial amount of hard data. This situation can change if more data is added during the development of the research project. Assuming that one has very scarce (or any) conditioning hard data to start with, choosing SISIM would be more appropriate since it does not need as input a lithotype rule. If a TPS approach is pursuit even in the absence of conditioning hard data, maybe the best way to proceed would be trying several lithotype rules and assessing qualitatively the output simulations in contrast with the available regional/local geological information coming from different sources (e.g., surface lithological maps, outcrop information, previous studies/surveys in the same area or its premises/vicinities, etc.). The problem in this case would be coming up with a rather sensible facies configuration in the absence of conditioning hard data. Therefore, when enough conditioning hard data is available, TPS might be an appropriate choice since it allows a more complex treatment of the heterogeneity embedded in the actual groundwater system.

In terms of implementation and computational cost, once the input parameters are assessed for the two employed methodologies, both are comparable. The same applies in terms of post-processing of the data. As a whole, we spent less than a week (per method) for computing the geostatistical simulations using a regular PC. It took about a week to run each of the two sets of 1000 MC flow simulations, for both SISIM and TPS, with the same computer. Finally, the post-processing and analysis of the output data took several months due to the big amount of information stored and the various statistical analyses that were performed.

We are conscious that for actual practitioners this kind of analysis might sound a bit cumbersome, but could be used as a preliminary step in the context of groundwater vulnerability assessments related to excessive drawdowns (due to different existing forcing terms, for instance water overabstractions) that could represent a real menace to water resources or protected areas such as springs networks or wetlands. Choosing one or another model, or both, would be a selection made from the experienced modeler. When pursuing a worst case scenario analysis, TPS would be the best choice (among the proposed two) since it gives a better scan (due to its higher variability of its output) of the possible drawdown values.

7.4. Flow field simulations

We are considering superimposition of three-dimensional natural and forced flows which, to the best of our knowledge, has not been addressed previously with respect to the specific problem we analyze (i.e., assessment of the ***pdf*** of hydraulic heads). In addition to this, the effect of vertical averaging of hydraulic heads might also be influenced by the conceptual model adopted for the system and has not been analyzed in the available literature. Our results show that spatial correlation and probability distributions of point and vertically averaged values of hydraulic heads, display similar key representative features and patterns. Therefore, typical measurements taken in screened boreholes can be used to infer qualitative information about the correlation structure and the statistical properties of heads. The latter could then be employed within typical Probabilistic Risk Assessment procedures.

With reference to the effect of boundary conditions, we always have to deal with boundaries. This is the reason why analytical (or numerical) solutions extracted only in the central part of the system, where the boundary effects are minimized, are seldom applicable in practice. In the scenario we consider, we have a competition between the effect of the source term and the boundaries. One of the points we addressed is the way the empirical ***pdf*** of hydraulic heads (both point and vertically averaged) is deformed with relative distance from the well and boundaries and the way the position of a monitoring point is influenced by these competitive effects. Note that the extent of our domain is just a few correlation scales so that, technically all points are influenced by the boundaries under a uniform in the mean flow condition such as the one studied, for example, by Nowak et al. (2008).

7.4.1. Comparison of SISIM and TPS results

Figures **Figure 6.2.2** and **Figure 6.2.3** allowed us to illustrate the spatial distribution along selected cross-sections of the sample mean hydraulic heads calculated for both simulation methods. We pointed that, regardless the width of the selected vertical integration segment, the hydraulic head values are highest for SISIM in the northern and eastern subregions of the simulation domain. On the other hand, TPS renders largest average values in the southern and western parts of the system. The largest drawdown at the well is always obtained from the TPS method. TPS yields the largest sample standard deviation of hydraulic heads, consistent with the results illustrated in **Table 5.3.3.1**. The observed behavior can be related to the differences in the internal structure of the hydrofacies and hydraulic conductivity distributions generated with the two selected methodologies. To illustrate this, we used Figures **5.3.4.1** and **5.3.4.2** where we depicted vertical distributions of SISIM-based sample mean and variance of the decimal logarithm of hydraulic conductivities, Log$\boldsymbol{K}$, obtained along the two cross-sections represented in **Figure 6.2.2**. **Figure 6.2.3** shows corresponding results obtained from the TPS-based simulations. The cross-sections depicted in Figs. 6.2.2 and 6.2.3 do not contain conditioning data and show the way information about conditioning propagates in space for the two methods considered. In particular, it is noted that the SISIM-based scenario is associated with a more pronounced impact of the conditioning points than TPS-based results are, where the effect of the selected lithotype contact rule is superimposed to the impact of the conditioning points. This is also reflected by the different values of the variogram ranges which are estimated for the two methods (see Chapter 5).

Along the N-S direction the SISIM method yields persistent clusters characterized by small ($\approx 10^{-7}$ m/s) and large ($\approx 10^{-4}$ m/s) conductivity values while the TPS-based results are associated with a relatively uniform ($\approx 10^{-5}$ m/s) $\boldsymbol{K}$ distribution and a large Log$\boldsymbol{K}$ variance.

This observation is consistent with the quite regular behavior displayed in Fig. 6.2.2.a by the TPS-based mean head (μ_{TPS}) and its large associated variance, when compared to the corresponding moments estimated on the basis of SISIM results. A different behavior is noted along the W-E direction where a relatively uniform mean Log***K*** distribution associated with SISIM output is replaced by a series of elongated structures honoring jointly the conditioning data and the imposed contact rule adopted for the TPS simulation scheme. As a consequence, while the mean head profile based on SISIM results is approximately symmetric around the well in Fig. 6.2.2.b, the TPS results are characterized by large drawdowns in the eastern part of the domain where there is the occurrence of elongated structures associated with small Log***K*** (Fig. **5.3.4.2**.c).

In Chapter 6 we presented figures showing the vertical distribution of the variance of point values of ***h*** at various relative distances from the pumping well along the N-S and the W-E directions and calculated from the SISIM- and the TPS-based simulations.

Regarding the SISIM-based scenario:

- The variance of point values of ***h***, forms non-uniform vertical profiles which are almost symmetric around the intermediate depth of the system.
- Differences between values of variance at the top and bottom of the aquifer are mainly related to the conditional nature of the simulations.
- The largest values of variance occur at locations close to the well and to the impervious boundaries.

- Hydraulic head variance tends to decrease and its vertical profile to become more uniform with increasing relative distance from the extraction well measured along the mean flow direction. This result is similar to what observed by Guadagnini et al. (2003).
- Along the W-E direction the variance tends to first decrease and then to increase with distance from the well and reaches a local maximum at the no-flow boundaries.
- The qualitatively observed increase in the correlation between hydraulic head values at mid locations along the vertical and the wavy behavior noted for the vertical distribution of variance values are consistent with the persistence of clusters of fine materials in the area stemming from the SISIM generation method.

The variance distributions associated with the TPS method:

- They are typically characterized by a reduced vertical variability at locations along the N-S direction and generally display larger values than those associated with SISIM-based results.
- Along the W-E direction, it is noted that the variance associated with locations at the bottom of the system is consistently larger than that related to points close to the top. These effects are due to the imposed contact rules between hydrofacies, which tend to reproduce the natural dip of the geological structures in the system and increase the possibility of occurrence of vertical fluxes.

The imposed contact rules tend to increase the internal variability of the system and result in a negative impact on the predictability of hydraulic heads which tend to be characterized by large variances. The general behavior of the covariance matrix calculated between point values of hydraulic heads is qualitatively similar for the two simulation methods (see Figs. 6.3.1.d-i and 6.3.2.d-i). A strong non-stationary behavior and heterogeneous distribution of typical scales of head correlation can be qualitatively inferred from Figs. 6.3.1 and 6.3.2. Regardless of the generation scheme, along the mean flow direction (N-S) the rate of decrease of the vertical covariance of ***h*** appears to increase (thus suggesting a decrease of vertical correlation scales) with increasing distance from the pumping well (see Fig. 6.3.1.d-f and Fig. 6.3.2.d-f). On the other hand, along the W-E direction (perpendicular to the mean base flow), the generation scheme strongly influences the correlation structure of ***h***. SISIM-based results suggest a degree of vertical correlation of ***h*** that tends to increase with the distance from the pumping well (see Figs. 6.3.1.g-i). TPS-based outcomes are not prone to an immediate interpretation. The degree of vertical correlation of hydraulic heads appear to be higher at locations in the western than in the eastern region, consistent with the occurrence of elongated structures in the latter region and the almost uniform distribution of Log***K*** along the western area (Fig. 5.3.4.2.c). A corresponding analysis (details included in the **Appendix to Chapter 7**) revealed that (integrated and point-wise) hydraulic head values display an increased degree of horizontal correlation along the direction perpendicular to mean flow and when an SISIM rather than a TPS approach is used. It is also noted that the horizontal head covariance tends to display the slowest rates of decay (thus suggesting relatively large horizontal correlation scales) for reference points located close to the impervious (horizontal and vertical) boundaries. These types of results can be useful during typical statistical analyses of monitored ***h*** values, which are often performed assuming that variables are uncorrelated in space. Our study shows that

this latter assumption is roughly satisfied only when considering points which (*a*) lie along the mean direction of the system base flow and (*b*) are located relatively far from the source/sink terms.

We reported in Chapter 6, examples of quantitative results on the effect that vertical averaging of hydraulic heads along different depth intervals can have on the vertical correlation structure. Despite the loss of resolution and information along the vertical direction due to spatial averaging, the main representative features and patterns observed for point-values based covariances remain visible. The same observation can be made for TPS-based simulations.

Also in Chapter 6 we presented results concerning the N-S and W-E spatial dependence of the sample ***pdf*** of hydraulic heads averaged over the whole aquifer thickness and calculated via the SISIM- and TPS-based reconstruction methods. The SISIM-based setting appears to be associated with the largest peakedness of the empirical distributions. Visual inspection of sample ***pdfs*** suggests that a Gaussian model might not always be appropriate to characterize the observed behavior. These ***pdfs*** are sometimes characterized by heavy tails, for which, e.g., an α-stable distribution might be an appropriate interpretive model. At the light of these results, hydraulic head values calculated at different locations in the system and averaged along vertical segments of various thicknesses were examined.

We recall that an α-stable distribution is described by four real-valued parameters: stability index $\alpha \in (0, 2]$, skewness $\beta \in [-1, 1]$, scale $\sigma > 0$ and shift μ. The following parameterized form, described by Samorodnitsky and Taqqu (1994), is applied to define the log characteristic function of an α-stable variable, X:

$$\ln\left\langle e^{i\phi X}\right\rangle = i\mu\phi - \sigma^{\alpha}|\phi|^{\alpha}\left[1+i\beta\,\mathrm{sign}(\phi)\,\omega(\phi,\alpha)\right]; \quad \omega(\phi,\alpha)=\begin{cases} -\tan\dfrac{\pi\alpha}{2} & \text{if } \alpha\neq 1 \\ \dfrac{2}{\pi}\ln|\phi| & \text{if } \alpha = 1 \end{cases} \tag{1}$$

Here, $\langle\ \rangle$ indicates the expected value (ensemble mean), ϕ is a real-valued parameter and $\mathrm{sign}(\phi)$ = 1, 0, –1 if ϕ > 0, = 0, < 0, respectively. The optimal estimated values $\hat{\boldsymbol{\theta}} = (\hat{\alpha}, \hat{\beta}, \hat{\sigma}, \hat{\mu})$ of the parameters array $\boldsymbol{\theta} = (\alpha, \beta, \sigma, \mu)$ are obtained through the maximum likelihood (ML) approach (Nolan, 2001) upon maximizing the likelihood

$$l(\boldsymbol{\theta}) = \sum_{i=1}^{n} \log f(X_i \mid \boldsymbol{\theta}) \tag{2}$$

with respect to $\boldsymbol{\theta}$, n and $f(X \mid \boldsymbol{\theta})$ respectively being the sample size and the conditional probability density function of *X*. ML is implemented through the program STABLE (Nolan, 2001) that provides reliable estimates of stable densities for α > 0.1. A Gaussian distribution is recovered when α = 2.

We performed a statistical analysis, at selected locations, to examine the influence of the averaging procedure along the vertical direction on the simulation results. The point-wise and vertically averaged values of ***h*** share some notable statistical properties. The tails of the hydraulic heads ***pdfs*** along the N-S direction become increasingly evident for both simulation schemes and hence best interpreted through an α-stable distribution, as the distance from the pumping well increases and the boundaries are approached. The observed similarities between the shapes of the sample ***pdfs*** of point-wise and vertically averaged heads suggests the possibility of capturing the key features of the statistical behavior of ***h*** by means of vertically integrated observations.

The results introduced by **Figure 6.5.5**.a show that in general:

- The tails of the head distributions are longer for TPS- than for SISIM- based simulations and that they decrease as the distance from the prescribed (deterministic) head boundaries increases.
- For large distances from the prescribed flow boundaries or close to the pumping well the distributions tends to become Gaussian (i.e., $\hat{\alpha}$ = 2.0).
- At locations close to the fixed head boundaries, the distribution is skewed towards values which are representative of the inner portion of the domain.
- The ***pdfs*** of vertically averaged heads along the W-E direction appear to be well interpreted by the Gaussian model (i.e., $\hat{\alpha} \approx 2.0$), regardless the thickness of the vertical averaging segment and the generation model adopted.
- The prescribed flux boundary conditions introduce less constraints (through the Monte Carlo realizations) to the heads computed along the W-E direction and the shape of the sample head distributions is not significantly modified when approaching the boundaries.

Figure 6.5.5.b reports the N-S spatial dependence of estimates $\hat{\sigma}$ obtained for the distribution of vertically averaged hydraulic heads for both methodologies. Since the scale parameter σ is linked to the (ensemble) variability of the variable, we observe an increase of $\hat{\sigma}$ with the distance from the fixed head boundaries. Consistently, $\hat{\sigma}$ is significantly larger for the TPS-based results than for their SISIM counterparts.

7.4.2. Providing guidelines

NUMERICAL GRID

The numerical solution of the grid associated with flow (and eventually transport) can and in some cases should be finer than the one adopted for the generation of the hydrofacies. In particular, accurate numerical solution of flow requires a fine grid close to source/sink terms such as wells. This is not associated with downscaling. We are stating that a generated value of a property is representative of a given volume (or block) and, as such, is constant within the volume itself (even if this volume cell is subdivided for an accurate solution of the flow problem). Assignment of hard data (which in our case is just hydrofacies category) to the finer grid employed for flow, has been accomplished the way described in Chapter 4. A similar strategy for the setting of the numerical grid associated with the flow problem has been adopted in previous works (e.g., Riva et al., 2006, 2008 and 2010).

SISIM vs TPS

The difference between the TPS and the SISIM reconstruction of facies and associated Log$\boldsymbol{K}$ distribution is not only localized along the boundaries, but is distributed across the simulated domain. An example of quantitative comparison between the two Log$\boldsymbol{K}$ reconstructions (in terms of ensemble mean and variance) is offered in Chapter 5. Therefore, the ***pdf*** of hydraulic heads obtained via SISIM- or TPS-based simulation are different not only close to the boundaries.

MOMENTS' CONVERGENCE

We think that this is related to the more structured heterogeneity which is embedded in the conceptual model underlying the TPS scheme. Each realization in the TPS method is constrained by the lithotype contact rule. This implies that the occurrence of a given facies at

a location is accompanied by the appearance of other facies in the surrounding blocks in compliance with the contact rule selected. This would enhance the variability of proportions across realizations, thus lowering the speed of convergence of moments. We note that this effect is not dramatic in the setting considered, probably due to the contact rule selected, where all facies are in contact with F1 (the most abundant, fine materials).

With reference to the stabilization of second order moments, the work of Ballio and Guadagnini (2004) points out the need to increase by at least an order of magnitude the number of simulations to discern some significant effects. We anticipate the computational demand to be more severe for the stabilization of the complete ***pdf***. Nevertheless, on the basis of our experience, we think that the number of realizations performed allows to capture the key points and shape (albeit not all the details) of the distributions. We further note that the hydraulic head is a regular function, in the sense that it smoothes the high wave-number components of hydraulic conductivity (***K***) spatial distribution which (in our setting) is in turn related to facies proportion.

PDF TAIL OSCILLATIONS

It is likely that these oscillations are an artifact of the number of Monte Carlo iterations performed. We adopted different binning strategies for the representation of the simulation results and oscillations at the tails were always present to some extent. On the basis of our experience, it is always difficult to stabilize all moments of a probability distribution and there is not a universally recognized criterion to assess stability of all nodal ***pdfs*** of state variables of interest (e.g., hydraulic heads). The problem is exacerbated for long-tailed ***pdf*** distributions, where oscillations in the tails are visible even with a very large number of data (such as 100,000 data as shown for example by Guadagnini et al., 2012).

7.4.2.1. Vulnerability issues

Probabilistic risk assessment (PRA) is a key application of stochastic hydrogeology and relies on the characterization of the probability distribution of target state variables of groundwater flow and transport. To the best of our knowledge, the characterization of the probability distribution of point and vertically averaged hydraulic heads in large scale randomly heterogeneous aquifers subject to pumping (and described by different hydrofacies generation schemes of the kind we consider) is still lacking in the literature.

For the purpose of our work we think that a qualitative assessment based on visual inspection of generated fields and a discussion grounded on low order-moments enables one to grasp the key elements controlling the probabilistic distribution of the hydraulic heads.

Concerning the conclusions of our study, and the way they can inform how a given application is approached, we highlight that a TPS-based approach can be considered as more conservative than its SISIM-based counterpart because it renders an increased range of variability in the collection of realizations of hydraulic heads.

8. Conclusions

Our work leads to the following major conclusions.

- Hydraulic heads deduced from TPS-based flow simulations exhibit larger variability than their counterparts evaluated by an SISIM-based modeling strategy. This is a consequence of the fact that setting geological contact rules, as considered within a TPS simulation scheme, can lead to an increased variability in the internal architecture of hydrofacies distributions within a relatively large-scale aquifer model of the kind we consider.

- Covariance matrices and probability distributions of point and vertically averaged values of hydraulic heads, display similar key representative features and patterns. Therefore, typical measurements taken in screened boreholes can be used to infer qualitative information about the correlation structure and the statistical properties of heads. The latter can then be employed within typical Probabilistic Risk Assessment procedures.

- Probability distributions of heads close to prescribed head boundaries are skewed, show a long tailing behavior and are accurately fitted by α-stable distributions. The tails of the distributions are longer for TPS- than for SISIM- based results.

- Probability distributions of heads close to impervious boundaries or to source terms (such as pumping wells) appear to be almost symmetric and reasonably well interpreted by Gaussian models.

- Due to the enhanced degree of variability displayed within the collection of simulations and to the occurrence of long-tailed ***pdfs***, reliance on a TPS scheme yields a broader range of possible drawdown values for the simulated groundwater system. As such, TPS-based results are associated with the most conservative (in terms of extreme values) drawdown estimates which can then be related to a given threshold probability of occurrence in the context of PRA protocols where the target environmental metric is the piezometric drawdown.

8.1. Future work

Intuitively a further step towards enriching the current stage of research would be exploring the effect of other commonly used geostatistical algorithms/techniques/procedures on the hydraulic heads ***pdfs***. Ideally they should treat natural heterogeneity in a similar way (pixel-based methods) likewise the two explored models, allowing to condition the stochastic simulations by means of hard and/or soft data of the kind presented in our study (i.e. lithological information, extracted from a borehole network). Among the interesting available schemes, Transition Probabilities would be an appropriate choice.

Choosing to simulate a bigger area, and a thicker groundwater system, would improve the aim of characterizing aquifer vulnerability. Especially relevant is the cell size (that should be decreased in the three space dimensions), as well as the interesting effect of introducing more wells in the simulation domain. In the real double aquifer system, the existing aquitard plays a crucial role. The aforementioned structure separates the shallow aquifer, polluted from agricultural fertilizers, from the deeper almost pristine aquifer (preventing a fatal link) used mainly for irrigation and drinking purposes. In other words, the aquitard protects the confined aquifer while feeding the overlying natural springs' network. So it appears to be of

paramount importance to characterize the spatial variability of the aquitard, in terms of lateral/vertical continuity and thickness. Capturing potential discontinuities in the aquitard would be useful to predict vulnerable locations where would be recommended to avoid further drilling of boreholes that might end polluting the confined water body by means of connecting vertically both water reservoirs.

Another limitation of our model is the use of stationary facies volumetric proportions across the full domain. Vertical and lateral variability of a given hydrofacies needs to be studied in detail by the modeler. Special attention and care are required, since vertical and lateral resolution of our conditioning data are not the same, being the former higher than the latter. Having built a simpler model does not subtract validity to our results. The model could be improved by subdividing the simulated volume into regions with vertically variable lithotype proportions (we do refer the reader to works carried out by Deraisme and Farrow, 2004; Riquelme et al., 2008 and Emery et al., 2008) and/or varying locally the truncation or lithotype rules (Fontaine and Beucher, 2006). Even a more realistic approach would require varying laterally the hydrofacies volumetric proportions. The hard data is out there and the implementation of the aforesaid procedure is feasible and therefore doable.

There is typically conceptual uncertainty associated with the selection of a model which can represent the heterogeneity of an aquifer at different scales of observation. Here, we are interested in an observation window which encompasses horizontal and vertical length scales of the order of 4000 and 100 m, respectively. At these scales the distribution of lithotypes in the system is a key driver for the distribution of groundwater flow quantities. On the other hand, the spatial heterogeneity of hydraulic parameters within a given lithotype is relevant at smaller scales of observation as seen, for example, in the works of Winter et al.

(2003), and Riva et al. (2006, 2008, 2010). Treating both sources of uncertainty (i.e., uncertainty in the location of the boundaries between different materials and in the distribution of attributes within each material) can be performed, e.g., in a composite medium framework, along the lines of the references cited above. Here, we are indeed adopting a composite medium approach where facies distribution is uncertain and hydraulic attributes are deterministically known. Therefore, working at a smaller scale, additional realism and consequently more complexity can be added to the model by embedding non-stationary hydraulic conductivity (***K***) values for each simulated lithofacies. A set of tools and techniques exist and could be applied in order to achieve the suggested enhancement (see works cited above).

Last but not least a study on hydrofacies connectivity, of the kind conducted by Knudby and Carrera (2005), would be an option to extend the work to characterize the aquitard in the real aquifer system. We think that such a study should be aimed at providing quantitative assessment of the relationship between such indicators and the shape and parameters of the probability distribution of groundwater flow state variables, e.g. hydraulic heads. The result of such an analysis on fields which are conditional on data, including geological information which is embodied in the contact rules required for the application of the TPS approach, would depend on the amount and location of the abovementioned data. As a consequence, we do think that this type of quantitative analysis and exploration would deserve a separate work, most likely to be performed on the basis of synthetic scenarios associated with different variogram parameters and types of contact rules.

9. Annexes / Appendixes

In the following we present a list of published material as a direct and/or indirect outcome of the current Ph.D. thesis and a set of dissemination activities carried out to spread the word of the current research activity.

9.1. Publications

- Perulero Serrano, R.; Guadagnini, L.; Riva, M.; Giudici, M. and Guadagnini, A. "***Impact of two geostatistical hydrofacies simulation strategies on head statistics under non-uniform groundwater flow***". Journal of Hydrology, Volume 508, 16 January 2014, Pages 343-355.

  http://dx.doi.org/10.1016/j.jhydrol.2013.11.009

- Perulero Serrano, R.; Guadagnini, L.; Giudici, M., Guadagnini, A. And Riva, M. "***Application of the Truncated Plurigaussian method to delineate hydrofacies distribution in heterogeneous aquifers***". Included in the Proceedings of the XIXth International Conference, "Computational Methods in Water Resources" (17th – 21st June 2012, Champaign-Urbana; Illinois, USA).

  http://cmwr2012.cee.illinois.edu/Papers/Special%20Sessions/Optimization%20and%20Uncertainty%20Analysis%20of%20Water%20Resources%20from%20a%20Systems%20Perspective/Perulero%20Serrano.Raul.pdf

9.2. Dissemination activities

9.2.1. Conferences and workshops

- ***IMVUL 2nd Annual Meeting***; Barcelona, SPAIN; 2010
- ***Summer School in Flow and transport in porous media***; Cargèse, Corsica, FRANCE; 2010.
- ***IMVUL 3rd Annual Meeting***; Trondheim, Norway; 2011,
- ***IMVUL Network Conference hosted by UPMC-Sisyphe; Groundwater Vulnerability – Emerging Issues and New Approaches***; 9th – 12th July, 2012; Paris, France.
- ***XIXth International Conference on Computational Methods in Water Resources***; 17th – 21st June, 2012; University of Illinois, Champaign-Urbana, USA.

9.2.2. Posters at international conferences

Perulero Serrano, R.; Riva, M. and Guadagnini, A. "***Delineation of geologic facies in heterogeneous aquifers by the Truncated Plurigaussian Method***". It was presented at the International Conference EGU 2011 (Vienna, Austria), in the Poster Programme HS8.2.1. ("Stochastic Groundwater Hydrology").

Perulero Serrano, R.; Guadagnini, L.; Giudici, M., Guadagnini, A. and Riva, M. "***Delineation of geologic facies in heterogeneous aquifers using the Truncated Plurigaussian method: a real case study in northern Italy***". Presented at XIXth International Conference, "Computational Methods in Water Resources" (17th – 21st June 2012, Champaign-Urbana; Illinois, USA).

9.2.3. Oral presentations

Perulero Serrano, R.; Guadagnini, A. and Riva, M. "***Probability distributions of vertically-integrated heads during a pumping test in three-dimensional heterogeneous porous media***". Presented at IMVUL Network Conference hosted by UPMC-Sisyphe; Groundwater Vulnerability – Emerging Issues and New Approaches; 9th – 12th July, 2012; Paris, France.

Perulero Serrano, R. "***Probability distributions of vertically-integrated heads during a pumping test in three-dimensional heterogeneous porous media***". Invited presentation at "Séminaire de l'équipe hydro", OSUR, University of Rennes 1 (8th November 2012; Rennes, France).

9.3. Appendix to Chapter 7

We include in this appendix the additional material referred in Chapter 7. We did calculate the horizontal covariance matrices of $\boldsymbol{h}$ at several lines (i.e. rows/columns along the N-S and W-E directions) across the simulation domain. We performed point-wise (at three different depths, namely: top, middle and bottom layers) and full vertically averaged calculations. We repeated this procedure along various straight lines, both parallel and perpendicular to the main flow direction, as well as at different distances from the pumping well (which is placed, approximately, in the middle of the domain).

Moreover, to assess the impact of the correlation scale, we performed the same covariance calculation and afterwards we divided it by the variance of the reference point. This was done only for the full vertically averaged case.

Here we present the results corresponding to the lines that pass through the pumping well location, along the N-S and the W-E directions. The aforementioned analyses revealed that (integrated and point-wise) hydraulic head values display an increased degree of horizontal correlation along the direction perpendicular to mean flow and when an SISIM rather than a TPS approach is used.

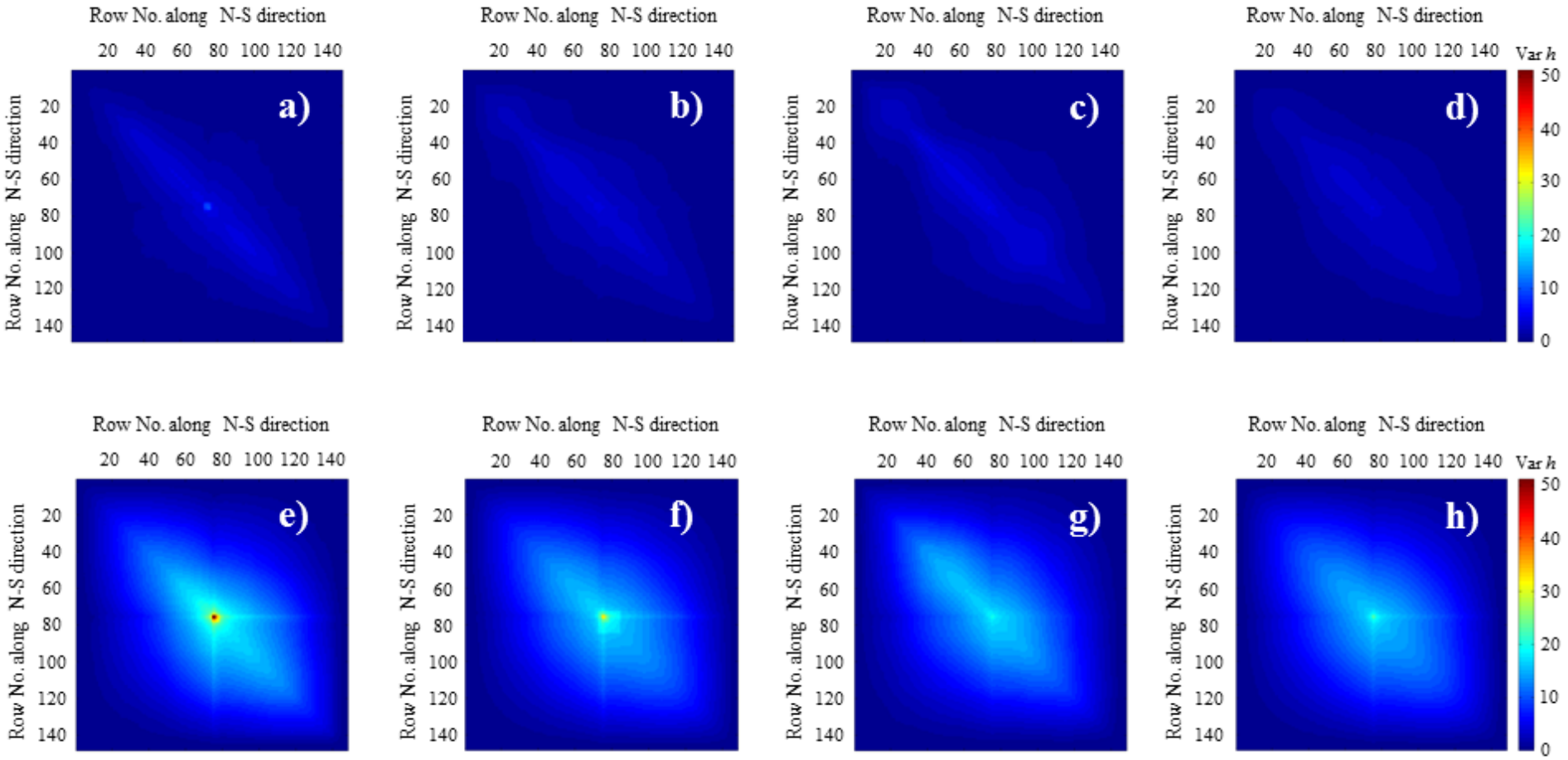

Figure 9.3.1: Covariance matrices calculated along the horizontal direction, of point values of hydraulic heads at different depths (a-c and e-g) and full vertically averaged (d, h) taken along the N-S line passing through the pumping well (see Figure 6.2.1). Namely: top layer (a, e), middle layer (b, f) and bottom layer (c, g). Results (a-d) correspond to the SISIM-based results whereas the plots (e-h) correspond to the TPS counterparts. "Var" stands for variance.

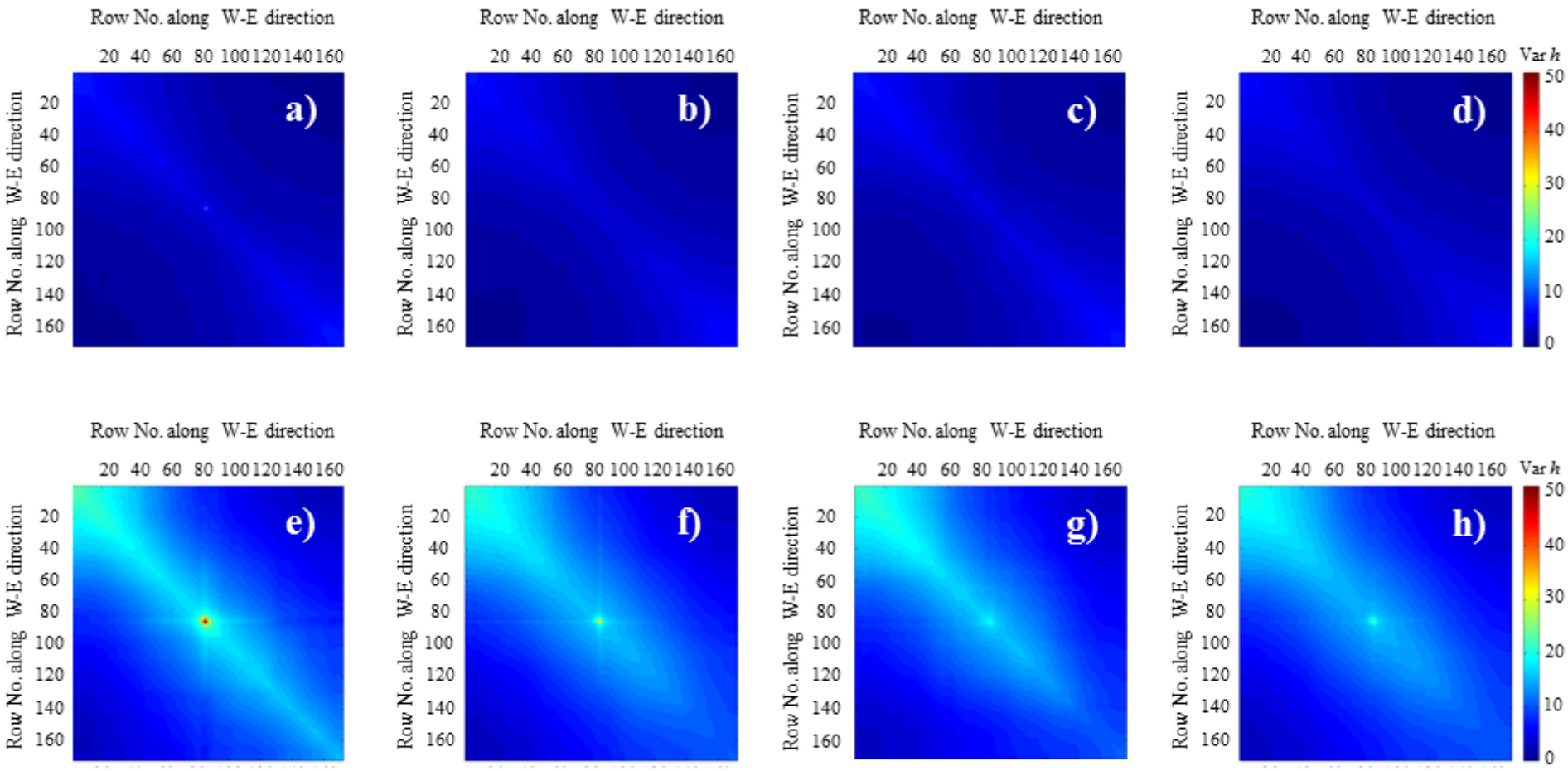

Figure 9.3.2: Covariance matrices calculated along the horizontal direction, of point values of hydraulic heads at different depths (a-c and e-g) and full vertically averaged (d, h) taken along the W-E line passing through the pumping well (see Figure 6.2.1). Namely: top layer (a, e), middle layer (b, f) and bottom layer (c, g). Results (a-d) correspond to the SISIM-based results whereas the plots (e-h) correspond to the TPS counterparts. "Var" stands for variance.

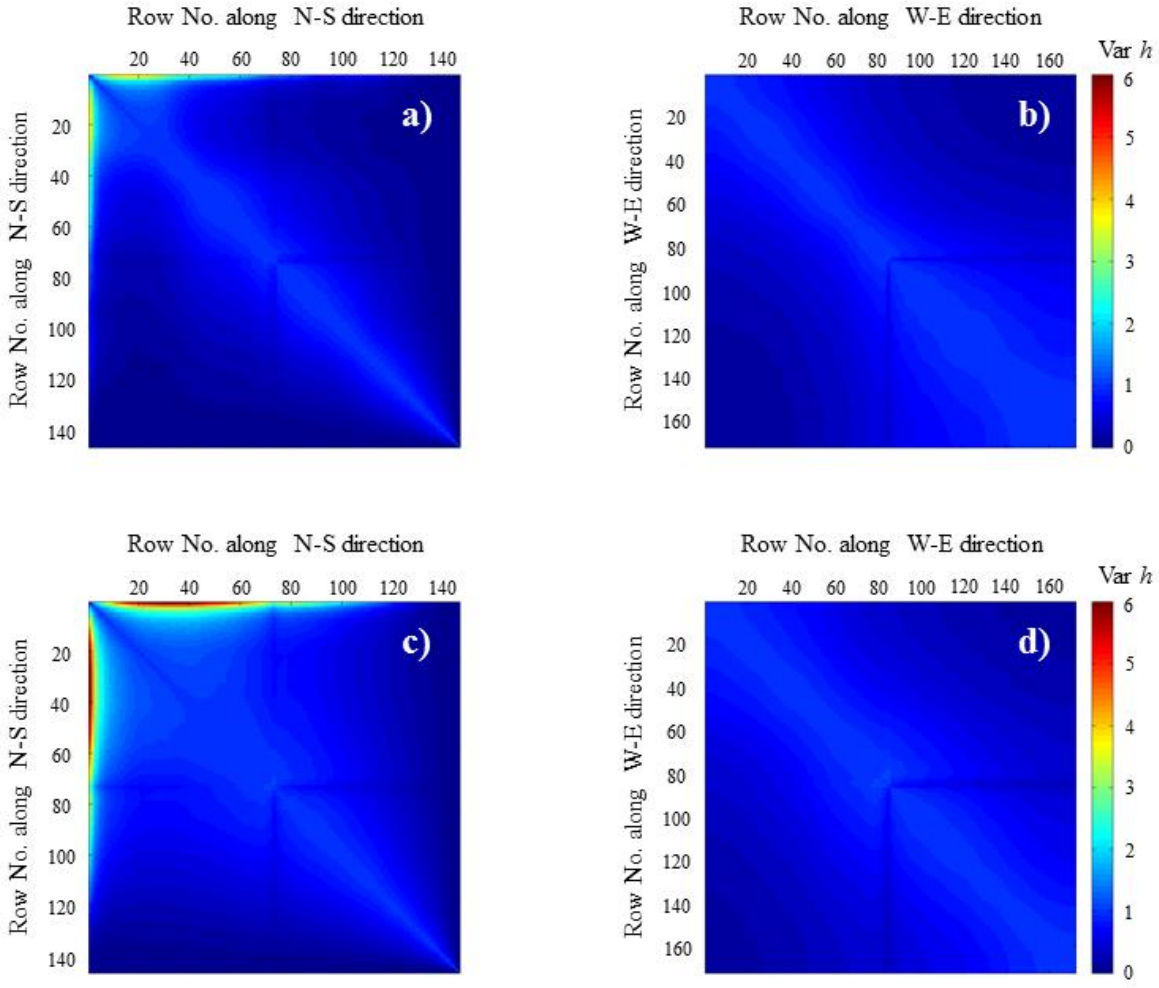

Figure 9.3.3: Covariance matrices along the horizontal direction, normalized by the variance of the reference point, of full vertically averaged hydraulic heads taken along the N-S (a, c) and the W-E (b, d) line passing through the pumping well (see Figure 6.2.1). Results (a, b) correspond to the SISIM-based results whereas the plots (c, d) correspond to the TPS counterparts. "Var" stands for variance.

10. References

Ababou, R., McLaughlin, D., Gelhar, L.W. and Tompson, A. F. B., 1989. Numerical simulation of three-dimensional saturated flow in randomly heterogeneous porous media. Transport Porous Med. 4, 6, 549-565.

Ballio, F., and Guadagnini, A., 2004. Convergence assessment of numerical Monte Carlo simulations in groundwater hydrology. Water Resour. Res. 40, W04603, doi:10.1029/2003WR002876.

Bellin, A., Tonina, D., 2007. Probability density function of non-reactive solute concentration in heterogeneous porous formations. J. Contam. Hydrol. 94, 1-2, 109-125, doi: 10.1016/j.jconhyd.2007.05.005.

Betzhold, J., Roth, C., 2000. Characterizing the mineralogical variability of a Chilean copper deposit using plurigaussian simulations. J. S. Afr. Inst. Min. Metall. 100, 2, 111-119.

Bianchi Janetti, E., Guadagnini, L., Riva, M., Larcan, E., Guadagnini, A., 2011. Geostatistical characterization of a regional scale sedimentary aquifer, in: F. Ubertini, E. Viola, S. de Miranda and G. Castellazzi (Eds.), Prof. of XX Congresso dell'Associazione Italiana di Meccanica Teorica e Applicata, Bologna 12-15 September 2011; ISBN 978-88-906340-1-7 (online), pp. 1-10.

Bolster, D., Barahona, M., Dentz, M., Fernández-García, D., Sánchez-Vila, X., Trinchero, P., Valhondo, C., Tartakovsky, D. M., 2009. Probabilistic risk analysis of groundwater remediation strategies. Water Resour. Res. 45, doi: 10.1029/2008WR007551

Carle, S. F., 1999. T-PROGS: transition probability geostatistical software version 2.1. University of California, Davis, CA.

Casar-González, R., 2001. Two procedures for stochastic simulation of vuggy formations. SPE Paper 69663, SPE, Richardson, TX.

Clark, I., 1979. Practical Geostatistics. Applied Science Publishers, Barking, Essex. 129p.

Dagan, G., 1985. A note on higher-order corrections of the head covariances in steady aquifer flow. Water Resour. Res. 21, 4, 573-578.

Dagan, G., 1989. Flow and Transport in Porous Formations. Springer-Verlag, New York.

De Barros, F. P. J., Ezzedine, S. and Rubin, Y., 2012. Impact of hydrogeological data on measures of uncertainty, site characterization and environmental performance metrics. Adv. Water Resour. 36, 51-64. doi: 10.1016/j.advwatres.2011.05.004.

Dell'Arciprete, D., Bersezio, R., Felletti, F., Giudici, M., Comunian, A., Renard, P., 2012. Comparison of three geostatistical methods for hydrofacies simulation: a test on alluvial sediments. Hydrogeol. J. 20, 299-311, doi: 10.1007/s10040-011-0808-0.

Deraisme, J. and Farrow, D., Geostatistical Simulation Techniques applied to kimberlite orebodies and risk assessment of sampling strategies. 7th Geostatistics Congress, Banff, 2004.

Deutsch, C. V., Journel, A. G., 1997. GSLIB: Geostatistical software library and user's guide, second ed. Oxford University Press, UK.

Dowd, P., Xu, C., Mardia, K. V., Fowell, R. J., 2007. A comparison of methods for the stochastic simulation of rock fractures. Math. Geol. 39, 7, 697-714.

Emery, X., 2004. Properties and limitations of sequential indicator simulation. Stoch. Env. Res. Risk. A. 18, 414-424.

Emery, X., 2007. Simulation of geological domains using the plurigaussian model: New developments and computer programs. Comput. Geosci. 33, 1189-1201.

Emery, X., Ortiz, J. M., and Cáceres, A. M., 2008. Geostatistical modeling of rock type domains with spatially varying proportions: Application to a porphyry copper deposit. Journal of the South African Institute of Mining and Metallurgy, vol. 108, n. 5, pp. 285-292.

Englert, A., Vanderborght, J. & Vereecken, H., 2006. Prediction of velocity statistics in three-dimensional multi-Gaussian hydraulic conductivity fields. Water Resour. Res. 42, 3, W03418, doi: 10.1029/2005WR004014.

Enzenhoefer, R., Nowak, W., Helmig, R., 2012. Probabilistic exposure risk assessment with advective dispersive well vulnerability criteria. Adv. Water Resour. 36, 121-132, doi: 10.1016/j.advwatres.2011.04.018.

Falivene, O., Arbués, P., Gardiner, A., Pickup, G., Muñoz, J.A., Cabrera, L., 2006. Best practice stochastic facies modeling from a channel-fill turbidite sandstone analog (the Quarry outcrop, Eocene Ainsa basin, northeast Spain). AAPG Bull., 90, 1003-1029.

Falivene, O., Cabrera, L., Muñoz, J. A., Arbués, P., Fernández, O., Sáez, A., 2007. Statistical grid-based facies reconstruction and modeling for sedimentary bodies. Alluvial-palustrine and turbiditic examples. Geol. Acta. 5, 199-230.

Fiorotto, V., Caroni, E., 2002. Solute concentration statistics in heterogeneous aquifers for finite Peclet values. Transport Porous Med. 48, 3, 331-351, doi: 10.1023/A:1015744421033.

Fontaine, L. and Beucher, H. 2006. Simulation of the Muyumkum uranium roll front deposit by using truncated plurigaussian method. In 6th international mining geology conference, Darwin.

Galli, A. G., Beucher, H., Le Loc'h, G., Doligez, B., Heresim group, 1994. The Pros and Cons of the truncated Gaussian method, in: Armstrong, M., Dowd, P. A., (Eds.), Geostatistical Simulations. Kluwer Academic Publishers, Netherlands, pp. 217-233.

Gandolfi, C., Ponzini, G. and Giudici, M., 2007. Realizzazione di un modello preliminare del flusso idrico nel sistema acquifero della Provincia di Cremona.

Guadagnini, A., Neuman, S. P., 1999a. Nonlocal and localized analyses of conditional mean steady state flow in bounded, randomly nonuniform domains 2. Computational examples. Water Resour. Res. 35, 10, 2999-3018, doi: 10.1029/1999WR900159.

Guadagnini, A., Neuman, S. P., 1999b. Nonlocal and localized analyses of conditional mean steady state flow in bounded, randomly nonuniform domains 1. Theory and computational approach. Water Resour. Res. 35, 10, 2999-3018, doi: 10.1029/1999WR900160.

Guadagnini, A., Riva, M., Neuman, S. P., 2003. Three-dimensional Steady State Flow to a Well in a Randomly Heterogeneous Bounded Aquifer. Water Resour. Res. 39(3) 1048, doi: 10.1029/2002WR001443.

Guadagnini, A., Neuman, S. P., Riva, M., 2012. Numerical Investigation of Apparent Multifractality of Samples from Processes Subordinated to Truncated fBm. Hydrol. Process. 26, 19, 2894-2908, doi: 10.1002/hyp.8358.

Guadagnini, L. et al. "Modello quali-quantitativo per la tutela della 'Fascia dei Fontanili' nella fase di pianificazione della risorsa acqua". Relazione tecnica; January 2007–December 2008.

Hernández, A. F.,. Neuman, S. P., Guadagnini, A., Carrera, J., 2006. Inverse stochastic moment analysis of steady state flow in randomly heterogeneous media. Water Resour. Res. 42, W05425, doi:10.1029/2005WR004449.

Isaaks, E. H., Srivastava, R. M., 1989. An Introduction to Applied Geostatistics. N.Y.: OUP. 561p.

Jones, L., 1990. Explicit Monte Carlo Simulation Head Moment Estimates for Stochastic Confined Groundwater Flow. Water Resour. Res. 26, 6, 1145-1153, doi: 10.1029/WR026i006p01145.

Journel, A. G., Alabert, F. G., 1989. Non-Gaussian data expansion in the earth sciences. Terra Nova, 1, 123-134.

Jurado, A., De Gaspari, F., Vilarrasa, V., Bolster, D., Sánchez-Vila, X., Fernández-García, D., Tartakovsky, D. M., 2012. Probabilistic analysis of groundwater-related risks at subsurface excavation sites. Eng. Geol.. 125, 35-44, doi: 10.1016/j.enggeo.2011.10.015.

Kitanidis, P. K., 1997. Introduction to Geostatistics. Applications in Hydrogeology. Cambridge, New York, Port Chester, Melbourne, Sydney: Cambridge University Press. 249 pp.

Kunstmann, H., Kastens, M., 2006. Determination of stochastic well head protection zones by direct propagation of uncertainties of particle tracks. J. Hydrol. 323, 1-4, 215-229, doi: 10.1016/j.jhydrol.2005.09.003.

Lee, S-Y., Carle, S. F., Fogg, G. E., 2007. Geologic heterogeneity and a comparison of two geostatistical models: sequential Gaussian and transition probability-based geostatistical simulation. Adv. Water Resour. 30, 1914-1932.

Maione, U., Paoletti, A., Grezzi, G., 1991. Studio di gestione coordinata delle acque di superficie e di falda nel territorio compreso fra i fiumi Adda e Oglio e delimitato dalle Prealpi e dalla linea settentrionale di affioramento dei fontanili

Mariethoz, G., Renard, Ph., Cornaton, F., Jaquet, O., 2009. Truncated Plurigaussian Simulations to Characterize Aquifer Heterogeneity. Ground Water. 47, 13-24.

McDonald, M.G., Harbaugh, A.W., 1988. A modular three-dimensional finite-difference ground-water flow model. Techniques of Water-Resources Investigations of the United States Geological Survey, Book 6, Chapter A1.

Nolan, J. P., 2001. Maximum likelihood estimation of stable parameters. In: O. E. Barndorff-Nielsen, T. Mikosch, and S. I. Resnick (Eds.), Levy Processes:Theory and Applications, Boston: Birkhäuser, pp 379-400.

Nowak, W., Schwede, R. L., Cirpka, O. A., Neuweiler, I., 2008. Probability density functions of hydraulic head and velocity in three-dimensional heterogeneous porous media. Water Resour. Res. 44, W08452, doi: 10.1029/2007WR006383.

Osnes, H., 1995. Stochastic analysis of head spatial variability in bounded rectangular heterogeneous aquifers. Water Resour. Res. 31, 12, 2981-2990.

Rametta, D. (2008). Interazione tra reticolo idrografico superficiale e acquifero sotterraneo nella modellistica idrologica distribuita, Politecnico di Milano, Milano.

Remy, N., Alexandre, B., Jianbing, W., 2009. Applied Geostatistics with SGeMS: A user's guide. 1st ed. Cambridge University Press; doi: 10.1017/CBO9781139150019.

Riquelme Tapia, R., Le Loc'H G., Carrasco Castelli, P., 2008. Truncated gaussian and plurigaussian simulations of lithological units in Mansa Mina deposit. VIII International Geostatistics Congress, GEOSTATS 2008, Santiago: Chile (2008).

Riva, M., Guadagnini, L., Guadagnini, A., Ptak, T., Martac, E., 2006. Probabilistic study of well capture zones distribution at the Lauswiesen field site. J. of Cont. Hydrol. 88, 92-118.

Riva, M., Guadagnini, A., Fernández-García, D., Sánchez-Vila, X., Ptak, T., 2008. Relative importance of geostatistical and transport models in describing heavily tailed breakthrough curves at the Lauswiesen site. J. Contam. Hydrol. 101, 1-13.

Riva, M., Guadagnini, A., 2009. Effects of evolving scales of heterogeneity on hydraulic head predictions under convergent flow conditions. Hydrogeol. J., 17, 817-825, doi:10.1007/s10040-008-0396-9.

Riva, M., Guadagnini, L., Guadagnini, A., 2010. Effects of uncertainty of litho-facies, conductivity and porosity distributions on stochastic interpretations of a field-scale tracer test. Stoch. Env. Res. Risk. A. 24, 955-970, doi: 10.1007/s00477-010-0399-7.

Rubin, Y., and Dagan, G., 1988. Stochastic analysis of boundaries effects on head spatial variability in heterogeneous aquifers: 1. Constant head boundary. Water Resour. Res. 24, 10. 1689-1697.

Rubin, Y., and Dagan, G., 1989. Stochastic analysis of boundaries effects on head spatial variability in heterogeneous aquifers: 2. Impervious boundary. Water Resour. Res. 25, 4, 707-712.

Samorodnitsky, G., Taqqu, M., 1994. Stable Non-Gaussian Random Processes. New York: Chapman and Hall.

Scheibe, T.D., Murray, C.J., 1998. Simulation of geologic patterns: a comparison of stochastic simulation techniques for groundwater transport modelling. In: Fraser GS, Davis JM (eds) Special publication of the SEPM (Society for Sedimentary Geology), Tulsa, OK, 107-118.

Schwede, R. L., Cirpka, O. A., Nowak, W., Neuweiler, I., 2008. Impact of sampling volume on the probability density function of steady state concentration. Water Resour. Res. 44, 12, doi: 10.1029/2007WR006668.

Strebelle, S., 2002. Conditional simulation of complex geological structures using multiple point statistics. Math. Geosci. 34, 1-22.

Tartakovsky, D. M., 2013. Assessment and management of risk in subsurface hydrology: A review and perspective. Adv. Water Resour., 51, 247-260, doi: 10.1016/j.advwatres.2012.04.007.

Vassena, C., Rienzner, M., Ponzini, G., Giudici, M., Gandolfi, C., Durante, C., Agostani, D., 2012. Modeling water resources of a highly irrigated alluvial plain (Italy): calibrating soil and groundwater models. Hydrogeol. J. 20, 3, 449-467, doi: 10.1007/s10040-011-0822-2.

Xu, C., Dowd, P. A., Mardia, K. V., Fowell, R. J., 2006. A flexible true plurigaussian code for spatial facies simulations. Comput. Geosci. 32, 1629-1645.

Winter, C. L, Tartakovsky, D. M., Guadagnini, A., 2003. Moment differential equations for flow in highly heterogeneous porous media. Surveys in Geophysics, 24(1), 81-106.

Wu, J., Boucher, A., Zhang, T., 2008. SGeMS code for pattern simulation of continuous and categorical variables: FILTERSIM. Computers & Geosciences. 34, 728, 1863-1876.

Zarlenga, A., Fiori, A., Soffia, C., and Jankovic, I., 2012. Flow velocity statistics for uniform flow through 3D anisotropic formations. Adv. Water Resour. 40, 37-45.

Zhang, T., Switzer, P., Journel, A. G., 2006. Filter-based classification of training image patterns for spatial simulation Math. Geosci. 38, 63-80.